

Unclassified
Security Classification

DOCUMENT CONTROL DATA - R&D	
<i>(Security classification of title, body of abstract and indexing annotation must be entered when the overall report is classified)</i>	
1. ORIGINATING ACTIVITY (Corporate author) Air Force Cambridge Research Laboratories (OP) L. G. Hanscom Field Bedford, Massachusetts 01730	20. REPORT SECURITY CLASSIFICATION Unclassified 2A. GROUP
3. REPORT TITLE OPTICAL PROPERTIES OF THE ATMOSPHERE (Third Edition)	
4. DESCRIPTIVE NOTES (Type of report and inclusive dates) Scientific. Interim.	
5. AUTHOR(S) (First name, middle initial, last name) R. A. McClatchey F. E. Volz R. W. Fenn J. S. Garing J. E. A. Selby	
6. REPORT DATE 24 August 1972	7A. NO. OF REFS 63
8A. CONTRACT OR GRANT NO.	9A. ORIGINATOR'S REPORT NUMBER(S) AFCLR-72-0497
a. PROJECT, TASK, WORK UNIT NOS. 7670-09-01	9B. OTHER REPORT NUMBER(S) (Any other numbers that may be assigned this report) ERP No. 411
c. DOD ELEMENT 62101F	
d. DOD SUPPLEMENT 681000	
10. DISTRIBUTION STATEMENT Approved for public release; distribution unlimited.	
11. SUPPLEMENTARY NOTES TECH, OTHER	12. SPONSORING MILITARY ACTIVITY Air Force Cambridge Research Laboratories (OP) L. G. Hanscom Field Bedford, Massachusetts 01730
13. ABSTRACT A series of tables and charts is presented from which the atmospheric transmittance between any two points in the terrestrial atmosphere can be determined. This material is based on a set of five atmospheric models ranging from tropical to arctic and two aerosol models. A selected set of laser frequencies has been defined for which monochromatic transmittance values have been given. For low resolution transmittance prediction, a series of charts has been drawn providing the capability for predicting transmittance at a resolution of 20 wave-numbers. Separate sections are included on scattered solar radiation, infrared emission, refractive effects, and attenuation by cloud and fog. This report represents the third edition of an earlier report bearing a similar title (McClatchey, et al, 1970). Although subsequent editions have been published primarily to accommodate demand, the opportunity has been used to make minor revisions, corrections and additions. This third edition differs from the others in that the low resolution spectral curves for the uniformly mixed gases and in the short wavelength region for water vapor have been revised, providing some overall improvement in accuracy; and more importantly, an appendix has been added providing model data and equivalent sea level path data for the U.S. Standard Atmosphere, 1962.	

DD FORM 1473
1 NOV 66

Unclassified
Security Classification

Unclassified
Security Classification

14. KEY WORDS	LINK A		LINK B		LINK C	
	ROLE	WT	ROLE	WT	ROLE	WT
Atmospheric transmittance Laser transmittance Infrared Radiative transfer Atmospheric optics						

Unclassified
Security Classification

AFCRL-72-0497
24 AUGUST 1972
ENVIRONMENTAL RESEARCH PAPERS, NO. 411



OPTICAL PHYSICS LABORATORY PROJECT 7670

AIR FORCE CAMBRIDGE RESEARCH LABORATORIES

L. G. HANSCOM FIELD, BEDFORD, MASSACHUSETTS

Optical Properties of the Atmosphere (Third Edition)

R.A. McCLATCHEY
R.W. FENN
J.E.A. SELBY
F.E. VOLZ
J.S. GARING

Approved for public release; distribution unlimited.

AIR FORCE SYSTEMS COMMAND
United States Air Force

- iii -



Contents

1. INTRODUCTION	1
2. MODEL ATMOSPHERES USED IN OPTICAL CALCULATIONS	2
2.1 Standard Model Atmospheres	2
2.2 Concentrations of Uniformly Mixed Gases	2
2.3 Aerosol Distributions	8
3. FUNDAMENTALS OF ATMOSPHERIC TRANSMITTANCE	10
4. ATMOSPHERIC TRANSMITTANCE AT SELECTED FREQUENCIES	13
4.1 List of Laser Frequencies	13
4.2 Scattering and Absorption Coefficients	13
4.3 Interpolation Procedures	14
5. ATMOSPHERIC TRANSMITTANCE AT LOW RESOLUTION FROM 0.25 to 25 μm	27
5.1 Continuum Absorption in the Atmospheric Window Regions	28
5.2 Outline of Band Model Techniques	29
5.3 Equivalent Constant Pressure Paths and Absorber Amounts	32
5.4 Description and Use of Prediction Charts	35
5.5 Absorption in the Region 0.25 to 0.75 μm	36
5.6 Accuracy of Low Resolution Transmittance Calculations	37
6. SCATTERED SOLAR RADIATION AND INFRARED EMISSION	38
6.1 Transmitted and Reflected Sky Radiance in Clear and Cloudy Sky	38
6.2 Infrared Emission of the Atmosphere	40
7. REFRACTIVE EFFECTS IN THE ATMOSPHERE	41
8. EFFECT OF CLOUDS AND FOG ON ATMOSPHERIC RADIATION	42

Preceding page blank

v

Contents

ACKNOWLEDGMENT	81
REFERENCES	83
APPENDIX A: Units and Conversion Factors	87
APPENDIX B: Equivalent Sea Level Path Charts for U. S. Standard Atmosphere, 1962	93

Illustrations

1. Normalized Particle Size Distribution for Aerosol Models	44
2. Equivalent Sea Level Path Lengths of Water Vapor as a Function of Altitude for Horizontal Atmospheric Paths	45
3. Equivalent Sea Level Path Length of Water Vapor as a Function of Altitude for Vertical Atmospheric Paths	46
4. Equivalent Sea Level Path Lengths of Uniformly Mixed Gases as a Function of Altitude for Horizontal Atmospheric Paths	47
5. Equivalent Sea Level Path Lengths of Uniformly Mixed Gases as a Function of Altitude for Vertical Atmospheric Paths	48
6. Equivalent Sea Level Path Length of Ozone as a Function of Altitude for Horizontal Atmospheric Paths	49
7. Equivalent Sea Level Path Length of Ozone as a Function of Altitude for Vertical Atmospheric Paths	50
8. Equivalent Sea Level Path Length of Nitrogen as a Function of Altitude for Horizontal Atmospheric Paths	51
9. Equivalent Sea Level Path Length of Nitrogen as a Function of Altitude for Vertical Atmospheric Paths	52
10. Equivalent Sea Level Path Length for Water Vapor Continuum as a Function of Altitude for Horizontal Atmospheric Paths	53
11. Equivalent Sea Level Path Length for Water Vapor Continuum as a Function of Altitude for Vertical Atmospheric Paths	54
12. Equivalent Sea Level Path Length for Molecular Scattering as a Function of Altitude for Horizontal Atmospheric Paths	55
13. Equivalent Sea Level Path Length for Molecular Scattering as a Function of Altitude for Vertical Atmospheric Paths	56
14. Equivalent Sea Level Path Length for Aerosol Extinction as a Function of Altitude for Horizontal Atmospheric Paths	57
15. Equivalent Sea Level Path Length for Aerosol Extinction as a Function of Altitude for Vertical Atmospheric Paths	58
16a. Prediction Chart for Water Vapor Transmittance (0.6 - 4.0 μm)	59
16b. Prediction Chart for Water Vapor Transmittance (4 - 26 μm)	60

Illustrations

17a. Prediction Chart for the Transmittance of Uniformly Mixed Gases (CO ₂ , N ₂ O, CO, CH ₄ , O ₂) (0.76 - 4.5 μm)	61
17b. Prediction Chart for the Transmittance of Uniformly Mixed Gases (CO ₂ , N ₂ O, CO, CH ₄) (4.5 - 19 μm)	62
18a. Prediction Chart for Ozone Transmittance (3-6.4 μm)	63
18b. Prediction Chart for Ozone Transmittance (8-18 μm)	64
19. Prediction Chart for Nitrogen Transmittance	65
20. Prediction Chart for Water Vapor Continuum	66
21. Prediction Chart for Transmittance Due to Molecular Scattering	67
22. Prediction Chart for Aerosol Transmittance (Scattering and Absorption)	68
23. Equivalent Sea Level Path Length for Ozone (0.25-0.75 μm) as a Function of Altitude for Horizontal Atmospheric Paths	69
24. Equivalent Sea Level Path Length for Ozone (0.25-0.75 μm) as a Function of Altitude for Vertical Atmospheric Paths	70
25. Prediction Chart for Ozone Transmittance (0.25-0.75 μm)	71
26. Normalized Scattering Phase Function of Aerosol and Air	72
27. Downward (a) and Upward (b) Radiance Computed by Monte Carlo Techniques	73
28. Downward (a) and Upward (b) Radiance Computed for a Dense Nimbostratus Cloud	74
29. Typical Reflectance of Water Surface, Snow, Dry Soil and Vegetation	75
30. Radiance as a Function of Wavelength Computed for Temperature Distribution Corresponding to the Midlatitude Winter Model	76
31. Spectral Radiance of a Clear Zenith Sky Showing the Effect of the Position of the Sun on the Radiation Scattered Below 3 μm and the Effect of Thermal Emission at Longer Wavelengths	77
32. Comparison of the Relative Air Mass [M(θ)] as a Function of Apparent Zenith Angle, θ.	78
33. The Attenuation as a Function of Wavelength Due to Fair Weather Cumulus Cloud	79
34. Particle Size Distribution for Fair Weather Cumulus Cloud Model	80
A1. Water Vapor Concentration per Kilometer Path Length as a Function of Temperature and Relative Humidity	91
B1. Equivalent Sea Level Path Length of Water Vapor as a Function of Altitude for Horizontal Atmospheric Paths	95
B2. Equivalent Sea Level Path Length of Water Vapor as a Function of Altitude for Vertical Atmospheric Paths	96
B3. Equivalent Sea Level Path Length of Uniformly Mixed Gases as a Function of Altitude for Horizontal Atmospheric Paths	97
B4. Equivalent Sea Level Path Length of Uniformly Mixed Gases as a Function of Altitude for Vertical Atmospheric Paths	98
B5. Equivalent Sea Level Path Length of Ozone as a Function of Altitude for Horizontal Atmospheric Paths.	99

Illustrations

B6.	Equivalent Sea Level Path Length of Ozone as a Function of Altitude for Vertical Atmospheric Paths	100
B7.	Equivalent Sea Level Path Length of Nitrogen as a Function of Altitude for Horizontal Atmospheric Paths	101
B8.	Equivalent Sea Level Path Length of Nitrogen as a Function of Altitude for Vertical Atmospheric Paths	102
B9.	Equivalent Sea Level Path Length for Water Vapor Continuum as a Function of Altitude for Horizontal Atmospheric Paths	103
B10.	Equivalent Sea Level Path Length for Water Vapor Continuum as a Function of Altitude for Vertical Atmospheric Paths	104
B11.	Equivalent Sea Level Path Length for Molecular Scattering as a Function of Altitude for Horizontal Atmospheric Paths	105
B12.	Equivalent Sea Level Path Length for Molecular Scattering as a Function of Altitude for Vertical Atmospheric Paths	106
B13.	Equivalent Sea Level Path Length for Ozone (0.25-0.75 μm) as a Function of Altitude for Horizontal Atmospheric Paths	107
B14.	Equivalent Sea Level Path Length for Ozone (0.25-0.75 μm) as a Function of Altitude for Vertical Atmospheric Paths	108

Tables

1.	Model Atmospheres Used as a Basis of the Computation of Atmospheric Optical Properties	3
2.	Concentration of Uniformly Mixed Gases	8
3.	Aerosol Models - Vertical Distributions for a "Clear" and "Hazy" Atmosphere	9
4.	Laser Wavelengths	14
5.	Values of Attenuation Coefficient/km as a Function of Altitude for Each Laser Wavelength and Each Atmospheric Model in Section 2	15
6.	Difference Between Actual and Apparent Zenith Angle as a Function of Apparent Zenith Angle	42
7.	Relative Optical Path of a Thin, High Altitude Layer as a Function of Zenith Angle θ	43
B1.	Model Atmosphere Used as a Basis for the Computation of Atmospheric Optical Properties	94

Optical Properties of the Atmosphere (Third Edition)

I. INTRODUCTION

This report is intended to provide data from which the attenuation or emission of radiation along a path in a given model atmosphere can be determined. The spectral region covered is from 0.25 to 25 micrometers. We have not concerned ourselves with the atmosphere above 100 km, thereby neglecting less than one-millionth of the total atmospheric mass.

We have defined five model atmospheres each for temperature, pressure and absorbing gas concentrations. In addition to these, two aerosol models have been defined. Thus, one effectively has 10 models from which to choose in order to use the data as presented without interpolation. However, interpolation schemes are described in order to allow the user to obtain optical data for intermediate conditions.

As it is not possible to cover all conceivable atmospheric models, neither is it possible to provide data in a short report for any spectral resolution. Thus, we are forced to limit the high resolution calculations to a few specific wavelengths. A list of laser emission wavelengths was chosen for this purpose. We attempted to pick those lasers most commonly used in practical applications and as research tools. In addition to the laser beam transmittance table, we have provided in graphical form a calculation scheme for determining atmospheric absorption and

(Received for publication 22 August 1972)

scattering at about a 20 wavenumber resolution across the entire spectral region. These curves, although appropriate for low resolution transmittance calculations would produce serious error if used for estimates of laser propagation in the atmosphere. For high resolution curves appropriate to the laser propagation problem, additional reports have been published (McClatchey, 1971 and McClatchey & Selby, 1972).

The models defined in Section 2 together with the low resolution absorption calculation techniques presented in Section 5, were used to compute the radiation emitted to space and the radiation as observed looking up at the sky from the surface (sky background) for wavelengths longer than $5 \mu\text{m}$ (Section 6). The radiation to space and sky backgrounds at shorter wavelengths is a complicated function of the solar zenith angle and the angle of observation, so only a few specific examples have been given.

The effect of the refractive index on the geometrical path length and the effect of cloud and fog on the attenuation of radiation are discussed in Sections 7 and 8, respectively.

2. MODEL ATMOSPHERES USED IN OPTICAL CALCULATIONS

2.1 Standard Model Atmospheres

A series of five model atmospheres is presented in Table 1. The pressure, temperature, density, water vapor concentrations are those of the U.S. Standard Atmosphere of 1932 and the Supplemental Atmospheres as compiled in the Handbook of Geophysics and Space Environment (Valley 1965). The ozone concentrations were extracted from Chapter 6 of the Handbook of Geophysics and Space Environment (Valley, 1965). The water vapor densities above 11 km have been taken from Sissenwine et al (1968). A discussion of units and conversion can be found in Appendix A.

2.2 Concentrations of Uniformly Mixed Gases

Table 2 is intended to provide the reader with the data for determining the concentrations of all uniformly mixed atmospheric gases in any horizontal or vertical path. Column 3 gives the concentrations in parts per million by volume. The fourth column gives the total amount of gas in a vertical path through the entire atmosphere. The fifth column lists the number of $(\text{cm-atm})_{\text{STP}}$ of gas in a one kilometer path at sea level. The number of $(\text{cm-atm})_{\text{STP}}$ in a horizontal path at any other altitude is given by Eq. (1).

$$(\text{cm-atm})_{\text{STP}} = L \left(\frac{\text{ppm}}{10} \right) \left(\frac{P_0 T_0}{P T} \right) \quad (1)$$

Table 1. Model Atmospheres Used as a Basis of the Computation of Atmospheric Optical Properties

TROPICAL					
Ht. (km)	Pressure (mb)	Temp. (°K)	Density (g/m ³)	Water Vapor (g/m ³)	Ozone (g/m ³)
0	1.013E+03	300.0	1.167E+03	1.9E+01	5.6E-05
1	9.040E+02	294.0	1.064E+03	1.3E+01	5.6E-05
2	8.050E+02	288.0	9.689E+02	9.3E+00	5.4E-05
3	7.150E+02	284.0	8.756E+02	4.7E+00	5.1E-05
4	6.330E+02	277.0	7.951E+02	2.2E+00	4.7E-05
5	5.590E+02	270.0	7.199E+02	1.5E+00	4.5E-05
6	4.920E+02	264.0	6.501E+02	8.5E-01	4.3E-05
7	4.320E+02	257.0	5.855E+02	4.7E-01	4.1E-05
8	3.780E+02	250.0	5.258E+02	2.5E-01	3.9E-05
9	3.290E+02	244.0	4.708E+02	1.2E-01	3.9E-05
10	2.860E+02	237.0	4.202E+02	5.6E-02	3.9E-05
11	2.470E+02	230.0	3.740E+02	1.7E-02	4.1E-05
12	2.130E+02	224.0	3.316E+02	6.0E-03	4.3E-05
13	1.820E+02	217.0	2.929E+02	1.8E-03	4.5E-05
14	1.560E+02	210.0	2.578E+02	1.0E-03	4.5E-05
15	1.320E+02	204.0	2.260E+02	7.6E-04	4.7E-05
16	1.110E+02	197.0	1.972E+02	6.4E-04	4.7E-05
17	9.370E+01	195.0	1.676E+02	5.6E-04	6.9E-05
18	7.890E+01	189.0	1.382E+02	5.0E-04	9.0E-05
19	6.660E+01	203.0	1.145E+02	4.9E-04	1.4E-04
20	5.650E+01	207.0	9.515E+01	4.5E-04	1.9E-04
21	4.800E+01	211.0	7.938E+01	5.1E-04	2.4E-04
22	4.090E+01	215.0	6.645E+01	5.1E-04	2.8E-04
23	3.500E+01	217.0	5.618E+01	5.4E-04	3.2E-04
24	3.000E+01	219.0	4.763E+01	6.0E-04	3.4E-04
25	2.570E+01	221.0	4.045E+01	6.7E-04	3.4E-04
30	1.220E+01	232.0	1.831E+01	3.6E-04	2.4E-04
35	6.000E+00	243.0	8.600E+00	1.1E-04	9.2E-05
40	3.050E+00	254.0	4.181E+00	4.3E-05	4.1E-05
45	1.590E+00	265.0	2.097E+00	1.9E-05	1.3E-05
50	8.540E-01	270.0	1.101E+00	6.3E-06	4.3E-06
70	5.790E-02	219.0	9.210E-02	1.4E-07	8.6E-08
100	3.000E-04	210.0	5.000E-04	1.0E-09	4.3E-11

Table 1 (Contd). Model Atmospheres Used as a Basis of the Computation of Atmospheric Optical Properties

MIDLATITUDE SUMMER					
Ht. (km)	Pressure (mb)	Temp. (°K)	Density (g/m ³)	Water Vapor (g/m ³)	Ozone (g/m ³)
0	1.013E+03	294.0	1.191E+03	1.4E+01	6.0E-05
1	9.020E+02	290.0	1.080E+03	9.3E+00	6.0E-05
2	8.020E+02	285.0	9.757E+02	5.9E+00	6.0E-05
3	7.100E+02	279.0	8.846E+02	3.3E+00	6.2E-05
4	6.280E+02	273.0	7.998E+02	1.9E+00	6.4E-05
5	5.540E+02	267.0	7.211E+02	1.0E+00	6.6E-05
6	4.870E+02	261.0	6.487E+02	6.1E-01	6.9E-05
7	4.260E+02	255.0	5.830E+02	3.7E-01	7.5E-05
8	3.720E+02	248.0	5.225E+02	2.1E-01	7.9E-05
9	3.240E+02	242.0	4.669E+02	1.2E-01	8.6E-05
10	2.810E+02	235.0	4.159E+02	6.4E-02	9.0E-05
11	2.430E+02	228.0	3.693E+02	2.2E-02	1.1E-04
12	2.090E+02	222.0	3.269E+02	6.0E-03	1.2E-04
13	1.790E+02	216.0	2.882E+02	1.8E-03	1.5E-04
14	1.530E+02	216.0	2.464E+02	1.0E-03	1.8E-04
15	1.300E+02	216.0	2.104E+02	7.6E-04	1.9E-04
16	1.110E+02	216.0	1.797E+02	6.4E-04	2.1E-04
17	9.500E+01	216.0	1.535E+02	5.6E-04	2.4E-04
18	8.120E+01	216.0	1.305E+02	5.0E-04	2.8E-04
19	6.950E+01	217.0	1.110E+02	4.9E-04	3.2E-04
20	5.950E+01	218.0	9.453E+01	4.5E-04	3.4E-04
21	5.100E+01	219.0	8.056E+01	5.1E-04	3.6E-04
22	4.370E+01	220.0	6.872E+01	5.1E-04	3.6E-04
23	3.760E+01	222.0	5.867E+01	5.4E-04	3.4E-04
24	3.220E+01	223.0	5.014E+01	6.0E-04	3.2E-04
25	2.770E+01	224.0	4.288E+01	6.7E-04	3.0E-04
30	1.320E+01	234.0	1.322E+01	3.6E-04	2.0E-04
35	6.520E+00	245.0	6.519E+00	1.1E-04	9.2E-05
40	3.330E+00	258.0	3.330E+00	4.3E-05	4.1E-05
45	1.760E+00	270.0	1.757E+00	1.9E-05	1.3E-05
50	9.510E-01	276.0	9.512E-01	6.3E-06	4.3E-06
70	6.710E-02	218.0	6.706E-02	1.4E-07	8.6E-08
100	3.000E-04	210.0	5.000E-04	1.0E-09	4.3E-11

Table 1 (Contd). Model Atmospheres Used as a Basis of the Computation of Atmospheric Optical Properties

MIDLATITUDE WINTER					
Ht (km)	Pressure (mb)	Temp. (°K)	Density (g/m ³)	Water Vapor (g/m ³)	Ozone (g/m ³)
0	1.018E+03	272.2	1.301E+03	3.5E+00	6.0E-05
1	8.973E+02	268.7	1.162E+03	2.5E+00	5.4E-05
2	7.897E+02	265.2	1.037E+03	1.8E+00	4.9E-05
3	6.938E+02	261.7	9.230E+02	1.2E+00	4.9E-05
4	6.081E+02	255.7	8.282E+02	6.6E-01	4.9E-05
5	5.313E+02	249.7	7.411E+02	3.8E-01	5.8E-05
6	4.627E+02	243.7	6.614E+02	2.1E-01	6.4E-05
7	4.016E+02	237.7	5.886E+02	8.5E-02	7.7E-05
8	3.473E+02	231.7	5.222E+02	3.5E-02	9.0E-05
9	2.992E+02	225.7	4.619E+02	1.6E-02	1.2E-04
10	2.568E+02	219.7	4.072E+02	7.5E-03	1.6E-04
11	2.199E+02	219.2	3.496E+02	6.9E-03	2.1E-04
12	1.882E+02	218.7	2.999E+02	6.0E-03	2.6E-04
13	1.610E+02	218.2	2.572E+02	1.8E-03	3.0E-04
14	1.378E+02	217.7	2.206E+02	1.0E-03	3.2E-04
15	1.178E+02	217.2	1.890E+02	7.6E-04	3.4E-04
16	1.007E+02	216.7	1.620E+02	6.4E-04	3.6E-04
17	8.610E+01	216.2	1.388E+02	5.6E-04	3.9E-04
18	7.350E+01	215.7	1.188E+02	5.0E-04	4.1E-04
19	6.280E+01	215.2	1.017E+02	4.9E-04	4.3E-04
20	5.370E+01	215.2	8.690E+01	4.5E-04	4.5E-04
21	4.580E+01	215.2	7.421E+01	5.1E-04	4.3E-04
22	3.910E+01	215.2	6.338E+01	5.1E-04	4.3E-04
23	3.340E+01	215.2	5.415E+01	5.4E-04	3.9E-04
24	2.860E+01	215.2	4.624E+01	6.0E-04	3.6E-04
25	2.430E+01	215.2	3.950E+01	6.7E-04	3.4E-04
30	1.110E+01	217.4	1.783E+01	3.6E-04	1.9E-04
35	5.180E+00	227.8	7.924E+00	1.1E-04	9.2E-05
40	2.530E+00	243.2	3.625E+00	4.3E-05	4.1E-05
45	1.290E+00	258.5	1.741E+00	1.9E-05	1.3E-05
50	6.820E-01	265.7	8.954E-01	6.3E-06	4.3E-06
70	4.670E-02	230.7	7.051E-02	1.4E-07	8.6E-08
100	3.000E-04	210.2	5.000E-04	1.0E-09	4.3E-11

Table 1 (Contd). Model Atmospheres Used as a Basis of the Computation of Atmospheric Optical Properties

SUBARCTIC SUMMER					
Ht. (km)	Pressure (mb)	Temp. (°K)	Density (g/m ³)	Water Vapor (g/m ³)	Ozone (g/m ³)
0	1.310E+03	287.0	1.220E+03	9.1E+00	4.9E-05
1	8.960E+02	282.0	1.110E+03	6.0E+00	5.4E-05
2	7.929E+02	276.0	9.971E+02	4.2E+00	5.6E-05
3	7.000E+02	271.0	8.985E+02	2.7E+00	5.8E-05
4	6.160E+02	266.0	8.077E+02	1.7E+00	6.0E-05
5	5.410E+02	260.0	7.244E+02	1.0E+00	6.4E-05
6	4.730E+02	253.0	6.519E+02	5.4E-01	7.1E-05
7	4.130E+02	246.0	5.849E+02	2.9E-01	7.5E-05
8	3.590E+02	239.0	5.231E+02	1.3E-02	7.9E-05
9	3.107E+02	232.0	4.663E+02	4.2E-02	1.1E-04
10	2.677E+02	225.0	4.142E+02	1.5E-02	1.3E-04
11	2.300E+02	225.0	3.559E+02	9.4E-03	1.8E-04
12	1.977E+02	225.0	3.059E+02	6.0E-03	2.1E-04
13	1.700E+02	225.0	2.630E+02	1.8E-03	2.6E-04
14	1.460E+02	225.0	2.260E+02	1.0E-03	2.8E-04
15	1.250E+02	225.0	1.943E+02	7.6E-04	3.2E-04
16	1.080E+02	225.0	1.671E+02	6.4E-04	3.4E-04
17	9.280E+01	225.0	1.436E+02	5.6E-04	3.9E-04
18	7.980E+01	225.0	1.235E+02	5.0E-04	4.1E-04
19	6.860E+01	225.0	1.062E+02	4.9E-04	4.1E-04
20	5.890E+01	225.0	9.128E+01	4.5E-04	3.9E-04
21	5.070E+01	225.0	7.849E+01	5.1E-04	3.6E-04
22	4.360E+01	225.0	6.750E+01	5.1E-04	3.2E-04
23	3.750E+01	225.0	5.805E+01	5.4E-04	3.0E-04
24	3.227E+01	226.0	4.963E+01	6.0E-04	2.8E-04
25	2.780E+01	228.0	4.247E+01	6.7E-04	2.6E-04
30	1.340E+01	235.0	1.338E+01	3.6E-04	1.4E-04
35	6.610E+00	247.0	6.614E+00	1.1E-04	9.2E-05
40	3.400E+00	262.0	3.404E+00	4.3E-05	4.1E-05
45	1.810E+00	274.0	1.817E+00	1.9E-05	1.3E-05
50	9.870E-01	277.0	9.868E-01	6.3E-06	4.3E-06
70	7.070E-02	216.0	7.071E-02	1.4E-07	8.6E-08
100	3.000E-04	210.0	5.000E-04	1.0E-09	4.3E-11

Table 1 (Contd). Model Atmospheres Used as a Basis of the Computation of Atmospheric Optical Properties

SUBARCTIC WINTER					
Ht. (km)	Pressure (mb)	Temp. (°K)	Density (g/m ³)	Water Vapor (g/m ³)	Ozone (g/m ³)
0	1.013E+03	257.1	1.372E+03	1.2E+00	4.1E-05
1	8.878E+02	259.1	1.193E+03	1.2E+00	4.1E-05
2	7.775E+02	255.9	1.058E+03	9.4E-01	4.1E-05
3	6.798E+02	252.7	9.366E+02	6.8E-01	4.3E-05
4	5.932E+02	247.7	8.339E+02	4.1E-01	4.5E-05
5	5.158E+02	240.9	7.457E+02	2.0E-01	4.7E-05
6	4.467E+02	234.1	6.646E+02	9.8E-02	4.9E-05
7	3.853E+02	227.3	5.904E+02	5.4E-02	7.1E-05
8	3.308E+02	220.6	5.226E+02	1.1E-02	9.6E-05
9	2.829E+02	217.2	4.538E+02	8.4E-03	1.6E-04
10	2.418E+02	217.2	3.879E+02	5.5E-03	2.4E-04
11	2.067E+02	217.2	3.315E+02	3.8E-03	3.2E-04
12	1.766E+02	217.2	2.834E+02	2.6E-03	4.3E-04
13	1.510E+02	217.2	2.422E+02	1.3E-03	4.7E-04
14	1.291E+02	217.2	2.071E+02	1.0E-03	4.9E-04
15	1.103E+02	217.2	1.770E+02	7.6E-04	5.6E-04
16	9.431E+01	216.6	1.517E+02	6.4E-04	6.2E-04
17	8.058E+01	216.0	1.300E+02	5.6E-04	6.2E-04
18	6.882E+01	215.4	1.113E+02	5.0E-04	6.2E-04
19	5.875E+01	214.8	9.529E+01	4.9E-04	6.0E-04
20	5.014E+01	214.1	8.155E+01	4.5E-04	5.6E-04
21	4.277E+01	213.6	6.976E+01	5.1E-04	5.1E-04
22	3.647E+01	213.0	5.966E+01	5.1E-04	4.7E-04
23	3.109E+01	212.4	5.100E+01	5.4E-04	4.3E-04
24	2.649E+01	211.8	4.358E+01	6.0E-04	3.6E-04
25	2.256E+01	211.2	3.722E+01	6.7E-04	3.2E-04
30	1.020E+01	216.0	1.645E+01	3.6E-04	1.5E-04
35	4.701E+00	222.2	7.368E+00	1.1E-04	9.2E-05
40	2.243E+00	234.7	3.330E+00	4.3E-05	4.1E-05
45	1.113E+00	247.0	1.569E+00	1.9E-05	1.3E-05
50	5.719E-01	259.3	7.682E-01	6.3E-06	4.3E-06
70	4.016E-02	245.7	5.695E-02	1.4E-07	8.6E-08
100	3.000E-04	210.0	5.000E-04	1.0E-09	4.3E-11

Table 2. Concentrations of Uniformly Mixed Gases

Constituent	Molecular Wt.	ppm by Vol.	(cm-atm) _{STP} in vertical path from sea level	(cm-atm) _{STP} /km in horizontal path at sea level	gm cm ⁻² /mb	Ref.
Air	28.97	10 ⁶	8x10 ⁵	10 ⁵	1.02	*
CO ₂	44	330	264	33	5.11x10 ⁻⁴	†
N ₂ O	44	0.28	0.22	0.028	4.34x10 ⁻⁷	†
CO	28	0.075	0.06	0.0075	7.39x10 ⁻⁸	0
CH ₄	16	1.6	1.28	0.16	9.01x10 ⁻⁷	**
O ₂	32	2.095x10 ⁵	1.68x10 ⁵	2.095x10 ⁴	0.236	*

where L is the path length in km, and P₀ and T₀ refer to STP (P₀ = 1 atm and T₀ = 273K).

The sixth column provides values from which the amount of gas between any two pressure levels in the atmosphere can be determined by multiplication of the tabulated values by the pressure increment in millibars (Δp) times the secant of the zenith angle (see Appendix).

2.3 Aerosol Distributions

The two aerosol models (Table 3) describe a "clear" and a "hazy" atmosphere corresponding to a visibility of 23 and 5 km respectively at ground level. The aerosol size distribution function for both models is the same at all altitudes and is similar to the one suggested by Deirmendjian (1963) for continental haze (Figure 1), whereby the relationship between the number density [n(r)] and the particle radius is given by:

$$\frac{n(r)}{\Delta r} = C_1 \cdot r^{-4} \text{ for } 0.1 \mu\text{m} < r < 10 \mu\text{m}$$

$$\frac{n(r)}{\Delta r} = C_1 \cdot 10^4 \text{ for } 0.02 \mu\text{m} < r < 0.1 \mu\text{m} \quad (2)$$

$$\frac{n(r)}{\Delta r} = 0 \text{ for } r < 0.02 \text{ and } r > 10.0.$$

It differs from Deirmendjian's model "C" in that the large particle cutoff has been extended from 5 μm to 10 μm. This distribution function is normalized with

* Valley (1965), † Fink et al (1964), ‡ Birkland and Shaw (1959), ° Shaw (1968), ** Shaw (1969).

Table 3. Aerosol Models - Vertical Distributions for a "Clear" and "Hazy" Atmosphere

Altitude (km)	PARTICLE DENSITY N (PARTICLES PER cm ³)	
	23 km Visibility Clear	5 km Visibility Hazy
0	2.828E+03	1.378E+04
1	1.244E+03	5.030E+03
2	5.371E+02	1.844E+03
3	2.256E+02	6.731E+02
4	1.192E+02	2.453E+02
5	8.987E+01	8.987E+01
6	6.337E+01	6.337E+01
7	5.890E+01	5.890E+01
8	6.069E+01	6.069E+01
9	5.818E+01	5.818E+01
10	5.675E+01	5.675E+01
11	5.317E+01	5.317E+01
12	5.585E+01	5.585E+01
13	5.156E+01	5.156E+01
14	5.048E+01	5.048E+01
15	4.744E+01	4.744E+01
16	4.511E+01	4.511E+01
17	4.458E+01	4.458E+01
18	4.314E+01	4.314E+01
19	3.634E+01	3.634E+01
20	2.667E+01	2.667E+01
21	1.933E+01	1.933E+01
22	1.455E+01	1.455E+01
23	1.113E+01	1.113E+01
24	8.826E+00	8.826E+00
25	7.429E+00	7.429E+00
30	2.238E+00	2.238E+00
35	5.890E-01	5.890E-01
40	1.550E-01	1.550E-01
45	4.082E-02	4.082E-02
50	1.078E-02	1.078E-02
70	5.550E-05	5.550E-05
100	1.969E-08	1.969E-08

$\Delta r = 1 \mu\text{m}$ and $C_1 = 0.883 \times 10^{-3}$, (Figure 1), that is, the integral over the whole size range becomes 1. One need only multiply the normalized distribution function by the values of N in Table 3 in order to obtain the actual size distribution at any height in the atmosphere.

The refractive index for the aerosol particles has been assumed real (that is, no absorption) for $\lambda \leq 0.6 \mu\text{m}$. For $\lambda > 0.6 \mu\text{m}$ the imaginary part of the refractive index (that is, absorption) is assumed to increase linearly to a value of 0.1 for $\lambda \geq 2 \mu\text{m}$. This model for the refractive index is based on measurements by Volz (1957).

The total numbers (Table 3) of aerosol particles N per unit volume for the "clear" atmosphere have been adjusted so that the total extinction coefficient at

wavelength $\lambda = 0.55 \mu\text{m}$ becomes identical to the values used in the atmospheric attenuation model by Elterman (1968, 1970) at each altitude. This model corresponds to an atmospheric condition of approximately 23 km ground visibility. The "hazy" model is identical to the "clear" model for altitudes $H \geq 5 \text{ km}$. For $H < 5 \text{ km}$, the total number of aerosol particles increases exponentially to reach a value at ground level corresponding to a ground visibility of approximately 5 km.

3. FUNDAMENTALS OF ATMOSPHERIC TRANSMITTANCE

Transmittance of radiation in the atmosphere is complex owing to the dependence of scattering and absorption coefficients on a number of different physical properties of the atmosphere (Goody, 1964). In general, we have for the monochromatic transmittance of radiation along a path in the atmosphere

$$\tau = \exp(-\gamma \Delta L) \quad (3)$$

where γ is an attenuation coefficient and ΔL is the length of the path traversed by the radiation. The attenuation coefficient (γ) is given by

$$\gamma = \sigma + k \quad (4)$$

where σ is the scattering coefficient and k is the absorption coefficient. Both of these coefficients are defined in km^{-1} . Equation 3 is only strictly valid when applied to monochromatic radiation.

The scattering and absorption coefficients defined in Eq. (4) depend on both molecules and aerosols in the atmospheric path. If electromagnetic radiation is incident on a molecule or an aerosol, a portion of the radiation is absorbed and the rest is scattered in all directions. Thus, we must make the following definitions:

$$\sigma = \sigma_m + \sigma_a \quad (4a)$$

$$k = k_m + k_a \quad (4b)$$

where the subscripts, m and a, indicate molecule and aerosol respectively. We will endeavor in this report to provide quantitative information on all four of the quantities defined in Eqs. (4a) and (4b).

The molecular scattering coefficient depends only on the number density of molecules in the radiation path, whereas the molecular absorption coefficient is

a function of not only the amount of absorbing gas, but also the local temperature and pressure of the gas. The wavelength dependence of molecular (Rayleigh) scattering is very nearly $\sigma_m \sim \lambda^{-4}$. The variation of the molecular absorption coefficient with wavelength is much more complicated, being a highly oscillatory function of wavelength due to the presence of numerous molecular absorption band complexes. These band complexes result for the most part from minor atmospheric constituents. The responsible molecules are (in order of importance): H_2O , CO_2 , O_3 , N_2O , CO , O_2 , CH_4 , N_2 . All of these molecules except H_2O and O_3 are assumed to be uniformly mixed by volume.

The quantities σ_a and k_a depend on the number density and size distribution of aerosols as well as on their complex index of refraction. The amount of absorbed radiation and the distribution of scattered light can be derived theoretically for spherical particles (and some other simple forms) by a theory developed by Mie (1908). According to this theory the distribution of radiation with scattering angle ϕ can be expressed as:

$$i(\phi) = I_0 \cdot \frac{\lambda^2}{4\pi} \cdot \left[\frac{i_1(\phi) + i_2(\phi)}{2} \right] \left[\frac{\text{Watt}}{\text{cm}^2} \times \frac{\text{cm}^2}{\text{ster}} \right] \quad (5)$$

where i_1 and i_2 represent the two polarized components of the scattered radiation (van deHulst, 1957). They are functions of the ratio of particle size to wavelength, the particle refractive index, and the scattering angle ϕ . I_0 is the intensity of incident radiation. If there are N particles per unit scattering volume with a size distribution $n(r)$, replacing i_1 and i_2 by $\int i_{1,2}(r)n(r)dr$ will yield the integrated angular scattering intensity $I(\phi)$ from the unit volume of the particle cloud into one steradian.

The integral $\int_0^{4\pi} i(\phi) d\Omega$ gives the total amount of scattered radiation which is also equal to $I_0 \cdot \sigma_a$.

Eq. (5) can be written as:

$$I(\phi) = I_0 \cdot \sigma \cdot \mathcal{F}(\phi) \quad (6)$$

where $\mathcal{F}(\phi)$ is the normalized scattering function, and the integral

$\int_0^{4\pi} \mathcal{F}(\phi) d\Omega$ becomes 1.

Figure 26 shows $\mathcal{F}(\phi)$ for molecular scattering (wavelength independent) and aerosol scattering for two wavelengths for the aerosol model described in Section 2.3. An absorption coefficient, k_a , for aerosol particles can be defined in the same manner as the scattering coefficient, σ_a . The absorption and scattering coefficients due to aerosol distributions are usually smooth functions of wavelength.

The molecular absorption coefficient for a single spectral line can be given to good accuracy in the lower 50 km of the atmosphere by

$$k_m(\nu) = \frac{S\alpha}{\pi[(\nu - \nu_0)^2 + \alpha^2]} \quad (7)$$

where S is the line intensity, α is the line half-width, ν_0 is the frequency of the line center and ν is the frequency at which the absorption coefficient is required. See the Appendix for the relationship between ν and λ . The half-width depends on the pressure and temperature approximately as follows:

$$\alpha = \alpha_0 \frac{P}{P_0} \sqrt{\frac{T_0}{T}} \quad (8)$$

The line intensity also depends on the temperature through the Boltzmann factor and the partition function (Goody, 1964 and Penner, 1959). Above 50 km, Doppler broadening (Goody, 1964) should be considered.

Let us consider a plane parallel atmosphere and a frequency at which several lines belonging to one or more molecular constituents contribute to the absorption coefficient. The molecular absorption coefficient in any one of the (j) layers will be given by:

$$k_{mj} = \sum_i k_{mji} \quad (9)$$

where the (i) summation is over all molecular absorption lines due to all absorbing species which are close enough to the frequency ν to contribute significantly to the total molecular absorption coefficient defined in Eq. (9). Introducing the molecular scattering (σ_m), and the absorption (k_a) and scattering (σ_a) due to aerosols as defined in Eqs. (4a) and (4b), we have for the total attenuation coefficient in the (j)th layer:

$$\gamma_j = k_{mj} + \sigma_{mj} + k_{aj} + \sigma_{aj} \quad (10)$$

Thus, according to Eq. (3), the transmittance of an atmosphere having (j) layers is given by:

$$\tau(\nu) = \exp \left(- \sum_j \gamma_j \Delta L_j \right) \quad (11)$$

It should be noted from Eq. (11) that ΔL does not necessarily denote vertical distance. The problem of slant path transmittance is easily solved by writing $\Delta L_j = (\Delta z_j) \sec \theta$ where Δz_j represents the increment of vertical distance. In this case, Eq. (11) becomes

$$\tau_M(\nu) = [\tau(\nu)]^M \quad (12)$$

where $M = \sec \theta$ is the secant of the angle between the vertical and the direction of observation. Thus it becomes very easy to convert vertical transmittance values to slant path transmittance. As θ approaches 90° , the result becomes meaningless due to the plane parallel atmosphere assumption (see Section 7).

All of the above discussion is valid only at a single wavelength (or very narrow wavelength interval which is known to be small compared with the width of any absorption lines in the vicinity). A sufficiently narrow spectral interval for most purposes is 0.001 wavenumber (cm^{-1}). The process which so limits the validity of the above relations is molecular absorption. As noted above, $k_m(\nu)$ is a highly oscillatory function of frequency whereas $k_a(\nu)$, $\sigma_m(\nu)$, and $\sigma_a(\nu)$ are much more slowly varying functions.

When it is desired to calculate the atmospheric transmittance over a large spectral interval, it is necessary to average Eq. (11) or Eq. (12) over the desired spectral interval [see Eq. (14)]. When many absorption lines are present, this can be a particularly tedious job (even on a computer). Various techniques have been developed to treat this problem and are discussed in Section 5.

4. ATMOSPHERIC TRANSMITTANCE AT SELECTED FREQUENCIES

4.1 List of Laser Frequencies

It is necessary to limit the number of specific frequencies at which we quote atmospheric absorption and scattering coefficients. We have therefore chosen the list of specific laser wavelengths (Table 4) at which values of these coefficients are given in Table 5.

4.2 Scattering and Absorption Coefficients

Each atmospheric model defined in Section 2 has been used as a basis for calculating the absorption and scattering coefficients given in Table 5 for each laser wavelength. Numerical values for the coefficients were computed for the 0, 1, 2, etc., km levels and then logarithmically interpolated for each atmospheric layer. The aerosol attenuation coefficients given in Table 5, which correspond to

Table 4. Laser Wavelengths[†]

0.3371 μm	Nitrogen
0.4880 μm	Argon
0.5145 μm	Argon
0.6328 μm	Helium-Neon
0.6943 μm	Ruby
0.86 μm	Gallium Arsenide
1.06 μm	Neodymium in Glass
1.536 μm	Erbium in Glass
3.39225 μm	Helium Neon
10.591 μm	Carbon Dioxide
27.9 μm	Water Vapor
337 μm	Hydrogen Cyanide

the clear and hazy atmospheres defined in Section 2.3, are identical for all geographical and seasonal models. In Table 5, the four extinction coefficients are listed as a function of altitude for each model: k_m and σ_m are the molecular absorption and scattering coefficients, and k_a and σ_a are the aerosol absorption and scattering coefficients. If the total attenuation coefficient is required, the four coefficients can be summed:

$$\gamma = k_m + \sigma_m + k_a + \sigma_a. \quad (13)$$

4.3 Interpolation Procedures

In general, it is permissible to interpolate linearly with respect to wavelength between tabulated values in Table 5 except for molecular absorption coefficient (k_m). This is true because of the smooth variation of scattering coefficients and of aerosol absorption coefficients with wavelength, and the rapid spectral variations in molecular absorption coefficients. The tables have been constructed so that linear interpolation with respect to height is expected to give correct values to ± 8 percent. If a given atmospheric condition differs from one of the ten models of Section 2, larger errors may result.

Again it should be remembered that one should never attempt to interpolate with respect to wavelength between molecular absorption coefficient values (k_m) given in Table 5.

[†] These lasers may emit over a range of wavelengths. However, the computed values in Table 5 were derived for the specific wavelength values of Table 4.

Table 5. Values of Attenuation Coefficient/km as a Function of Altitude for Each Laser Wavelength and Each Atmospheric Model in Section 2 (k_{kr} = molecular absorption, σ_m = molecular scattering, k_a = aerosol absorption, σ_a = aerosol scattering)

Alt (km)	$\lambda = 0.337 \mu\text{m}$																						
	TROPICAL			MID-LATITUDE SUMMER			MID-LATITUDE WINTER			SUBARCTIC SUMMER			SUBARCTIC WINTER			CLEAR		HAZY					
	k_m (km^{-1})	σ_m (km^{-1})	k_a (km^{-1})	k_m (km^{-1})	σ_m (km^{-1})	k_a (km^{-1})	k_m (km^{-1})	σ_m (km^{-1})	k_a (km^{-1})	k_m (km^{-1})	σ_m (km^{-1})	k_a (km^{-1})	k_m (km^{-1})	σ_m (km^{-1})	k_a (km^{-1})	k_m (km^{-1})	σ_m (km^{-1})	k_a (km^{-1})	k_m (km^{-1})	σ_m (km^{-1})	k_a (km^{-1})		
0	2.34E-04	8.48E-02	2.52E-04	8.64E-02	2.52E-04	9.34E-02	2.07E-04	8.83E-02	1.71E-04	9.88E-02	2.35E-01	2.35E-01	2.35E-01	2.35E-01	2.35E-01	2.35E-01	2.35E-01	2.35E-01	2.35E-01	2.35E-01	2.35E-01	2.35E-01	1.14E-00
0-1	2.32E-04	8.07E-02	2.52E-04	8.25E-02	2.52E-04	8.73E-02	2.15E-04	8.40E-02	1.71E-04	9.44E-02	1.56E-01	1.56E-01	1.56E-01	1.56E-01	1.56E-01	1.56E-01	1.56E-01	1.56E-01	1.56E-01	1.56E-01	1.56E-01	1.56E-01	6.92E-01
1-2	2.27E-04	7.54E-02	2.52E-04	7.47E-02	2.16E-04	7.94E-02	2.10E-04	7.59E-02	1.71E-04	8.24E-02	6.39E-02	6.39E-02	6.39E-02	6.39E-02	6.39E-02	6.39E-02	6.39E-02	6.39E-02	6.39E-02	6.39E-02	6.39E-02	6.39E-02	2.53E-01
2-3	2.18E-04	6.88E-02	2.57E-04	6.76E-02	2.07E-04	7.23E-02	2.09E-04	6.85E-02	1.76E-04	8.11E-02	2.89E-02	2.89E-02	2.89E-02	2.89E-02	2.89E-02	2.89E-02	2.89E-02	2.89E-02	2.89E-02	2.89E-02	2.89E-02	2.89E-02	9.25E-02
3-4	1.93E-04	6.03E-02	2.65E-04	6.12E-02	2.03E-04	5.32E-02	2.48E-04	6.15E-02	1.85E-04	7.19E-02	1.36E-02	1.36E-02	1.36E-02	1.36E-02	1.36E-02	1.36E-02	1.36E-02	1.36E-02	1.36E-02	1.36E-02	1.36E-02	1.36E-02	3.37E-02
4-5	1.84E-04	5.48E-02	2.74E-04	5.53E-02	2.25E-04	5.66E-02	2.31E-04	5.52E-02	1.94E-04	6.38E-02	8.60E-03	8.60E-03	8.60E-03	8.60E-03	8.60E-03	8.60E-03	8.60E-03	8.60E-03	8.60E-03	8.60E-03	8.60E-03	8.60E-03	1.23E-02
5-6	1.75E-04	4.96E-02	2.83E-04	4.96E-02	2.83E-04	5.06E-02	2.84E-04	4.96E-02	2.03E-04	5.08E-02	6.27E-03	6.27E-03	6.27E-03	6.27E-03	6.27E-03	6.27E-03	6.27E-03	6.27E-03	6.27E-03	6.27E-03	6.27E-03	6.27E-03	6.27E-03
6-7	1.66E-04	4.47E-02	2.92E-04	4.47E-02	2.92E-04	4.51E-02	2.96E-04	4.45E-02	2.52E-04	4.52E-02	5.07E-03	5.07E-03	5.07E-03	5.07E-03	5.07E-03	5.07E-03	5.07E-03	5.07E-03	5.07E-03	5.07E-03	5.07E-03	5.07E-03	5.07E-03
7-8	1.62E-04	4.02E-02	3.23E-04	4.01E-02	3.11E-04	4.01E-02	3.24E-04	3.99E-02	3.02E-04	4.01E-02	4.87E-03	4.87E-03	4.87E-03	4.87E-03	4.87E-03	4.87E-03	4.87E-03	4.87E-03	4.87E-03	4.87E-03	4.87E-03	4.87E-03	4.87E-03
8-9	1.62E-04	3.61E-02	3.44E-04	3.59E-02	3.59E-04	4.30E-02	3.87E-04	3.57E-02	3.27E-04	3.52E-02	4.94E-03	4.94E-03	4.94E-03	4.94E-03	4.94E-03	4.94E-03	4.94E-03	4.94E-03	4.94E-03	4.94E-03	4.94E-03	4.94E-03	4.94E-03
9-10	1.62E-04	3.23E-02	3.67E-04	3.67E-02	3.67E-04	3.14E-02	4.95E-04	3.17E-02	3.18E-04	3.03E-02	4.77E-03	4.77E-03	4.77E-03	4.77E-03	4.77E-03	4.77E-03	4.77E-03	4.77E-03	4.77E-03	4.77E-03	4.77E-03	4.77E-03	4.77E-03
10-11	1.65E-04	2.88E-02	4.14E-04	2.85E-02	2.85E-04	2.73E-02	5.44E-04	2.78E-02	1.17E-03	2.58E-02	4.56E-03	4.56E-03	4.56E-03	4.56E-03	4.56E-03	4.56E-03	4.56E-03	4.56E-03	4.56E-03	4.56E-03	4.56E-03	4.56E-03	4.56E-03
11-12	1.75E-04	2.56E-02	4.86E-04	2.53E-02	2.53E-04	2.53E-02	6.33E-04	2.53E-02	3.38E-04	2.58E-02	4.53E-03	4.53E-03	4.53E-03	4.53E-03	4.53E-03	4.53E-03	4.53E-03	4.53E-03	4.53E-03	4.53E-03	4.53E-03	4.53E-03	4.53E-03
12-13	1.82E-04	2.28E-02	5.70E-04	2.45E-02	2.45E-04	1.65E-02	8.89E-04	2.05E-02	1.83E-03	1.89E-02	4.46E-03	4.46E-03	4.46E-03	4.46E-03	4.46E-03	4.46E-03	4.46E-03	4.46E-03	4.46E-03	4.46E-03	4.46E-03	4.46E-03	4.46E-03
13-14	1.91E-04	1.76E-02	7.74E-04	1.86E-02	1.86E-04	1.42E-02	1.25E-03	1.76E-02	2.03E-03	1.62E-02	4.24E-03	4.24E-03	4.24E-03	4.24E-03	4.24E-03	4.24E-03	4.24E-03	4.24E-03	4.24E-03	4.24E-03	4.24E-03	4.24E-03	4.24E-03
14-15	1.96E-04	1.54E-02	8.54E-04	1.66E-02	1.66E-04	1.37E-02	1.48E-03	1.51E-02	2.22E-03	1.38E-02	3.84E-03	3.84E-03	3.84E-03	3.84E-03	3.84E-03	3.84E-03	3.84E-03	3.84E-03	3.84E-03	3.84E-03	3.84E-03	3.84E-03	3.84E-03
15-16	2.43E-04	1.33E-02	9.56E-04	1.22E-02	1.22E-04	1.64E-02	1.08E-03	1.12E-02	2.58E-03	1.01E-02	3.72E-03	3.72E-03	3.72E-03	3.72E-03	3.72E-03	3.72E-03	3.72E-03	3.72E-03	3.72E-03	3.72E-03	3.72E-03	3.72E-03	3.72E-03
16-17	3.33E-04	1.10E-02	1.10E-03	1.04E-02	1.04E-04	1.73E-02	9.29E-03	1.65E-03	8.69E-03	8.69E-03	3.64E-03	3.64E-03	3.64E-03	3.64E-03	3.64E-03	3.64E-03	3.64E-03	3.64E-03	3.64E-03	3.64E-03	3.64E-03	3.64E-03	3.64E-03
17-18	4.86E-04	9.12E-03	1.25E-03	8.79E-03	1.84E-03	1.84E-03	7.97E-03	1.71E-03	8.27E-03	7.44E-03	3.29E-03	3.29E-03	3.29E-03	3.29E-03	3.29E-03	3.29E-03	3.29E-03	3.29E-03	3.29E-03	3.29E-03	3.29E-03	3.29E-03	3.29E-03
18-19	6.98E-04	7.57E-03	1.40E-03	7.46E-03	1.84E-03	1.84E-03	6.82E-03	1.65E-03	7.11E-03	6.37E-03	2.59E-03	2.59E-03	2.59E-03	2.59E-03	2.59E-03	2.59E-03	2.59E-03	2.59E-03	2.59E-03	2.59E-03	2.59E-03	2.59E-03	2.59E-03
19-20	8.89E-04	6.32E-03	1.49E-03	6.38E-03	1.86E-03	1.86E-03	5.81E-03	1.58E-03	6.11E-03	5.45E-03	1.89E-03	1.89E-03	1.89E-03	1.89E-03	1.89E-03	1.89E-03	1.89E-03	1.89E-03	1.89E-03	1.89E-03	1.89E-03	1.89E-03	1.89E-03
20-21	1.06E-03	5.28E-03	1.56E-03	5.45E-03	1.80E-03	1.80E-03	4.95E-03	1.45E-03	5.26E-03	4.68E-03	1.39E-03	1.39E-03	1.39E-03	1.39E-03	1.39E-03	1.39E-03	1.39E-03	1.39E-03	1.39E-03	1.39E-03	1.39E-03	1.39E-03	1.39E-03
21-22	1.23E-03	4.44E-03	1.47E-03	4.63E-03	1.71E-03	1.71E-03	4.24E-03	1.34E-03	4.52E-03	3.98E-03	1.06E-03	1.06E-03	1.06E-03	1.06E-03	1.06E-03	1.06E-03	1.06E-03	1.06E-03	1.06E-03	1.06E-03	1.06E-03	1.06E-03	1.06E-03
22-23	1.40E-03	3.76E-03	1.40E-03	3.95E-03	1.61E-03	1.61E-03	3.62E-03	1.23E-03	3.88E-03	3.41E-03	8.23E-04	8.23E-04	8.23E-04	8.23E-04	8.23E-04	8.23E-04	8.23E-04	8.23E-04	8.23E-04	8.23E-04	8.23E-04	8.23E-04	8.23E-04
23-24	1.44E-03	3.18E-03	1.33E-03	3.38E-03	1.48E-03	1.48E-03	3.09E-03	1.12E-03	3.32E-03	2.91E-03	6.73E-04	6.73E-04	6.73E-04	6.73E-04	6.73E-04	6.73E-04	6.73E-04	6.73E-04	6.73E-04	6.73E-04	6.73E-04	6.73E-04	6.73E-04
24-25	1.24E-03	2.12E-03	1.06E-03	2.28E-03	1.10E-03	1.10E-03	2.18E-03	8.24E-04	2.23E-03	1.93E-03	5.33E-04	5.33E-04	5.33E-04	5.33E-04	5.33E-04	5.33E-04	5.33E-04	5.33E-04	5.33E-04	5.33E-04	5.33E-04	5.33E-04	5.33E-04
25-30	9.98E-04	3.72E-04	6.13E-04	1.05E-03	5.84E-04	1.04E-03	4.86E-04	4.99E-04	1.63E-03	1.56E-04	4.66E-04	4.66E-04	4.66E-04	4.66E-04	4.66E-04	4.66E-04	4.66E-04	4.66E-04	4.66E-04	4.66E-04	4.66E-04	4.66E-04	4.66E-04
30-35	2.78E-04	4.63E-04	4.63E-04	5.09E-04	2.79E-04	4.16E-04	2.79E-04	4.99E-04	4.99E-04	4.99E-04	3.98E-04	3.98E-04	3.98E-04	3.98E-04	3.98E-04	3.98E-04	3.98E-04	3.98E-04	3.98E-04	3.98E-04	3.98E-04	3.98E-04	3.98E-04
35-40	1.13E-04	2.28E-04	1.13E-04	2.46E-04	1.13E-04	1.94E-04	1.13E-04	2.46E-04	1.13E-04	1.76E-04	9.53E-05	9.53E-05	9.53E-05	9.53E-05	9.53E-05	9.53E-05	9.53E-05	9.53E-05	9.53E-05	9.53E-05	9.53E-05	9.53E-05	9.53E-05
40-45	3.60E-05	1.16E-04	3.60E-05	1.26E-04	3.60E-05	3.48E-05	3.60E-05	1.26E-04	3.48E-05	3.42E-05	1.74E-06	1.74E-06	1.74E-06	1.74E-06	1.74E-06	1.74E-06	1.74E-06	1.74E-06	1.74E-06	1.74E-06	1.74E-06	1.74E-06	1.74E-06
45-50	9.00E-06	4.31E-05	9.00E-06	4.75E-05	9.00E-06	3.48E-06	9.00E-06	4.75E-05	3.42E-06	2.97E-05	1.00E-06	1.00E-06	1.00E-06	1.00E-06	1.00E-06	1.00E-06	1.00E-06	1.00E-06	1.00E-06	1.00E-06	1.00E-06	1.00E-06	1.00E-06
50-70	<E-06	3.35E-06	<E-06	3.82E-06	<E-06	2.56E-06	<E-06	3.82E-06	<E-06	2.07E-06	<E-06	<E-06	<E-06	<E-06	<E-06	<E-06	<E-06	<E-06	<E-06	<E-06	<E-06	<E-06	<E-06
70-100	<E-06	<E-06	<E-06	<E-06	<E-06	<E-06	<E-06	<E-06	<E-06	<E-06	<E-06	<E-06	<E-06	<E-06	<E-06	<E-06	<E-06	<E-06	<E-06	<E-06	<E-06	<E-06	<E-06

NOT REPRODUCIBLE

Table 5 (Contd). Values of Attenuation Coefficient/km as a Function of Altitude for Each Laser Wavelength and Each Atmospheric Model in Section 2 (k_m = molecular absorption, σ_m = molecular scattering, k_a = aerosol absorption, σ_a = aerosol scattering)

H(km)	TROPICAL		MIDLATITUDE SUMMER		MIDLATITUDE WINTER		SUBARCTIC SUMMER		SUBARCTIC WINTER		CLEAP		AEROSOL		HAZY
	k_m (km^{-1})	σ_m (km^{-1})	k_m (km^{-1})	σ_m (km^{-1})	k_m (km^{-1})	σ_m (km^{-1})	k_m (km^{-1})	σ_m (km^{-1})	k_m (km^{-1})	σ_m (km^{-1})	k_m (km^{-1})	σ_m (km^{-1})	k_a (km^{-1})	σ_a (km^{-1})	
0	<E-05	1.87E-12	<E-06	1.86E-02	<E-06	2.02E-02	<E-06	1.60E-02	<E-06	<E-06	2.13E-02	<E-06	1.76E-01	8.51E-01	
0-1		1.74E-02		1.77E-02		1.91E-02		1.80E-02			1.99E-02		1.17E-01	5.15E-01	
1-2		1.58E-02		1.60E-02		1.70E-02		1.63E-02			1.74E-02		5.03E-02	1.96E-01	
2-3		1.43E-02		1.45E-02		1.52E-02		1.47E-02			1.55E-02		2.17E-02	6.94E-02	
3-4		1.30E-02		1.31E-02		1.36E-02		1.32E-02			1.37E-02		1.02E-02	2.53E-02	
4-5		1.18E-02		1.18E-02		1.22E-02		1.19E-02			1.22E-02		6.45E-03	9.23E-03	
5-6		1.06E-02		1.06E-02		1.09E-02		1.07E-02			1.08E-02		4.70E-03	4.70E-03	
6-7		9.56E-03		9.54E-03		9.88E-03		9.57E-03			9.72E-03		3.80E-03	3.80E-03	
7-8		8.61E-03		8.55E-03		8.60E-03		8.58E-03			8.62E-03		3.72E-03	3.72E-03	
8-9		7.72E-03		7.65E-03		7.62E-03		7.68E-03			7.58E-03		3.70E-03	3.70E-03	
9-10		6.89E-03		6.89E-03		6.73E-03		6.83E-03			6.52E-03		3.58E-03	3.58E-03	
10-11		6.18E-03		6.08E-03		5.88E-03		5.97E-03			5.37E-03		3.42E-03	3.42E-03	
11-12		5.48E-03		5.40E-03		5.03E-03		5.13E-03			4.76E-03		3.39E-03	3.39E-03	
12-13		4.83E-03		4.77E-03		4.31E-03		4.41E-03			4.07E-03		3.34E-03	3.34E-03	
13-14		4.27E-03		4.15E-03		3.70E-03		3.79E-03			3.48E-03		3.18E-03	3.18E-03	
14-15		3.75E-03		3.53E-03		3.17E-03		3.23E-03			2.97E-03		3.05E-03	3.05E-03	
15-16		3.27E-03		3.01E-03		2.72E-03		2.79E-03			2.54E-03		2.88E-03	2.88E-03	
16-17		2.82E-03		2.57E-03		2.33E-03		2.41E-03			2.18E-03		2.19E-03	2.19E-03	
17-18		2.37E-03		2.20E-03		1.99E-03		2.07E-03			1.87E-03		2.73E-03	2.73E-03	
18-19		1.93E-03		1.88E-03		1.71E-03		1.78E-03			1.60E-03		2.47E-03	2.47E-03	
19-20		1.62E-03		1.60E-03		1.46E-03		1.52E-03			1.37E-03		1.94E-03	1.94E-03	
20-21		1.35E-03		1.33E-03		1.25E-03		1.31E-03			1.17E-03		1.41E-03	1.41E-03	
21-22		1.12E-03		1.16E-03		1.09E-03		1.13E-03			1.00E-03		1.04E-03	1.04E-03	
22-23		9.48E-04		9.24E-04		9.06E-04		9.72E-04			8.57E-04		7.53E-04	7.53E-04	
23-24		8.04E-04		7.66E-04		7.77E-04		7.35E-04			7.32E-04		6.17E-04	6.17E-04	
24-25		6.83E-04		7.23E-04		6.63E-04		7.14E-04			6.26E-04		5.04E-04	5.04E-04	
25-30		4.56E-04		4.86E-04		4.42E-04		4.83E-04			4.16E-04		2.54E-04	2.54E-04	
30-35		2.08E-04		2.24E-04		1.88E-04		2.26E-04			1.84E-04		1.15E-05	1.15E-05	
35-40		8.90E-05		1.07E-04		8.94E-05		1.07E-04			8.28E-05		1.88E-05	1.88E-05	
40-45		4.86E-05		5.24E-05		4.15E-05		5.28E-05			4.79E-05		4.85E-06	4.85E-06	
45-50		2.47E-05		2.69E-05		2.04E-05		2.74E-05			1.81E-05		1.31E-05	1.31E-05	
50-70		8.24E-06		1.01E-05		7.47E-06		1.03E-05			6.39E-06		<E-06	<E-06	
70-100		<E-06		<E-06		<E-06		<E-06			<E-06		<E-06	<E-06	

$\lambda=0.4880\mu\text{m}$

Table 5 (Contd). Values of Attenuation Coefficient/km as a Function of Altitude for Each Laser Wavelength and Each Atmospheric Model in Section 2 (k_m = molecular absorption, σ_m = molecular scattering, k_a = aerosol absorption, σ_a = aerosol scattering)

H(km)	$\lambda=0.5145\mu m$													
	TROPICAL		MID-LATITUDE SUMMER		MID-LATITUDE WINTER		SUB-ARCTIC SUMMER		SUB-ARCTIC WINTER		CLEAR AEROSOL		HAZY AEROSOL	
	k_m (km^{-1})	σ_m (km^{-1})	k_m (km^{-1})	σ_m (km^{-1})	k_m (km^{-1})	σ_m (km^{-1})	k_m (km^{-1})	σ_m (km^{-1})	k_m (km^{-1})	σ_m (km^{-1})	k_m (km^{-1})	σ_m (km^{-1})	k_a (km^{-1})	σ_a (km^{-1})
0	<E-06	1.47E-02	1.50E-02	1.63E-02	1.63E-02	1.53E-02	<E-06	1.53E-02	1.71E-02	1.71E-02	<E-06	1.68E-01	<E-06	8.26E-01
0-1		1.40E-02	1.43E-02	1.54E-02	1.54E-02	1.46E-02		1.46E-02	1.60E-02	1.60E-02		1.62E-01		4.96E-01
1-2		1.28E-02	1.29E-02	1.37E-02	1.37E-02	1.32E-02		1.32E-02	1.41E-02	1.41E-02		1.41E-01		1.81E-01
2-3		1.15E-02	1.16E-02	1.22E-02	1.22E-02	1.19E-02		1.19E-02	1.25E-02	1.25E-02		2.07E-02		6.53E-02
3-4		1.04E-02	1.05E-02	1.09E-02	1.09E-02	1.06E-02		1.06E-02	1.10E-02	1.10E-02		9.76E-03		2.42E-02
4-5		9.48E-03	9.48E-03	8.79E-03	8.79E-03	9.51E-03		9.51E-03	9.86E-03	9.86E-03		6.16E-03		8.88E-03
5-6		8.55E-03	8.56E-02	8.75E-03	8.75E-03	8.58E-03		8.58E-03	8.80E-03	8.80E-03		4.19E-03		4.45E-03
6-7		7.70E-03	7.78E-02	7.80E-03	7.80E-03	7.80E-03		7.80E-03	7.83E-03	7.83E-03		3.64E-03		3.56E-03
7-8		6.94E-03	6.89E-02	6.89E-03	6.89E-03	6.91E-03		6.91E-03	6.94E-03	6.94E-03		3.56E-03		3.56E-03
8-9		6.22E-03	6.16E-03	6.16E-03	6.16E-03	6.14E-03		6.14E-03	6.09E-03	6.09E-03		3.54E-03		3.54E-03
9-10		5.55E-03	5.50E-03	5.50E-03	5.50E-03	5.50E-03		5.50E-03	5.25E-03	5.25E-03		3.42E-03		3.42E-03
10-11		4.96E-03	4.96E-03	4.96E-03	4.96E-03	4.80E-03		4.80E-03	4.72E-03	4.72E-03		3.27E-03		3.27E-03
11-12		4.40E-03	4.35E-03	4.35E-03	4.35E-03	4.05E-03		4.05E-03	4.05E-03	4.05E-03		3.24E-03		3.24E-03
12-13		3.89E-03	3.85E-03	3.85E-03	3.85E-03	3.47E-03		3.47E-03	3.47E-03	3.47E-03		3.19E-03		3.19E-03
13-14		3.44E-03	3.34E-03	3.34E-03	3.34E-03	2.98E-03		2.98E-03	2.98E-03	2.98E-03		3.04E-03		3.04E-03
14-15		3.02E-03	2.85E-03	2.85E-03	2.85E-03	2.55E-03		2.55E-03	2.55E-03	2.55E-03		2.91E-03		2.91E-03
15-16		2.63E-03	2.42E-03	2.42E-03	2.42E-03	2.19E-03		2.19E-03	2.19E-03	2.19E-03		2.75E-03		2.75E-03
16-17		2.27E-03	2.07E-03	2.07E-03	2.07E-03	1.88E-03		1.88E-03	1.88E-03	1.88E-03		2.67E-03		2.67E-03
17-18		1.91E-03	1.77E-03	1.77E-03	1.77E-03	1.67E-03		1.67E-03	1.67E-03	1.67E-03		2.61E-03		2.61E-03
18-19		1.57E-03	1.51E-03	1.51E-03	1.51E-03	1.38E-03		1.38E-03	1.38E-03	1.38E-03		2.36E-03		2.36E-03
19-20		1.31E-03	1.29E-03	1.29E-03	1.29E-03	1.18E-03		1.18E-03	1.18E-03	1.18E-03		1.85E-03		1.85E-03
20-21		1.09E-03	1.10E-02	1.10E-02	1.10E-02	1.01E-03		1.01E-03	1.06E-03	1.06E-03		1.35E-03		1.35E-03
21-22		9.08E-04	9.38E-04	9.38E-04	9.38E-04	8.57E-04		8.57E-04	9.11E-04	9.11E-04		9.98E-04		9.98E-04
22-23		6.48E-04	6.82E-04	6.82E-04	6.82E-04	6.26E-04		6.26E-04	7.32E-04	7.32E-04		7.58E-04		7.58E-04
23-24		5.50E-04	5.83E-04	5.83E-04	5.83E-04	5.34E-04		5.34E-04	6.72E-04	6.72E-04		5.90E-04		5.90E-04
24-25		3.67E-04	3.91E-04	3.91E-04	3.91E-04	3.56E-04		3.56E-04	3.89E-04	3.89E-04		4.82E-04		4.82E-04
25-30		1.68E-04	1.80E-04	1.80E-04	1.80E-04	1.60E-04		1.60E-04	1.82E-04	1.82E-04		2.43E-04		2.43E-04
35-40		7.97E-05	8.58E-05	8.58E-05	8.58E-05	7.20E-05		7.20E-05	8.64E-05	8.64E-05		1.00E-05		1.00E-05
40-45		3.91E-05	4.22E-05	4.22E-05	4.22E-05	3.35E-05		3.35E-05	4.26E-05	4.26E-05		3.06E-05		3.06E-05
45-50		1.99E-05	2.17E-05	2.17E-05	2.17E-05	1.64E-05		1.64E-05	2.21E-05	2.21E-05		1.46E-05		1.46E-05
50-70		7.45E-06	8.15E-06	8.15E-06	8.15E-06	6.01E-06		6.01E-06	8.45E-06	8.45E-06		5.15E-06		5.15E-06
70-100		<E-06	<E-06	<E-06	<E-06	<E-06		<E-06	<E-06	<E-06		<E-06		<E-06

NOT REPRODUCIBLE

Table 5 (Contd). Values of Attenuation Coefficient/km as a Function of Altitude for Each Laser Wavelength and Each Atmospheric Model in Section 2 (k_m = molecular absorption, σ_m = molecular scattering, k_a = aerosol absorption, σ_a = aerosol scattering)

PH(Alt)	TROPICAL		MIDLATITUDE SUMMER		MIDLATITUDE WINTER		SUBARCTIC SUMMER		SUBARCTIC WINTER		CLEAR AEROSOL		HAZY AEROSOL	
	k_m (km ⁻¹)	σ_m (km ⁻¹)	k_m (km ⁻¹)	σ_m (km ⁻¹)	k_m (km ⁻¹)	σ_m (km ⁻¹)	k_m (km ⁻¹)	σ_m (km ⁻¹)	k_m (km ⁻¹)	σ_m (km ⁻¹)	k_a (km ⁻¹)	σ_a (km ⁻¹)	k_a (km ⁻¹)	σ_a (km ⁻¹)
0	<E-06	6.31E-03	<E-06	6.44E-03	<E-06	6.79E-03	<E-06	6.58E-03	7.37E-03	7.37E-03	1.34E-01	1.53E-02	1.53E-02	5.63E-01
0-1		5.03E-03	6.13E-03	6.62E-03	6.62E-03	6.62E-03	6.29E-03	6.29E-03	6.88E-03	6.88E-03	2.02E-02	9.03E-02	9.25E-03	4.01E-01
1-2		5.49E-03	5.54E-03	5.61E-03	5.61E-03	5.61E-03	5.66E-03	5.66E-03	6.04E-03	6.04E-03	9.09E-04	3.93E-02	3.79E-03	1.47E-01
2-3		4.97E-03	5.01E-03	5.26E-03	5.26E-03	5.26E-03	5.10E-03	5.10E-03	5.36E-03	5.36E-03	3.87E-04	1.67E-02	1.24E-03	5.36E-02
3-4		4.49E-03	4.53E-03	4.70E-03	4.70E-03	4.70E-03	4.58E-03	4.58E-03	4.75E-03	4.75E-03	1.82E-04	7.89E-03	4.52E-04	1.96E-02
4-5		4.07E-03	4.08E-03	4.21E-03	4.21E-03	4.21E-03	4.11E-03	4.11E-03	4.24E-03	4.24E-03	1.15E-04	4.98E-03	1.55E-04	7.14E-03
5-6		3.68E-03	3.68E-03	3.76E-03	3.76E-03	3.76E-03	3.69E-03	3.69E-03	3.79E-03	3.79E-03	6.79E-05	3.63E-03	3.63E-03	2.94E-03
6-7		3.31E-03	3.31E-03	3.35E-03	3.35E-03	3.35E-03	3.32E-03	3.32E-03	3.37E-03	3.37E-03	5.79E-05	2.86E-03	2.86E-03	2.86E-03
7-8		2.89E-03	2.89E-03	2.86E-03	2.86E-03	2.86E-03	2.87E-03	2.87E-03	2.92E-03	2.92E-03	6.61E-05	2.88E-03	2.88E-03	2.88E-03
8-9		2.67E-03	2.67E-03	2.66E-03	2.66E-03	2.66E-03	2.65E-03	2.65E-03	2.69E-03	2.69E-03	6.61E-05	2.86E-03	2.86E-03	2.86E-03
9-10		2.39E-03	2.39E-03	2.37E-03	2.37E-03	2.37E-03	2.36E-03	2.36E-03	2.43E-03	2.43E-03	6.61E-05	2.86E-03	2.86E-03	2.86E-03
10-11		2.13E-03	2.13E-03	2.12E-03	2.12E-03	2.12E-03	2.07E-03	2.07E-03	2.19E-03	2.19E-03	6.11E-05	2.64E-03	2.64E-03	2.64E-03
11-12		1.89E-03	1.87E-03	1.87E-03	1.87E-03	1.87E-03	1.78E-03	1.78E-03	1.93E-03	1.93E-03	6.06E-05	2.62E-03	2.62E-03	2.62E-03
12-13		1.67E-03	1.66E-03	1.66E-03	1.66E-03	1.66E-03	1.53E-03	1.53E-03	1.61E-03	1.61E-03	5.97E-05	2.58E-03	2.58E-03	2.58E-03
13-14		1.42E-03	1.42E-03	1.42E-03	1.42E-03	1.42E-03	1.31E-03	1.31E-03	1.21E-03	1.21E-03	5.57E-05	2.45E-03	2.45E-03	2.45E-03
14-15		1.30E-03	1.23E-03	1.23E-03	1.23E-03	1.23E-03	1.13E-03	1.13E-03	1.02E-03	1.02E-03	5.44E-05	2.35E-03	2.35E-03	2.35E-03
15-16		1.13E-03	1.04E-03	1.04E-03	1.04E-03	1.04E-03	9.68E-04	9.68E-04	8.82E-04	8.82E-04	5.14E-05	2.23E-03	2.23E-03	2.23E-03
16-17		8.76E-04	8.32E-04	8.32E-04	8.32E-04	8.32E-04	8.34E-04	8.34E-04	7.56E-04	7.56E-04	4.95E-05	2.16E-03	2.16E-03	2.16E-03
17-18		8.10E-04	7.63E-04	7.63E-04	7.63E-04	7.63E-04	7.17E-04	7.17E-04	6.47E-04	6.47E-04	4.98E-05	2.11E-03	2.11E-03	2.11E-03
18-19		6.77E-04	6.51E-04	6.51E-04	6.51E-04	6.51E-04	6.17E-04	6.17E-04	5.54E-04	5.54E-04	4.40E-05	1.91E-03	1.91E-03	1.91E-03
19-20		5.62E-04	5.55E-04	5.55E-04	5.55E-04	5.55E-04	5.30E-04	5.30E-04	4.78E-04	4.78E-04	3.49E-05	1.50E-03	1.50E-03	1.50E-03
20-21		3.91E-04	4.03E-04	4.03E-04	4.03E-04	4.03E-04	3.82E-04	3.82E-04	3.47E-04	3.47E-04	1.87E-05	8.07E-04	8.07E-04	8.07E-04
21-22		3.28E-04	3.44E-04	3.44E-04	3.44E-04	3.44E-04	3.37E-04	3.37E-04	2.97E-04	2.97E-04	1.42E-05	6.13E-04	6.13E-04	6.13E-04
22-23		2.79E-04	2.89E-04	2.89E-04	2.89E-04	2.89E-04	2.88E-04	2.88E-04	2.54E-04	2.54E-04	4.77E-04	1.10E-03	1.10E-03	1.10E-03
23-24		2.37E-04	2.51E-04	2.51E-04	2.51E-04	2.51E-04	2.48E-04	2.48E-04	2.17E-04	2.17E-04	9.00E-06	3.60E-04	3.60E-04	3.60E-04
24-25		1.98E-04	1.68E-04	1.68E-04	1.68E-04	1.68E-04	1.67E-04	1.67E-04	1.44E-04	1.44E-04	4.53E-06	1.95E-04	1.95E-04	1.95E-04
25-30		7.22E-05	7.16E-05	7.16E-05	7.16E-05	7.16E-05	7.83E-05	7.83E-05	6.39E-05	6.39E-05	1.28E-06	5.52E-05	5.52E-05	5.52E-05
30-35		3.43E-05	3.69E-05	3.69E-05	3.69E-05	3.69E-05	3.72E-05	3.72E-05	2.87E-05	2.87E-05	<E-06	1.45E-05	1.45E-05	1.45E-05
35-40		1.68E-05	1.82E-05	1.82E-05	1.82E-05	1.82E-05	1.82E-05	1.82E-05	1.39E-05	1.39E-05	3.83E-06	3.83E-06	3.83E-06	3.83E-06
45-50		3.57E-06	9.31E-06	9.31E-06	9.31E-06	9.31E-06	9.51E-06	9.51E-06	6.27E-06	6.27E-06	1.01E-06	1.01E-06	1.01E-06	1.01E-06
50-70		3.20E-06	3.51E-06	3.51E-06	3.51E-06	3.51E-06	2.59E-06	2.59E-06	2.23E-06	2.23E-06	<E-06	<E-06	<E-06	<E-06
70-100		<E-06	<E-06	<E-06										

$\lambda = 0.6328 \mu\text{m}$

Table 5 (Contd). Values of Attenuation Coefficient/km as a Function of Altitude for Each Laser Wavelength and Each Atmospheric Model in Section 2 (k_m = molecular absorption, σ_m = molecular scattering, k_a = aerosol absorption, σ_a = aerosol scattering)

H(km)	$\lambda=0.694\text{-}\mu\text{m}$																								
	TROPICAL			MIDLATITUDE SUMMER			MIDLATITUDE WINTER			SUBARCTIC SUMMER			SUBARCTIC WINTER			CLEAR AEROSOL			HAZY						
	k_m (km^{-1})	σ_m (km^{-1})	k_a (km^{-1})	k_m (km^{-1})	σ_m (km^{-1})	k_a (km^{-1})	k_m (km^{-1})	σ_m (km^{-1})	k_a (km^{-1})	k_m (km^{-1})	σ_m (km^{-1})	k_a (km^{-1})	k_m (km^{-1})	σ_m (km^{-1})	k_a (km^{-1})	k_m (km^{-1})	σ_m (km^{-1})	k_a (km^{-1})	k_m (km^{-1})	σ_m (km^{-1})	k_a (km^{-1})	k_m (km^{-1})	σ_m (km^{-1})	k_a (km^{-1})	k_m (km^{-1})
0	2.62E-02	4.29E-03	6.44E-02	4.37E-03	1.55E-02	4.75E-03	4.07E-02	4.47E-05	4.48E-03	5.00E-03	7.60E-03	1.20E-01	3.70E-02	5.95E-01											
0-1	6.84E-02	4.10E-03	5.07E-02	4.16E-03	1.29E-02	4.50E-03	3.19E-02	4.25E-03	4.19E-03	4.68E-03	5.04E-03	7.97E-02	2.24E-02	3.54E-01											
1-2	4.22E-02	3.73E-03	3.03E-02	3.78E-03	8.13E-03	4.01E-03	1.83E-02	3.84E-03	3.56E-03	4.11E-03	2.20E-03	3.47E-02	8.18E-03	1.29E-01											
2-3	2.73E-02	3.36E-03	1.72E-02	3.40E-03	5.13E-03	3.57E-03	1.13E-02	3.47E-03	2.56E-03	3.64E-03	9.39E-04	1.42E-02	2.99E-03	4.73E-02											
3-4	1.23E-02	3.05E-03	8.67E-03	3.09E-03	3.06E-03	3.19E-03	6.79E-03	3.11E-03	1.65E-03	3.23E-03	4.41E-04	6.56E-03	1.09E-03	1.73E-02											
4-5	5.24E-03	2.77E-03	4.45E-03	2.78E-03	1.48E-03	2.85E-03	3.15E-03	2.79E-03	3.50E-04	2.88E-03	2.78E-04	4.40E-03	3.69E-04	6.30E-03											
5-6	3.09E-03	2.50E-03	2.06E-03	2.50E-03	2.06E-03	2.56E-03	1.95E-03	2.79E-03	3.66E-04	2.57E-03	2.03E-03	3.20E-03	2.03E-04	3.20E-03											
6-7	1.59E-03	2.25E-03	1.11E-03	2.25E-03	1.26E-04	2.28E-03	9.49E-04	2.25E-03	1.54E-04	2.29E-03	1.64E-04	2.58E-03	1.64E-04	2.59E-03											
7-8	7.61E-04	2.03E-03	5.87E-04	2.03E-03	4.29E-04	2.02E-03	4.32E-04	2.05E-03	7.25E-05	2.03E-03	1.61E-04	2.54E-03	1.61E-04	2.54E-03											
8-9	3.54E-04	1.82E-03	2.92E-04	1.82E-03	4.42E-05	1.79E-03	1.68E-04	1.83E-03	1.27E-05	1.78E-03	1.60E-04	2.52E-03	1.60E-04	2.52E-03											
9-10	1.47E-04	1.62E-03	1.44E-04	1.61E-03	1.73E-05	1.59E-03	4.64E-05	1.43E-03	8.23E-06	1.53E-03	1.54E-04	2.44E-03	1.54E-04	2.44E-03											
10-11	5.28E-05	1.45E-03	6.86E-05	1.44E-03	6.87E-06	1.38E-03	1.43E-05	1.41E-03	4.65E-06	1.31E-03	1.49E-04	2.33E-03	1.49E-04	2.33E-03											
11-12	1.55E-05	1.29E-03	1.95E-05	1.27E-03	5.51E-06	1.18E-03	7.70E-06	1.21E-03	2.76E-06	1.12E-03	1.48E-04	2.31E-03	1.48E-04	2.31E-03											
12-13	4.63E-06	1.14E-03	4.54E-06	1.12E-03	4.07E-06	1.01E-03	4.23E-06	1.04E-03	1.59E-06	9.56E-04	1.44E-04	2.28E-03	1.44E-04	2.28E-03											
13-14	1.19E-06	1.00E-03	1.18E-06	1.03E-03	1.05E-06	8.70E-04	1.10E-06	8.92E-04	<E-06	8.18E-04	1.37E-04	2.17E-03	1.37E-04	2.17E-03											
14-15	<E-06	8.82E-04	3.32E-04	8.32E-04	<E-06	7.46E-04	<E-06	7.65E-04	6.39E-04	7.00E-04	1.31E-04	2.08E-03	1.31E-04	2.08E-03											
15-16	7.68E-04	7.68E-04	6.59E-04	6.59E-04	6.59E-04																				
16-17	6.63E-04	6.63E-04	6.02E-04	6.02E-04	6.02E-04																				
17-18	5.37E-04	5.37E-04	5.18E-04	5.18E-04	5.18E-04																				
18-19	4.60E-04	4.60E-04	4.42E-04	4.42E-04	4.42E-04																				
19-20	3.81E-04	3.81E-04	3.76E-04	3.76E-04	3.76E-04																				
20-21	3.18E-04	3.18E-04	3.21E-04	3.21E-04	3.21E-04																				
21-22	2.65E-04	2.65E-04	2.74E-04	2.74E-04	2.74E-04																				
22-23	2.23E-04	2.23E-04	2.34E-04	2.34E-04	2.34E-04																				
23-24	1.90E-04	1.90E-04	1.99E-04	1.99E-04	1.99E-04																				
24-25	1.61E-04	1.61E-04	1.70E-04	1.70E-04	1.70E-04																				
25-30	1.07E-04	1.07E-04	1.14E-04	1.14E-04	1.14E-04																				
30-35	4.90E-05	4.90E-05	5.27E-05	5.27E-05	5.27E-05																				
35-40	1.14E-05	1.14E-05	1.23E-05	1.23E-05	1.23E-05																				
40-45	5.81E-06	5.81E-06	5.34E-06	5.34E-06	5.34E-06																				
50-70	2.17E-06	2.17E-06	2.38E-06	2.38E-06	2.38E-06																				
70-100	<E-06	<E-06	<E-06	<E-06	<E-06	<E-06	<E-06	<E-06	<E-06	<E-06	<E-06	<E-06	<E-06	<E-06											

NOT REPRODUCIBLE

Table 5 (Contd). Values of Attenuation Coefficient/km as a Function of Altitude for Each Laser Wavelength and Each Atmospheric Model in Section 2 (k_m = molecular absorption, σ_m = molecular scattering, k_a = aerosol absorption, σ_a = aerosol scattering)

Ht(km)	TROPICAL		MIDLATITUDE SUMMER		MIDLATITUDE WINTER		SUBARCTIC SUMMER		SUBARCTIC WINTER		CLEAR		AEROSOL HAZY	
	k_m (km^{-1})	σ_m (km^{-1})	k_m (km^{-1})	σ_m (km^{-1})	k_m (km^{-1})	σ_m (km^{-1})	k_m (km^{-1})	σ_m (km^{-1})	k_m (km^{-1})	σ_m (km^{-1})	k_m (km^{-1})	σ_m (km^{-1})	k_a (km^{-1})	σ_a (km^{-1})
0	<E-06	8.04E-04	<E-06	8.20E-04	<E-06	8.91E-04	8.39E-04	<E-06	8.77E-04	8.39E-04	1.98E-02	6.79E-02	9.63E-02	3.31E-01
0-1		7.61E-04		7.81E-04		8.43E-04	7.98E-04		7.21E-04		1.31E-02	4.50E-02	5.82E-02	2.00E-01
1-2		6.96E-04		7.06E-04		7.52E-04	7.21E-04		6.50E-04		5.71E-03	1.96E-02	2.13E-02	7.31E-02
2-3		6.33E-04		6.38E-04		6.70E-04	6.50E-04		5.84E-04		4.33E-03	8.36E-03	7.78E-03	2.67E-02
3-4		5.72E-04		5.77E-04		5.99E-04	5.84E-04		5.24E-04		1.15E-03	3.94E-03	2.84E-03	9.76E-03
4-5		5.19E-04		5.21E-04		5.37E-04	5.24E-04		4.71E-04		7.23E-04	2.49E-03	1.04E-03	3.56E-03
5-6		4.65E-04		4.68E-04		4.80E-04	4.71E-04		4.23E-04		4.82E-04	1.61E-03	5.27E-04	1.81E-03
6-7		4.22E-04		4.21E-04		4.27E-04	4.23E-04		3.81E-04		4.27E-04	1.47E-03	4.27E-04	1.47E-03
7-8		3.80E-04		3.76E-04		3.80E-04	3.79E-04		3.34E-04		4.18E-04	1.44E-03	4.18E-04	1.44E-03
8-9		3.41E-04		3.38E-04		3.36E-04	3.38E-04		2.89E-04		4.01E-04	1.38E-03	4.01E-04	1.38E-03
9-10		3.04E-04		3.02E-04		2.97E-04	3.01E-04		2.46E-04		3.84E-04	1.32E-03	3.84E-04	1.32E-03
10-11		2.72E-04		2.69E-04		2.64E-04	2.64E-04		2.10E-04		3.61E-04	1.26E-03	3.61E-04	1.26E-03
11-12		2.41E-04		2.39E-04		2.32E-04	2.32E-04		1.80E-04		3.39E-04	1.20E-03	3.39E-04	1.20E-03
12-13		2.13E-04		2.11E-04		2.03E-04	2.03E-04		1.54E-04		3.18E-04	1.14E-03	3.18E-04	1.14E-03
13-14		1.88E-04		1.83E-04		1.73E-04	1.73E-04		1.31E-04		2.97E-04	1.08E-03	2.97E-04	1.08E-03
14-15		1.66E-04		1.59E-04		1.49E-04	1.49E-04		1.12E-04		2.77E-04	1.02E-03	2.77E-04	1.02E-03
15-16		1.44E-04		1.33E-04		1.23E-04	1.23E-04		9.63E-05		2.58E-04	9.63E-04	2.58E-04	9.63E-04
16-17		1.24E-04		1.14E-04		1.03E-04	1.03E-04		8.23E-05		2.40E-04	9.06E-04	2.40E-04	9.06E-04
17-18		1.05E-04		9.72E-05		8.80E-05	8.80E-05		7.06E-05		2.23E-04	8.42E-04	2.23E-04	8.42E-04
18-19		8.63E-05		8.29E-05		7.53E-05	7.53E-05		6.05E-05		2.07E-04	7.86E-04	2.07E-04	7.86E-04
19-20		7.16E-05		7.07E-05		6.45E-05	6.45E-05		5.17E-05		1.90E-04	7.48E-04	1.90E-04	7.48E-04
20-21		5.96E-05		6.02E-05		5.51E-05	5.51E-05		4.42E-05		1.73E-04	7.08E-04	1.73E-04	7.08E-04
21-22		4.98E-05		5.14E-05		4.70E-05	4.70E-05		3.78E-05		1.56E-04	6.70E-04	1.56E-04	6.70E-04
22-23		4.19E-05		4.38E-05		4.01E-05	4.01E-05		3.23E-05		1.40E-04	6.32E-04	1.40E-04	6.32E-04
23-24		3.55E-05		3.74E-05		3.43E-05	3.43E-05		2.76E-05		1.24E-04	5.94E-04	1.24E-04	5.94E-04
24-25		3.02E-05		3.19E-05		2.93E-05	2.93E-05		2.33E-05		1.08E-04	5.56E-04	1.08E-04	5.56E-04
25-30		2.01E-05		2.15E-05		1.95E-05	1.95E-05		1.54E-05		9.63E-05	5.18E-04	9.63E-05	5.18E-04
20-35		9.20E-06		9.79E-06		8.79E-06	8.79E-06		7.06E-06		8.42E-05	4.80E-04	8.42E-05	4.80E-04
35-40		4.37E-06		4.71E-06		3.85E-06	3.85E-06		3.11E-06		7.86E-05	4.42E-04	7.86E-05	4.42E-04
40-45		2.15E-06		2.31E-06		1.83E-06	1.83E-06		1.68E-06		6.32E-05	4.04E-04	6.32E-05	4.04E-04
45-50		1.09E-06		1.19E-06		1.09E-06	1.09E-06		1.21E-06		4.42E-05	3.66E-04	4.42E-05	3.66E-04
50-70		<E-06		<E-06		<E-06	<E-06		<E-06		<E-06	<E-06	<E-06	<E-06
70-100														

NOT REPRODUCIBLE

Table 5 (Contd). Values of Attenuation Coefficient/km as a Function of Altitude for Each Laser Wavelength and Each Atmospheric Model in Section 2 (k_m = molecular absorption, σ_m = molecular scattering, k_a = aerosol absorption, σ_a = aerosol scattering)

Ht(km)	TROPICAL		MID-LATITUDE SUMMER		MID-LATITUDE WINTER		SUBARCTIC SUMMER		SUBARCTIC WINTER		CLEAR AEROSOL		HAZY	
	k_m (μm^{-1})	σ_m (μm^{-1})	k_m (μm^{-1})	σ_m (μm^{-1})	k_m (μm^{-1})	σ_m (μm^{-1})	k_m (μm^{-1})	σ_m (μm^{-1})	k_m (μm^{-1})	σ_m (μm^{-1})	k_m (μm^{-1})	σ_m (μm^{-1})	k_m (μm^{-1})	σ_m (μm^{-1})
0	1.47E-04	1.77E-04	1.52E-04	1.81E-04	1.81E-04	1.96E-04	1.74E-04	1.85E-04	2.22E-04	2.07E-04	2.35E-02	4.09E-02	1.15E-01	1.89E-01
0-1	1.31E-04	1.69E-04	1.35E-04	1.72E-04	1.62E-04	1.86E-04	1.55E-04	1.76E-04	1.98E-04	1.93E-04	1.56E-02	2.71E-02	8.89E-02	1.20E-01
1-2	1.09E-04	1.54E-04	1.11E-04	1.56E-04	1.30E-04	1.66E-04	1.27E-04	1.59E-04	1.63E-04	1.70E-04	6.80E-03	1.18E-02	2.53E-02	1.40E-02
2-3	8.99E-05	1.40E-04	9.24E-05	1.41E-04	1.04E-04	1.48E-04	1.04E-04	1.43E-04	1.20E-04	1.50E-04	2.90E-03	5.03E-03	9.27E-03	1.61E-02
3-4	7.48E-05	1.26E-04	7.63E-05	1.27E-04	8.39E-05	1.32E-04	8.54E-05	1.29E-04	9.64E-05	1.34E-04	1.36E-03	2.37E-03	3.36E-03	5.88E-03
4-5	6.14E-05	1.14E-04	6.09E-05	1.15E-04	5.82E-05	1.18E-04	6.80E-05	1.15E-04	7.68E-05	1.19E-04	8.62E-04	1.50E-03	1.24E-03	2.15E-03
5-6	5.06E-05	1.03E-04	5.09E-05	1.04E-04	5.45E-05	1.06E-04	5.69E-05	1.04E-04	6.20E-05	1.06E-04	6.28E-04	1.09E-03	6.28E-04	1.09E-03
6-7	4.12E-05	8.31E-05	4.20E-05	8.33E-05	4.38E-05	8.42E-05	4.51E-05	8.32E-05	4.95E-05	9.46E-05	8.43E-04	5.09E-04	8.83E-04	8.83E-04
7-8	3.36E-05	6.71E-05	3.35E-05	6.66E-05	3.47E-05	6.66E-05	3.69E-05	6.59E-05	3.32E-05	6.59E-05	8.65E-04	6.65E-04	8.65E-04	8.65E-04
8-8	2.75E-05	5.99E-05	2.63E-05	5.83E-05	2.77E-05	5.83E-05	2.97E-05	5.83E-05	3.04E-05	7.36E-05	4.95E-04	4.95E-04	4.95E-04	4.95E-04
9-10	2.17E-05	5.12E-05	2.15E-05	5.06E-05	2.19E-05	5.06E-05	2.35E-05	5.06E-05	2.26E-05	6.34E-05	4.78E-04	4.78E-04	4.78E-04	4.78E-04
10-11	1.77E-05	4.39E-05	1.73E-05	4.31E-05	1.55E-05	4.31E-05	1.79E-05	4.31E-05	1.65E-05	5.42E-05	4.57E-04	4.57E-04	4.57E-04	4.57E-04
11-12	1.38E-05	3.72E-05	1.36E-05	3.66E-05	1.20E-05	3.66E-05	1.36E-05	3.66E-05	1.20E-05	4.63E-05	4.54E-04	4.54E-04	4.54E-04	4.54E-04
12-13	1.12E-05	3.10E-05	1.07E-05	3.03E-05	8.87E-06	3.03E-05	1.07E-05	3.03E-05	8.64E-06	3.96E-05	4.47E-04	4.47E-04	4.47E-04	4.47E-04
13-14	8.40E-06	2.58E-05	8.15E-06	2.51E-05	6.65E-06	2.51E-05	7.45E-06	2.51E-05	6.59E-06	3.39E-05	4.25E-04	4.25E-04	4.25E-04	4.25E-04
14-15	6.87E-06	2.18E-05	6.08E-06	2.11E-05	4.81E-06	2.11E-05	5.45E-06	2.11E-05	4.69E-06	2.89E-05	4.07E-04	4.07E-04	4.07E-04	4.07E-04
15-16	5.28E-06	1.82E-05	4.30E-06	1.75E-05	3.51E-06	1.75E-05	3.85E-06	1.75E-05	3.44E-06	2.48E-05	3.85E-04	3.85E-04	3.85E-04	3.85E-04
16-17	3.76E-06	1.48E-05	3.10E-06	1.41E-05	2.59E-06	1.41E-05	2.96E-06	1.41E-05	2.33E-06	2.12E-05	3.73E-04	3.73E-04	3.73E-04	3.73E-04
17-18	2.70E-06	1.12E-05	2.29E-06	1.12E-05	1.93E-06	1.12E-05	2.18E-06	1.12E-05	1.86E-06	1.82E-05	3.65E-04	3.65E-04	3.65E-04	3.65E-04
18-19	1.85E-06	8.31E-06	1.66E-06	8.31E-06	1.40E-06	8.31E-06	1.61E-06	8.31E-06	1.38E-06	1.56E-05	3.30E-04	3.30E-04	3.30E-04	3.30E-04
19-20	1.25E-06	6.14E-06	1.21E-06	6.14E-06	1.01E-06	6.14E-06	1.42E-06	6.14E-06	1.38E-06	1.33E-05	4.50E-04	4.50E-04	4.50E-04	4.50E-04
20-21	8.31E-07	4.51E-06	8.31E-07	4.51E-06	6.65E-07	4.51E-06	5.06E-07	4.51E-06	4.63E-07	1.14E-05	1.98E-04	1.98E-04	1.98E-04	1.98E-04
21-22	6.14E-07	3.36E-06	6.14E-07	3.36E-06	4.81E-07	3.36E-06	3.69E-07	3.36E-06	3.39E-07	9.75E-06	1.40E-04	1.40E-04	1.40E-04	1.40E-04
22-23	4.51E-07	2.58E-06	4.51E-07	2.58E-06	3.51E-07	2.58E-06	2.74E-07	2.58E-06	2.48E-07	7.13E-06	1.06E-04	1.06E-04	1.06E-04	1.06E-04
23-24	3.36E-07	1.98E-06	3.36E-07	1.98E-06	2.59E-07	1.98E-06	2.11E-07	1.98E-06	1.86E-07	5.05E-06	8.25E-05	8.25E-05	8.25E-05	8.25E-05
24-25	2.58E-07	1.48E-06	2.58E-07	1.48E-06	1.98E-07	1.48E-06	1.59E-07	1.48E-06	1.41E-07	3.69E-06	6.74E-05	6.74E-05	6.74E-05	6.74E-05
25-30	1.98E-07	1.12E-06	1.98E-07	1.12E-06	1.48E-07	1.12E-06	1.12E-07	1.12E-06	1.06E-07	2.89E-06	5.90E-05	5.90E-05	5.90E-05	5.90E-05
30-35	1.48E-07	8.31E-07	1.48E-07	8.31E-07	1.12E-07	8.31E-07	8.31E-08	8.31E-07	7.74E-08	2.20E-06	1.66E-05	1.66E-05	1.66E-05	1.66E-05
35-40	1.12E-07	6.14E-07	1.12E-07	6.14E-07	8.31E-08	6.14E-07	6.14E-08	6.14E-07	5.57E-08	1.66E-06	1.15E-05	1.15E-05	1.15E-05	1.15E-05
40-45	8.31E-08	4.51E-07	8.31E-08	4.51E-07	6.14E-08	4.51E-07	4.51E-08	4.51E-07	4.01E-08	1.15E-06	8.25E-06	8.25E-06	8.25E-06	8.25E-06
45-50	6.14E-08	3.36E-07	6.14E-08	3.36E-07	4.51E-08	3.36E-07	3.36E-08	3.36E-07	3.01E-08	8.25E-07	6.74E-06	6.74E-06	6.74E-06	6.74E-06
50-70	4.51E-08	2.58E-07	4.51E-08	2.58E-07	3.36E-08	2.58E-07	2.58E-08	2.58E-07	2.20E-08	6.74E-07	5.90E-06	5.90E-06	5.90E-06	5.90E-06
70-100	3.36E-08	1.98E-07	3.36E-08	1.98E-07	2.58E-08	1.98E-07	1.98E-08	1.98E-07	1.74E-08	5.90E-07	5.90E-06	5.90E-06	5.90E-06	5.90E-06

NOT REPRODUCIBLE

Table 5 (Contd). Values of Attenuation Coefficient/km as a Function of Altitude for Each Laser Wavelength and Each Atmospheric Model in Section 2 (k_m = molecular absorption, σ_m = molecular scattering, k_a = aerosol absorption, σ_a = aerosol scattering)

Ht(km)	3.39225 μ m																	
	TROPICAL			MIDLATITUDE SUMMER			MIDLATITUDE WINTER			SUBARCTIC SUMMER			SUBARCTIC WINTER			CLEAR AEROSOL HAZY		
	k_m (km^{-1})	σ_m (km^{-1})	k_a (km^{-1})	k_m (km^{-1})	σ_m (km^{-1})	k_a (km^{-1})	k_m (km^{-1})	σ_m (km^{-1})	k_a (km^{-1})	k_m (km^{-1})	σ_m (km^{-1})	k_a (km^{-1})	k_m (km^{-1})	σ_m (km^{-1})	k_a (km^{-1})	k_m (km^{-1})	σ_m (km^{-1})	k_a (km^{-1})
0	1.77E+00	7.79E-06	1.83E+00	7.95E-06	1.98E+00	8.53E-06	1.88E+10	8.12E-06	2.03E+00	9.09E-06	1.58E-02	1.65E-02	7.71E-02	8.05E-02				
0-1	1.75E+00	7.44E-06	1.79E+00	7.56E-06	1.92E+00	8.17E-06	1.84E+10	7.72E-06	1.97E+00	8.50E-06	1.05E-02	1.09E-02	4.66E-02	4.86E-02				
1-2	1.68E+00	6.77E-06	1.70E+00	6.83E-06	1.79E+00	7.29E-06	1.79E+10	6.98E-06	1.84E+00	7.46E-06	4.57E-03	4.77E-03	1.70E-02	1.78E-02				
2-3	1.63E+00	6.13E-06	1.65E+00	6.18E-06	1.75E+00	6.49E-06	1.65E+10	6.29E-06	1.75E+00	6.69E-06	1.94E-03	2.03E-03	5.24E-03	5.38E-03				
3-4	1.59E+00	5.54E-06	1.60E+00	5.59E-06	1.65E+00	5.80E-06	1.68E+10	5.65E-06	1.67E+00	5.86E-06	8.18E-04	9.57E-04	2.27E-03	2.37E-03				
4-5	1.54E+00	5.02E-06	1.54E+00	5.05E-06	1.60E+00	5.29E-06	1.54E+10	5.07E-06	1.62E+00	5.23E-06	6.04E-04	6.40E-04	8.31E-04	8.67E-04				
5-6	1.52E+00	4.54E-06	1.54E+00	4.55E-06	1.54E+00	4.64E-06	1.51E+10	4.55E-06	1.57E+00	4.67E-06	4.22E-04	4.40E-04	4.22E-04	4.49E-04				
6-7	1.47E+00	4.09E-06	1.46E+00	4.08E-06	1.46E+00	4.14E-06	1.47E+10	4.09E-06	1.54E+00	4.16E-06	3.42E-04	3.57E-04	3.42E-04	3.57E-04				
7-8	1.45E+00	3.69E-06	1.43E+00	3.66E-06	1.46E+00	3.68E-06	1.45E+10	3.67E-06	1.50E+00	3.58E-06	3.35E-04	3.49E-04	3.35E-04	3.49E-04				
8-9	1.46E+00	3.30E-06	1.41E+00	3.27E-06	1.44E+00	3.26E-06	1.51E+10	3.28E-06	1.47E+00	3.23E-06	3.23E-04	3.47E-04	3.23E-04	3.47E-04				
9-10	1.41E+00	2.95E-06	1.43E+00	2.92E-06	1.49E+00	2.88E-06	1.46E+10	2.92E-06	1.44E+00	2.79E-06	3.22E-04	3.35E-04	3.22E-04	3.35E-04				
10-11	1.42E+00	2.63E-06	1.40E+00	2.60E-06	1.41E+00	2.51E-06	1.42E+10	2.55E-06	1.41E+00	2.38E-06	3.07E-04	3.21E-04	3.07E-04	3.21E-04				
11-12	1.37E+00	2.34E-06	1.38E+00	2.31E-06	1.39E+00	2.15E-06	1.38E+10	2.19E-06	1.38E+00	2.04E-06	3.05E-04	3.18E-04	3.05E-04	3.18E-04				
12-13	1.40E+00	2.06E-06	1.37E+00	2.04E-06	1.36E+00	1.81E-06	1.35E+10	1.89E-06	1.34E+00	1.74E-06	3.00E-04	3.13E-04	3.00E-04	3.13E-04				
13-14	1.31E+00	1.82E-06	1.34E+00	1.77E-06	1.30E+00	1.58E-06	1.34E+10	1.62E-06	1.31E+00	1.49E-06	2.86E-04	2.98E-04	2.86E-04	2.98E-04				
14-15	1.35E+00	1.60E-06	1.36E+00	1.51E-06	1.29E+00	1.36E-06	1.37E+10	1.39E-06	1.27E+00	1.27E-06	2.74E-04	2.86E-04	2.74E-04	2.86E-04				
15-16	1.32E+00	1.40E-06	1.28E+00	1.29E-06	1.24E+00	1.14E-06	1.21E+10	1.10E-06	1.21E+00	1.09E-06	2.59E-04	2.70E-04	2.59E-04	2.70E-04				
16-17	1.21E+00	1.20E-06	1.23E+00	1.10E-06	1.19E+00	1.19E-06	1.18E+10	1.07E-06	1.16E+00	1.09E-06	2.51E-04	2.62E-04	2.51E-04	2.62E-04				
17-18	1.17E+00	1.01E-06	1.14E+00	1.09E-06	1.13E+00	1.03E-06	1.13E+10	1.07E-06	1.09E+00	1.09E-06	2.45E-04	2.56E-04	2.45E-04	2.56E-04				
18-19	1.10E+00	0.95E-06	1.09E+00	1.00E+00	1.03E+00	0.97E-06	1.07E+10	1.07E-06	1.01E+00	1.01E+00	2.22E-04	2.31E-04	2.22E-04	2.31E-04				
19-20	8.95E-01	8.95E-01	8.95E-01	8.95E-01	8.95E-01	8.95E-01	8.95E-01	8.95E-01	8.95E-01	8.95E-01	1.74E-04	1.82E-04	1.74E-04	1.82E-04				
20-21	8.95E-01	8.95E-01	8.95E-01	8.95E-01	8.95E-01	8.95E-01	8.95E-01	8.95E-01	8.95E-01	8.95E-01	1.27E-04	1.33E-04	1.27E-04	1.33E-04				
21-22	7.82E-01	6.14E-01	6.14E-01	6.14E-01	6.14E-01	6.14E-01	6.14E-01	6.14E-01	6.14E-01	6.14E-01	9.32E-05	9.79E-05	9.32E-05	9.79E-05				
22-23	6.55E-01	6.62E-01	6.62E-01	6.62E-01	6.62E-01	6.62E-01	6.62E-01	6.62E-01	6.62E-01	6.62E-01	7.12E-05	7.43E-05	7.12E-05	7.43E-05				
23-24	5.48E-01	6.23E-01	6.23E-01	6.23E-01	6.23E-01	6.23E-01	6.23E-01	6.23E-01	6.23E-01	6.23E-01	5.55E-05	5.55E-05	5.55E-05	5.55E-05				
24-25	4.51E-01	4.76E-01	4.76E-01	4.76E-01	4.76E-01	4.76E-01	4.76E-01	4.76E-01	4.76E-01	4.76E-01	4.53E-05	4.53E-05	4.53E-05	4.53E-05				
25-30	2.33E-01	2.63E-01	2.63E-01	2.63E-01	2.63E-01	2.63E-01	2.63E-01	2.63E-01	2.63E-01	2.63E-01	2.28E-05	2.28E-05	2.28E-05	2.28E-05				
30-35	1.93E-01	2.07E-01	2.07E-01	2.07E-01	2.07E-01	2.07E-01	2.07E-01	2.07E-01	2.07E-01	2.07E-01	6.43E-06	6.43E-06	6.43E-06	6.43E-06				
35-40	9.21E-02	1.03E-01	1.03E-01	1.03E-01	1.03E-01	1.03E-01	1.03E-01	1.03E-01	1.03E-01	1.03E-01	1.69E-06	1.69E-06	1.69E-06	1.69E-06				
40-45	4.86E-02	5.30E-02	5.30E-02	5.30E-02	5.30E-02	5.30E-02	5.30E-02	5.30E-02	5.30E-02	5.30E-02	0.00E-06	0.00E-06	0.00E-06	0.00E-06				
45-50	2.45E-02	2.67E-02	2.67E-02	2.67E-02	2.67E-02	2.67E-02	2.67E-02	2.67E-02	2.67E-02	2.67E-02	0.00E-06	0.00E-06	0.00E-06	0.00E-06				
50-70	6.75E-03	7.50E-03	7.50E-03	7.50E-03	7.50E-03	7.50E-03	7.50E-03	7.50E-03	7.50E-03	7.50E-03	0.00E-06	0.00E-06	0.00E-06	0.00E-06				
70-100	3.21E-04	3.72E-04	3.72E-04	3.72E-04	3.72E-04	3.72E-04	3.72E-04	3.72E-04	3.72E-04	3.72E-04	0.00E-06	0.00E-06	0.00E-06	0.00E-06				

NOT REPRODUCIBLE

Table 5 (Contd). Values of Attenuation Coefficient/km as a Function of Altitude for Each Laser Wavelength and Each Atmospheric Model in Section 2 (k_m = molecular absorption, σ_m = molecular scattering, k_a = aerosol absorption, σ_a = aerosol scattering)

Ht(km)	$\lambda = 10.591 \mu\text{m}$													
	TROPICAL		MIDLATITUDE SUMMER		MIDLATITUDE WINTER		SUBARCTIC SUMMER		SUBARCTIC WINTER		CLEAR		HAZY	
	k_m (km^{-1})	σ_m (km^{-1})	k_m (km^{-1})	σ_m (km^{-1})	k_m (km^{-1})	σ_m (km^{-1})	k_m (km^{-1})	σ_m (km^{-1})	k_m (km^{-1})	σ_m (km^{-1})	k_a (km^{-1})	σ_a (km^{-1})	k_a (km^{-1})	σ_a (km^{-1})
0	5.785E-01	<1.0E-06	3.582E-01	<1.0E-06	1.937E-02	<1.0E-06	2.066E-01	<1.0E-06	4.118E-02	<1.0E-06	5.42E-03	4.65E-03	2.67E-02	2.27E-02
0-1	5.172E-01		3.256E-01		7.312E-02		1.818E-01		4.147E-02		3.64E-03	3.09E-03	1.61E-02	1.37E-02
1-2	2.845E-01		1.877E-01		5.295E-02		1.137E-01		4.002E-02		1.58E-03	1.34E-03	5.90E-03	5.01E-03
2-3	1.807E-01		1.152E-01		4.911E-02		8.152E-02		3.516E-02		6.75E-04	5.73E-04	2.15E-03	1.83E-03
3-4	9.616E-02		7.592E-02		4.043E-02		6.090E-02		3.048E-02		3.18E-04	2.70E-04	7.88E-04	6.88E-04
4-5	6.200E-02		5.544E-02		3.240E-02		4.863E-02		2.433E-02		2.01E-04	1.70E-04	2.88E-04	2.44E-04
5-6	5.019E-02		4.468E-02		2.622E-02		3.737E-02		1.932E-02		1.46E-04	1.24E-04	1.48E-04	1.24E-04
6-7	3.998E-02		3.752E-02		2.147E-02		2.861E-02		1.509E-02		1.18E-04	1.00E-04	1.18E-04	1.00E-04
7-8	3.200E-02		3.018E-02		1.728E-02		2.377E-02		1.171E-02		1.16E-04	9.83E-05	1.16E-04	9.83E-05
8-9	2.634E-02		2.378E-02		1.405E-02		1.788E-02		9.59E-03		1.15E-04	9.77E-05	1.15E-04	9.77E-05
9-10	2.074E-02		1.952E-02		1.083E-02		1.375E-02		8.92E-03		1.11E-04	9.45E-05	1.11E-04	9.45E-05
10-11	1.651E-02		1.574E-02		9.813E-03		1.195E-02		8.921E-03		1.06E-04	9.04E-05	1.06E-04	9.04E-05
11-12	1.237E-02		1.241E-02		9.484E-03		1.229E-02		8.908E-03		1.06E-04	9.04E-05	1.06E-04	9.04E-05
12-13	1.035E-02		9.534E-03		8.337E-03		1.181E-02		8.733E-03		1.04E-04	8.83E-05	1.04E-04	8.83E-05
13-14	7.362E-03		8.700E-03		8.307E-03		1.229E-02		9.109E-03		9.89E-05	8.39E-05	9.89E-05	8.39E-05
14-15	5.850E-03		8.491E-03		8.749E-03		1.166E-02		8.773E-03		9.48E-05	8.06E-05	9.48E-05	8.06E-05
16-17	3.318E-03		5.364E-03		8.573E-03		1.217E-02		8.559E-03		8.69E-05	7.38E-05	8.69E-05	7.38E-05
17-18	3.556E-03		8.467E-03		8.556E-03		1.203E-02		8.324E-03		8.50E-05	7.21E-05	8.50E-05	7.21E-05
18-19	4.350E-03		8.560E-03		8.011E-03		1.193E-02		8.269E-03		8.97E-05	7.61E-05	8.97E-05	7.61E-05
19-20	5.184E-03		8.529E-03		8.194E-03		1.186E-02		8.269E-03		7.68E-05	6.51E-05	7.68E-05	6.51E-05
20-21	6.273E-03		9.186E-03		8.186E-03		1.186E-02		7.744E-03		4.40E-05	3.74E-05	4.40E-05	3.74E-05
21-22	7.471E-03		9.719E-03		8.194E-03		1.209E-02		7.523E-03		3.25E-05	2.76E-05	3.25E-05	2.76E-05
22-23	8.351E-03		1.010E-02		8.161E-03		1.209E-02		7.309E-03		2.47E-05	2.09E-05	2.47E-05	2.09E-05
23-24	9.041E-03		1.114E-02		8.507E-03		1.197E-02		7.329E-03		1.92E-05	1.63E-05	1.92E-05	1.63E-05
24-25	9.908E-03		1.112E-02		8.378E-03		1.275E-02		5.837E-03		1.57E-05	1.33E-05	1.57E-05	1.33E-05
25-30	1.203E-02		1.327E-02		8.387E-03		1.453E-02		7.238E-03		7.50E-06	6.71E-06	7.50E-06	6.71E-06
30-35	1.180E-02		1.319E-02		6.848E-03		2.007E-02		5.785E-03		2.23E-06	1.89E-06	2.23E-06	1.89E-06
35-40	1.101E-02		1.269E-02		6.714E-03		1.393E-02		5.099E-03		<1.0E-06	<1.0E-06	<1.0E-06	<1.0E-06
40-45	8.865E-03		1.063E-02		6.023E-03		1.189E-02		4.100E-03					
45-50	6.038E-03		7.522E-03		4.405E-03		8.188E-03		3.082E-03					
50-70	9.007E-04		1.077E-03		2.744E-04		1.097E-03		7.761E-04					
70-100	1.535E-05		1.743E-05		1.560E-04		1.762E-05		1.785E-05					

NOT REPRODUCIBLE

Table 5 (Contd). Values of Attenuation Coefficient/km as a Function of Altitude for Each Laser Wavelength and Each Atmospheric Model in Section 2 (k_m = molecular absorption, σ_m = molecular scattering, k_a = aerosol absorption, σ_a = aerosol scattering)

Ht (km)	TROPICAL		MIDLATITUDE SUMMER		MIDLATITUDE WINTER		SUBARCTIC SUMMER		SUBARCTIC WINTER		CLEAR AEROSOL		HAZY AEROSOL	
	k_m (km^{-1})	σ_m (km^{-1})	k_m (km^{-1})	σ_m (km^{-1})	k_m (km^{-1})	σ_m (km^{-1})	k_m (km^{-1})	σ_m (km^{-1})	k_m (km^{-1})	σ_m (km^{-1})	k_a (km^{-1})	σ_a (km^{-1})	k_a (km^{-1})	σ_a (km^{-1})
0	>30	<E-06	7.78E-04	3.79E-03	9.49E-04	3.79E-03								
0-1	>30	>30	>30	>30	>30	>30	>30	>30	>30	>30	1.29E-03	5.16E-04	5.73E-04	2.29E-03
1-2	>30	>30	>30	>30	>30	>30	>30	>30	>30	>30	5.63E-04	2.25E-04	2.10E-04	8.36E-04
2-3	>30	>30	>30	>30	>30	>30	>30	>30	>30	>30	2.40E-04	9.58E-05	7.67E-04	3.07E-04
3-4	>30	>30	>30	>30	>30	>30	>30	>30	>30	>30	1.13E-04	4.51E-05	2.89E-04	1.12E-04
4-5	>30	>30	>30	>30	>30	>30	>30	>30	>30	>30	7.13E-05	2.85E-05	1.02E-04	4.08E-05
5-6	>30	>30	>30	>30	>30	>30	>30	>30	>30	>30	5.20E-05	2.08E-05	5.20E-05	2.08E-05
6-7	>30	>30	2.95E+01	4.29E+00	1.35E+01	4.29E+00	1.62E+01	4.69E+00	4.69E+00	4.69E+00	4.21E-05	1.68E-05	4.21E-05	1.68E-05
8-6	1.67E+01	1.32E+01	1.32E+01	1.32E+01	1.32E+01	1.32E+01	6.22E+00	3.08E-01	3.08E-01	3.08E-01	4.09E-05	1.64E-05	4.09E-05	1.64E-05
9-10	6.18E+00	5.77E+00	5.77E+00	4.69E-01	4.69E-01	4.69E-01	1.49E+00	1.97E-01	1.97E-01	1.97E-01	3.96E-05	1.58E-05	3.96E-05	1.58E-05
10-11	1.81E+00	2.33E+00	2.33E+00	1.73E-01	1.73E-01	1.73E-01	4.30E-01	1.14E-01	1.14E-01	1.14E-01	3.78E-05	1.51E-05	3.78E-05	1.51E-05
11-12	4.96E-01	5.87E-01	5.87E-01	1.39E-01	1.39E-01	1.39E-01	2.36E-01	6.90E-02	6.90E-02	6.90E-02	3.75E-05	1.50E-05	3.75E-05	1.50E-05
12-13	1.23E-01	1.15E-01	1.15E-01	1.04E-01	1.04E-01	1.04E-01	1.33E-01	4.07E-02	4.07E-02	4.07E-02	3.70E-05	1.48E-05	3.70E-05	1.48E-05
13-14	2.60E-02	2.77E-02	2.77E-02	2.68E-02	2.68E-02	2.68E-02	5.48E-02	2.46E-02	2.46E-02	2.46E-02	3.51E-05	1.40E-05	3.51E-05	1.40E-05
14-15	9.71E-03	1.28E-02	1.28E-02	1.28E-02	1.28E-02	1.28E-02	1.61E-02	1.14E-02	1.14E-02	1.14E-02	3.37E-05	1.35E-05	3.37E-05	1.35E-05
15-16	5.95E-03	8.46E-03	8.46E-03	7.94E-03	7.94E-03	7.94E-03	1.07E-02	7.44E-03	7.44E-03	7.44E-03	3.19E-05	1.27E-05	3.19E-05	1.27E-05
16-17	3.19E-03	6.33E-03	6.33E-03	5.85E-03	5.85E-03	5.85E-03	8.10E-03	5.46E-03	5.46E-03	5.46E-03	3.09E-05	1.23E-05	3.09E-05	1.23E-05
17-18	2.36E-03	4.63E-03	4.63E-03	4.20E-03	4.20E-03	4.20E-03	6.30E-03	3.80E-03	3.80E-03	3.80E-03	3.02E-05	1.21E-05	3.02E-05	1.21E-05
18-19	2.04E-03	3.80E-03	3.80E-03	3.35E-03	3.35E-03	3.35E-03	4.53E-03	3.09E-03	3.09E-03	3.09E-03	2.73E-05	1.09E-05	2.73E-05	1.09E-05
19-20	2.13E-03	3.15E-03	3.15E-03	2.65E-03	2.65E-03	2.65E-03	3.90E-03	2.42E-03	2.42E-03	2.42E-03	2.14E-05	8.57E-06	2.14E-05	8.57E-06
20-21	1.69E-03	2.61E-03	2.61E-03	2.12E-03	2.12E-03	2.12E-03	3.13E-03	1.90E-03	1.90E-03	1.90E-03	1.58E-05	6.25E-06	1.58E-05	6.25E-06
21-22	2.09E-03	2.63E-03	2.63E-03	2.07E-03	2.07E-03	2.07E-03	3.09E-03	1.71E-03	1.71E-03	1.71E-03	1.16E-05	4.62E-06	1.16E-05	4.62E-06
22-23	1.90E-03	2.20E-03	2.20E-03	1.66E-03	1.66E-03	1.66E-03	2.66E-03	1.52E-03	1.52E-03	1.52E-03	8.77E-06	3.50E-06	8.77E-06	3.50E-06
23-24	1.84E-03	2.26E-03	2.26E-03	1.61E-03	1.61E-03	1.61E-03	2.47E-03	1.35E-03	1.35E-03	1.35E-03	6.83E-06	2.73E-06	6.83E-06	2.73E-06
24-25	1.77E-03	2.23E-03	2.23E-03	1.53E-03	1.53E-03	1.53E-03	2.35E-03	1.20E-03	1.20E-03	1.20E-03	5.58E-06	2.23E-06	5.58E-06	2.23E-06
25-30	1.28E-03	1.48E-03	1.48E-03	8.61E-04	8.61E-04	8.61E-04	1.61E-03	7.36E-04	7.36E-04	7.36E-04	2.81E-06	1.12E-06	2.81E-06	1.12E-06
30-35	4.50E-04	5.15E-04	5.15E-04	2.62E-04	2.62E-04	2.62E-04	5.43E-04	2.14E-04	2.14E-04	2.14E-04	<E-06	<E-06	<E-06	<E-06
35-40	8.05E-05	1.05E-04	1.05E-04	5.53E-05	5.53E-05	5.53E-05	1.16E-04	4.08E-05	4.08E-05	4.08E-05	<E-06	<E-06	<E-06	<E-06
40-45	6.50E-05	2.84E-05	2.84E-05	1.58E-05	1.58E-05	1.58E-05	1.16E-05	1.09E-05	1.09E-05	1.09E-05	<E-06	<E-06	<E-06	<E-06
45-50	6.50E-06	8.01E-06	8.01E-06	4.67E-06	4.67E-06	4.67E-06	8.73E-06	3.26E-06	3.26E-06	3.26E-06	<E-06	<E-06	<E-06	<E-06
50-70	<E-06	<E-06												
70-160														

NOT REPRODUCIBLE

Table 5 (Contd). Values of Attenuation Coefficient/km as a Function of Altitude for Each Laser Wavelength and Each Atmospheric Model in Section 2 (k_m = molecular absorption, σ_m = molecular scattering, k_a = aerosol absorption, σ_a = aerosol scattering)

$\lambda = 337 \mu\text{m}$

Ht(km)	TROPICAL		MID-LATITUDE SUMMER		MID-LATITUDE WINTER		SUBARCTIC SUMMER		SUBARCTIC WINTER		CLEAR		HAZY	
	k_m (km^{-1})	σ_m (km^{-1})	k_m (km^{-1})	σ_m (km^{-1})	k_m (km^{-1})	σ_m (km^{-1})	k_m (km^{-1})	σ_m (km^{-1})	k_m (km^{-1})	σ_m (km^{-1})	k_a (km^{-1})	σ_a (km^{-1})	k_a (km^{-1})	σ_a (km^{-1})
0														
0-1	2.67E+01	<E-06	2.03E+01	<E-06	5.39E+00	<E-06	1.87E+01	<E-06	1.71E+00	<E-06	1.71E+00	<E-06	<E-06	<E-06
1-2	2.12E+01		1.60E+01		4.35E+00		1.07E+01		1.60E+00		1.60E+00			
2-3	1.35E+01		9.56E+00		2.84E+00		6.39E+00		1.39E+00		1.39E+00			
3-4	9.72E+00		5.58E+00		1.88E+00		4.08E+00		9.79E-01		9.79E-01			
4-5	4.00E+00		2.87E+00		1.10E+00		2.33E+00		6.33E-01		6.33E-01			
5-6	1.75E+00		1.50E+00		5.48E-01		1.31E+00		3.45E-01		3.45E-01			
6-7	1.06E+00		7.17E-01		2.83E-01		7.21E-01		1.52E-01		1.52E-01			
7-8	5.52E-01		3.87E-01		1.42E-01		3.50E-01		6.88E-02		6.88E-02			
8-9	2.78E-01		2.17E-01		5.13E-02		1.73E-01		3.29E-02		3.29E-02			
9-10	1.34E-02		1.12E-01		1.87E-02		6.90E-02		5.96E-03		5.96E-03			
10-11	5.78E-02		5.72E-02		7.73E-03		2.07E-02		3.81E-03		3.81E-03			
11-12	2.18E-02		2.75E-02		3.10E-03		6.33E-03		2.20E-03		2.20E-03			
12-13	6.64E-03		8.43E-03		2.48E-03		3.43E-03		1.30E-03		1.30E-03			
13-14	2.07E-03		2.05E-03		1.83E-03		1.88E-03		7.57E-04		7.57E-04			
14-15	5.59E-04		5.41E-04		4.61E-04		4.88E-04		4.53E-04		4.53E-04			
15-16	2.68E-04		2.47E-04		2.21E-04		2.34E-04		2.08E-04		2.08E-04			
16-17	1.79E-04		1.61E-04		1.48E-04		1.48E-04		1.36E-04		1.36E-04			
17-18	9.63E-05		8.73E-05		7.91E-05		8.19E-05		7.41E-05		7.41E-05			
18-19	6.82E-05		7.00E-05		6.38E-05		6.75E-05		5.98E-05		5.98E-05			
19-20	6.14E-05		5.59E-05		5.12E-05		5.28E-05		4.80E-05		4.80E-05			
20-21	4.13E-05		4.44E-05		4.08E-05		4.34E-05		3.84E-05		3.84E-05			
21-22	4.32E-05		4.32E-05		3.88E-05		4.17E-05		3.52E-05		3.52E-05			
22-23	3.54E-05		3.45E-05		3.19E-05		3.58E-05		3.21E-05		3.21E-05			
23-24	3.18E-05		3.32E-05		3.08E-05		3.27E-05		2.92E-05		2.92E-05			
24-25	2.85E-05		3.17E-05		2.84E-05		2.95E-05		2.64E-05		2.64E-05			
25-30	3.64E-05		1.74E-05		1.58E-05		1.74E-05		1.50E-05		1.50E-05			
30-35	4.02E-06		4.32E-06		3.93E-06		4.35E-06		3.56E-06		3.56E-06			
35-40	<E-06		<E-05		<E-06		<E-05		<E-06		<E-06			
40-45														
45-50														
50-70														
70-100														

NOT REPRODUCIBLE

Having obtained the attenuation coefficient, γ [Eq. (13)], the laser transmittance for a horizontal path of length, L , at height, h , is given by $\tau = \exp(-\gamma_j L)$ when the suffix j , refers to the layer at height, h . For slant paths between two altitudes, Eq. (11) should be used with the appropriate correction for zenith angle.

5. ATMOSPHERIC TRANSMITTANCE AT LOW RESOLUTION FROM 0.25 TO 25 μm

The calculations presented in Section 4 were made at infinite resolution (monochromatic calculations). In practice it is impossible to measure radiation transmitted at a single frequency. Instead one measures the transmittance $\bar{\tau}_{\Delta\nu}(\nu)$ averaged over the spectral interval, $\Delta\nu$, accepted by the receiver, as indicated in the equation

$$\bar{\tau}_{\Delta\nu}(\nu) = \frac{1}{\Delta\nu} \int \tau(\nu) d\nu, \quad (14)$$

where ν is the central frequency in the interval, $\Delta\nu$. Consequently for many applications one is interested in knowing the transmittance of the atmosphere averaged over a relatively wide spectral interval, that is, for low resolution.

Thus the term transmittance is somewhat ambiguous unless it is qualified by some indication of the spectral resolution, $\Delta\nu$, over which it is averaged. This is particularly true in the case of molecular absorption, since the absorption coefficient k_m is a rapidly varying function of frequency. It is because of the rapid variation of k_m with frequency that the averaged transmittance $\bar{\tau}$ does not, in general, obey the simple exponential law given in Eq. (3). That is,

$$\bar{\tau}_{\Delta\nu}(\nu) = \frac{1}{\Delta\nu} \int \exp[-k_m(\nu)\Delta L] d\nu \neq \exp(-\bar{K}(\nu)\Delta L) \quad (15)$$

where k_m represents the net monochromatic molecular absorption coefficient as given in Eq. (9) and where \bar{K} is an average absorption coefficient, which cannot in most cases be defined when $\Delta\nu$ is much greater than the half width of a spectral line [see Eq. (8)].

On the other hand the molecular scattering coefficient (σ_{rn}) and the aerosol scattering and absorption coefficients [σ_a and k_a , see Eqs. (4a) and (4b)] are slowly varying functions of frequency, and the average transmittance (which can easily be obtained by interpolation from the monochromatic values, see Figures 21 and 22) obeys the simple exponential law [Eq. (3)] provided only the direct transmitted beam is being observed (see Zuev et al, 1967).

There are four basic approaches to obtaining low resolution transmittance values for a given path through the atmosphere due to molecular absorption. These are: (1) direct measurements over the required path, (2) measurements in the laboratory under simulated conditions, (3) line-by-line (monochromatic) calculations based on detailed knowledge of spectroscopic line parameters (see Section 3) which are then averaged over the required spectral interval, and (4) calculations based on band model techniques (which use available laboratory and/or field transmittance measurements or actual line data as a basis).

From the point of view of computations, method 3 involves a considerable amount of work and computer time, and consequently method 4 has been used most frequently.

In this section we will briefly discuss the problem of continuum absorption in the atmospheric window region (Section 5.1). Then we will summarize the application of band models to molecular absorption calculations (section 5.2) and present a detailed description of a graphical prediction scheme for determining the transmittance of the atmosphere due to line absorption, continuum absorption, and scattering (average over 20 cm^{-1}) for a given atmospheric path. First, the reader is provided with figures for determining the relevant absorber amounts in the required atmospheric path (Section 5.3), which are then used in conjunction with the transmittance charts (Section 5.4) to determine (separately) the transmittance due to: (1) molecular (line) absorption (H_2O , O_3 , and the uniformly mixed gases), (2) molecular (continuum) absorption (H_2O , N_2), (3) molecular (Rayleigh) scattering, and (4) aerosol extinction (absorption and scattering), as a function of frequency (wavelength).

Finally the reader has to multiply together the individual transmittances at each wavelength in order to determine the total transmittance at that wavelength. That is:

$$\begin{aligned} \bar{\tau}_{\Delta\nu}(\nu) \text{ (Total)} &= \bar{\tau}_{\Delta\nu}(\nu) \text{ (line absorption)} \times \bar{\tau}_{\Delta\nu}(\nu) \text{ (continuum absorption)} \\ &\times \bar{\tau}_{\Delta\nu}(\nu) \text{ (Rayleigh)} \times \bar{\tau}_{\Delta\nu}(\nu) \text{ (aerosol)}. \end{aligned}$$

5.1 Continuum Absorption in the Atmospheric Window Regions

There are a number of spectral regions of weak or negligible absorption by atmospheric molecules in the infrared which are generally called atmospheric windows. Various attempts have been made to determine the transparency of these window regions (Yates and Taylor, 1960; and Streete, 1968). Yates and Taylor (1960) concluded that the opacity in the near infrared windows is limited at sea level by aerosol scattering. This conclusion is consistent with the results which are derived from our aerosol chart presented in Section 5.4

As there are no laboratory data presently available from which the molecular absorption between absorption bands can be inferred (with two important exceptions), we will here assume that the gaps in the charts presented in Figures 16 through 18 are real gaps of zero molecular absorption. Thus, the attenuation in these regions is dependent entirely on molecular and aerosol scattering.

However, laboratory absorption data are available for the water vapor continuum (Burch, 1970; and McCoy et al, 1969), from 8-13 μm and also for the pressure induced (continuous absorption) band of nitrogen (Reddy and Cho, 1965) centered near 4.3 μm . The strongest part of this nitrogen band is not too important as it is centered beneath the very strong 4.3 μm CO_2 band. However, the nitrogen absorption extends out beyond the region of CO_2 absorption near 4.0 μm and becomes predominant, accounting for 20 percent absorption in a 10 km path at sea level.

Due to the continuous nature of these absorbing regions, the transmittance follows a simple exponential law which is represented by the scale in Figures 19 and 20.

5.2 Outline of Band Model Techniques

Basically, a band model assumes an array of lines having chosen intensities, half-widths and spacings, which can be adjusted to represent the line structure in some part of a real band. For a particular band model the mean transmittance can be represented by a mathematical expression (transmittance function); for example

$$\bar{\tau}_{\Delta\nu}(\nu) = f(C(\nu), \Delta L, P) \quad (16)$$

expressed in terms of pressure, P , effective path length (or absorber concentration) ΔL , and one or more frequency dependent absorption coefficients ($C(\nu)$'s).

Several band models have been developed (see Goody, 1952 and 1964; Elsasser, 1938; Plass, 1958; King, 1959 and 1964; and Wyatt et al, 1964); the Elsasser model (1942) and the Goody model (1952 and 1964) being most well known. The Elsasser band model consists of an array of equally spaced identical lines of Lorentz shape [see Eq. (7)]. This model has been applied to absorption bands which have a regular line structure, for example, to some bands of CO_2 , N_2O , CO , CH_4 and O_2 . The Goody model, on the other hand, assumes that the band is composed of spectral lines with an exponential intensity distribution and with random spacing between lines. Again the lines are assumed to have a Lorentz shape. This model has generally been applied to bands which have an irregular line structure, for example, to some H_2O and O_3 bands.

In practice the wavelength dependent coefficients are determined for each absorbing gas separately using laboratory transmittance values measured under

known conditions, that is by solving Eq. (16) for the $C(\nu)$'s at each ν for known values of $\bar{\tau}(\nu)$, ΔL , and P .

The absorption coefficients obtained in this way are then used in the band model transmittance function [Eq. (16)] to determine $\bar{\tau}(\nu)$ as a function of frequency ν for other values of ΔL and P for each absorber. Finally, the total mean transmittance for molecular absorption is given by the product of the mean transmittances of the individual absorbers at each frequency.

$$\begin{aligned} \bar{\tau}_{\Delta\nu}(\nu) \text{ (molecular absorption)} &= \bar{\tau}_{\Delta\nu}(\nu) (\text{H}_2\text{O}) \times \bar{\tau}_{\Delta\nu}(\nu) (\text{CO}_2) \\ &\times \bar{\tau}_{\Delta\nu}(\text{N}_2\text{O}) \times \bar{\tau}_{\Delta\nu}(\nu) (\text{O}_3) \text{ etc.} \end{aligned} \quad (17)$$

Exact analytical expressions have been obtained for most of the band models. However, they are sometimes difficult to use and simpler approximations have been found to apply in two limiting conditions, which are common to all band models. These simpler expressions are the well known "weak line" and "strong line" approximations (see Goody, 1964; and Plass, 1958) for which the transmittance is a function of the absorber amount, ΔL , and the product of the pressure and absorber amount, $P\Delta L$, respectively (for a given temperature).

The weak line approximation, which corresponds to the exponential law, is valid when the absorption is small at the line centers (generally for high pressures and low absorber amounts). Unfortunately this case is rarely applicable to conditions existing in the terrestrial atmosphere.

The strong line approximation is applicable where the lines are completely absorbing at their centers; the effect of increasing the amount of absorber is then confined to the edges or wings of the lines.

The regions of validity of the strong and weak line approximations for the Elsasser and Goody models are discussed in Plass (1958).

For practical purposes most problems fall in either the strong line approximation region or the intermediate regime. It is perhaps interesting to compare the functional form of the strong line approximation for some of the models.

For the Elsasser Model

$$\bar{\tau}_{\Delta\nu}(\nu) = 1 - \text{erf} [C(\nu) \Delta LP]^{1/2} \quad (18)$$

where erf is the error function $\left[\text{erf}(z) = \frac{2}{\sqrt{\pi}} \int_z^\infty e^{-t^2} dt \right]$ and $C(\nu)$ is an average absorption coefficient which can be written in terms of average values of the molecular line constants defined in Section 3.

The strong line approximation for the Goody model is given by

$$\bar{\tau}_{\Delta\nu}(\nu) = \exp \left\{ [C'(\nu) \Delta L P]^{1/2} \right\} \quad (19)$$

where $C'(\nu)$ is defined in a similar manner to $C(\nu)$ above.

King (1959) attempted to generalize the above expressions by writing

$$\bar{\tau}_{\Delta\nu}(\nu) = f [C''(\nu) \Delta L P^n] \quad (20)$$

so that when n is set equal to zero or unity, the average transmittance agrees with the weak or strong line approximations respectively.

In this report we have determined from laboratory and synthetic transmittance data, * three empirical transmittance functions based on Eq. (20) for (1) H_2O , (2) O_3 , and (3) the combined contributions of the uniformly mixed gases. It was found that Eq. (20) gave the best fit to laboratory and theoretical data over a wide spectral interval when: (1) $n = 0.9$ for H_2O , (2) $n = 0.4$ for O_3 , and (3) $n = 0.75$ for the uniformly mixed gases.

The corresponding empirical transmittance functions were found to give better agreement with laboratory and synthetic transmittance data than the commonly used band models over a wide range of pressures and absorber amounts.

The procedure used for determining the parameter n and function, f , defined in Eq. (20) will be briefly outlined below. By taking the logarithm of the inverse of Eq. (20), it will be seen that

$$n \log P + \log \Delta L = \log f^{-1} [\bar{\tau}_{\Delta\nu}(\nu)] - \log C''(\nu). \quad (21)$$

Thus for a given frequency ν and fixed values of average transmittance $\bar{\tau}_{\Delta\nu}(\nu)$, the righthand side of Eq. (21) becomes a constant.

A mean value for n was determined from Eq. (21) for a wide range of frequencies and several values of $\bar{\tau}$. Then for each frequency, $\bar{\tau}$ was plotted against $\log \Delta L P^n$, and the curves superimposed and the best mean curve determined. The "mean" curve thus obtained constitutes the empirical transmittance function and is displayed as the transmittance scale and associated scaling factor, $\log (\Delta L P^n)$, in the prediction charts given in Figures 16 through 18.

So far the discussion has been restricted to constant pressure paths. In the following section we will discuss the application of band models to variable pressure paths.

*Synthetic spectra here refers to monochromatic (line by line) transmittance calculations degraded in resolution to 20 cm^{-1} .

5.3 Equivalent Constant Pressure Paths and Absorber Amounts

Atmospheric paths may be divided into two types, namely, constant pressure paths (that is, horizontal paths of up to about 100 km) and slant or variable pressure paths. The extent of the former types of path is limited due to the curvature of the earth. Since the transmittance functions for constant pressure paths are simpler to handle than those for variable pressure paths, the problem is simplified by reducing the slant path to an "equivalent constant pressure path"; that is, to a constant pressure path which, ideally, has the same transmittance at each wavelength as does the actual slant path.

In this section we will discuss the construction and application of charts for determining the equivalent sea level path quantities for molecular absorption (including continuum absorption in the 4 μm and 8-13 μm region), molecular scattering and aerosol extinction based on the model atmospheres presented in Section 2.

5.3.1 MOLECULAR ABSORPTION

It has been assumed that for most practical purposes, the average transmittance is dependent on the product $\Delta L P^n$ where ΔL is the absorber amount and P is the pressure.

Here we will define the equivalent sea level amounts for each of the five model atmospheres given in Section 2 as the value of the above product (reduced to STP) averaged over a given atmospheric path for a particular absorber, that is

$$\Delta L_o \left(\frac{P}{P_o} \right)^n \quad \text{where the subscript (o) refers to STP.}$$

Since H_2O and O_3 are distributed nonuniformly in the atmosphere, we must consider these gases separately from the uniformly mixed gases.

For water vapor, n is set equal to 0.9 and $\Delta L_o \left(\frac{P}{P_o} \right)^n = R w(z) \left(\frac{P}{P_o} \right)^{0.9}$ where $w(z)$ is the water vapor concentration at altitude, z , in units of $\text{gm cm}^{-2}/\text{km}$ (obtained from Table 1), and R is the range in km. Since $w(z)$ is given in mass units there is no temperature or pressure correction necessary to reduce this quantity to STP. The variation with altitude of $w(z) \left(\frac{P}{P_o} \right)^{0.9}$ and $\int_z^\infty w(z) \left(\frac{P}{P_o} \right)^{0.9} dz$ (denoted by w_h and w_v respectively) is shown in Figures 2 and 3. The subscripts, h and v , refer to horizontal and vertical paths respectively.

For the uniformly mixed gases, n is set equal to 0.75, but the absorber concentration, ΔL_o (reduced to STP) for a horizontal path of range R at altitude z is given by $\Delta L_o = cR \left(\frac{P}{P_o} \right) \left(\frac{T_o}{T} \right)$ where c is the fractional concentration by volume of the absorbing gas (see Table 2 and Appendix). The terms P and T refer to the pressure and temperature at altitude z . Therefore, we have in this case

$\Delta L_o \left(\frac{P}{P_o}\right)^n \propto \left(\frac{P}{P_o}\right)^{1.75} \left(\frac{T_o}{T}\right)$. The variation with altitude of $\left(\frac{P}{P_o}\right)^{1.75} \left(\frac{T_o}{T}\right)$ and $\int_z^\infty \left(\frac{P}{P_o}\right)^{1.75} \left(\frac{T_o}{T}\right) dz$ (denoted by t_h and t_v respectively), is shown in Figures 4 and 5.

For ozone, n is set equal to 0.4 (see Section 5.2), and $\Delta L_o \left(\frac{P}{P_o}\right)^n = u(z) \left(\frac{P}{P_o}\right)^{0.4}$ where $u(z)$ is the ozone concentration in units of (cm - atm)/km at STP (obtained from Table 1). The variation with altitude of $u(z) \left(\frac{P}{P_o}\right)^{0.4}$ and $\int_z^\infty u(z) \left(\frac{P}{P_o}\right)^{0.4} dz$ (denoted by u_h and u_v respectively) is shown in Figures 6 and 7.

5.3.2 NITROGEN CONTINUUM (4 μ m REGION)

The absorption due to the nitrogen collision induced band is proportional to the square of the pressure. The effective absorber amount (reduced to STP) for a horizontal path of range R at altitude z is $cR \left(\frac{P}{P_o}\right)^2 \left(\frac{T_o}{T}\right)$. The variation with altitude of $\left(\frac{P}{P_o}\right)^2 \left(\frac{T_o}{T}\right)$ for horizontal paths and $\int_z^\infty \left(\frac{P}{P_o}\right)^2 \left(\frac{T_o}{T}\right) dz$ for vertical paths (denoted by n_h and n_v respectively) is shown in Figures 8 and 9.

5.3.3 WATER VAPOR CONTINUUM

Laboratory measurements of the water vapor continuum indicate that self-broadening due to water vapor molecules is much more important than broadening due to other atmospheric molecules (Burch, 1970). The appropriate equivalent sea level absorber amount for the water vapor continuum is

$$b_h = \frac{1}{P_o} \left[p_{H_2O} + 0.005 \left(P - p_{H_2O} \right) \right] w(z)$$

for horizontal paths, where P is the total pressure and p_{H_2O} is the partial pressure of water vapor ($p_{H_2O} = 4.56 \times 10^{-5} w(z) T(z)$ atm, where the constant is given by the ratio of the universal gas constant to the molecular weight of water vapor) and $w(z)$ is the number of (gm cm⁻²/km) of water vapor at altitude z obtained from Table 1. The equivalent sea level amount for vertical paths is given by

$$b_v(z) = \int_z^\infty \frac{1}{P_o} \left[p_{H_2O} + 0.005 \left(P - p_{H_2O} \right) \right] w(z) dz .$$

The variation with altitude of these functions, denoted by b_h and b_v respectively, is shown in Figures 10 and 11.

5.3.4 MOLECULAR SCATTERING

Molecular scattering is a function of atmospheric density $\rho(z)$ (Section 3). For each of the five model atmospheres given in Section 2, Figures 12 and 13 show the variation with altitude z of $\rho(z)/\rho_0$ and $\int_z^\infty \rho(z)/\rho_0 dz$ (denoted by m_h and m_v respectively) where ρ_0 is the density of air at STP.

5.3.5 AEROSOL EXTINCTION

Aerosol extinction is a function of the height variation of the aerosol number density $N(z)$ for a given size distribution function (Section 2.3). Figures 14 and 15 show the variation with altitude of $\frac{N(z)}{N_0}$ and $\int_z^\infty \frac{N(z)dz}{N_0}$ (denoted by a_h and a_v respectively) for the two hazy models given in Section 2.3 where N_0 is the number density (cm^{-3}) of aerosols at sea level for a visibility of 23 km.

5.3.6 UTILIZATION OF EQUIVALENT PATH FIGURES

For a given atmospheric path, let us consider how to obtain the equivalent sea level quantities for H_2O , O_3 , the uniformly mixed gases, the nitrogen and water continua, molecular scattering and aerosol extinction which will be denoted by W , U , L , N , B , M , and A respectively. At this point the reader need not be concerned with the units of these quantities which were chosen to facilitate the use of the prediction charts given in Section 5.4. The subject of units will be discussed separately in the Appendix.

Figures 2 through 15 show the variation with altitude of the relevant quantities for both horizontal and vertical paths (distinguished by suffixes h and v respectively). The use of these figures can best be illustrated by the following examples:

5.3.6.1 Horizontal Paths

To determine the equivalent sea level quantities for a horizontal path of length R (< 100 km) at an altitude z , simply multiply each of the quantities w_h , t_h , u_h , n_h , b_h , m_h and a_h (obtained from Figures 2, 4, 6, 8, 10, 12, 14 for the appropriate altitude z), by R (in kms). For example in the case of molecular line absorption by water vapor, W is given by

$$W = w_h(z)R. \quad (21)$$

5.3.6.2 Slant Paths

(1) The equivalent sea level quantities (W , L , U , N , B , M and A) for a slant path from altitude z to the top of the atmosphere at zenith angle θ are determined by multiplying each of the quantities w_v , l_v , u_v , n_v , b_v , m_v , and a_v (obtained from Figures 3, 5, 7, 9, 11, 13, 15 for the appropriate altitude z) by $\sec \theta$ (where $\theta < 80^\circ$). For example, in the case of molecular line absorption by water vapor

$$W = w_v(z) \sec \theta. \quad (22)$$

For $\theta > 80^\circ$, $\sec \theta$ should be replaced by $M(\theta)$ given in Figure 32 (see Section 7).

(2) For a slant path of range R between altitudes z_1 and z_2 , the value of W for molecular line absorption by water vapor is given by

$$W = \left[w_v(z_1) - w_v(z_2) \right] \times \frac{R}{z_2 - z_1}. \quad (23)$$

Similar expressions hold for L , U , N , B , M and A .

Corrections can also be applied to account for atmospheric refraction and earth curvature and these will be briefly summarized in Section 7.

Having now determined W (gm. cm^{-2}), U (cm-atm at STP), L (km), N (km), B (gm cm^{-2}), M (km) and A (km) one can use the prediction charts given in Figures 16 through 22 (Section 5.4).

5.4 Description and Use of Prediction Charts

The purpose of this section is to present a simple method of predicting atmospheric transmittance (at low resolution) which is applicable over a wide spectral interval and for a wide range of atmospheric paths. Of the methods available, the one originally devised by Altshuler (1961) is the most comprehensive that meets the above requirements, although based on fairly old experimental data. In view of this, an attempt has been made here to further simplify Altshuler's method and to update it by (1) using more recent laboratory and field transmittance data (Burch et al, 1962, 1964, 1965a, 1965b, 1965c, 1965d, 1967, and 1968) and (2) making some line by line calculations for molecular absorption (as discussed in Section 5.4) and averaging over the spectral interval ($\Delta\nu = 20 \text{ cm}^{-1}$).

Charts for calculating the transmittance due to molecular line absorption by water vapor (H_2O), ozone (O_3), the uniformly mixed gases (CO_2 , N_2O , CH_4 , CO , O_2), the nitrogen $4 \mu\text{m}$ continuum, the water vapor $8\text{-}13 \mu\text{m}$ continuum, molecular scattering, and aerosol extinction and absorption are presented in Figures 16 through 22. It will be noted that the effects of the different uniformly mixed gases

have been combined into one chart (Figure 17) (assuming the mixing ratios given in Table 2).

A description and outline of the use of the charts will now be given.

Each figure shows the variation of an attenuation coefficient with respect to wavelength, relative to a horizontal datum line for a given effective sea level path length or absorber amount. Also shown in each figure is a vertical transmittance scale associated with a set of scaling factors (for the absorber amount). In order to use these charts efficiently, it is necessary to trace the transmittance scale and associated scaling factors for each of the figures on to some transparent paper.

If the transmittance scale is now placed on its appropriate chart so that the scaling factor 1 rests on the datum line (as shown in Figure 16(b)), then one is in a position to read off the transmittance (for 1 gm. cm^{-2} of H_2O) as a function of wavelength. Simply move the chart horizontally until the transmittance scale is vertically above the required wavelength and read off the transmittance where the scale crosses the curve. For example, in Figure 16(b) the scale is set at 21 microns and indicates a transmittance of 0.10 for $W = 1 \text{ gm cm}^{-2}$ of H_2O .* If the transmittance is required for a different amount of absorber, for example, $W = 10 \text{ gm cm}^{-2}$, just displace the transmittance scale vertically until the scaling factor 10 is coincident with the datum line. Then move the scale horizontally to the required wavelength and read off the transmittance as described above.

The same procedure applies to Figures 17 through 22, 25 and 33, where it will be noted the datum line for scaling the absorber amounts is expressed as $1 (\text{cm-atm})_{\text{STP}}$ for O_3 (Figures 18 and 25), 1 gm cm^{-2} for the water vapor continuum (Figure 20), and 1 km for each of the other charts.

Thus by displacing the transmittance scale horizontally according to wavelength and vertically according to the appropriate equivalent sea level quantity (W , U , L , N , B , M or A) for Figures 16 through 22 respectively, one can construct a low resolution transmittance spectrum (for $\Delta\nu \geq 20 \text{ cm}^{-1}$).

A method for calculating the equivalent sea level absorber amounts W , U , L , N , B , M and A respectively (in the appropriate units) for a given atmospheric path has been described in Section 5.3 based on the ten model atmospheres defined in Section 2. In the case where the relevant meteorological parameters are known for the atmospheric path, these quantities can be calculated by an alternative method described in the Appendix.

5.5 Absorption in the Region 0.25 to 0.75 μm

The only atmospheric molecule considered in this report in the spectral region from 0.25 to 0.70 μm is ozone. Weak absorption bands due to water vapor and oxygen

*This corresponds to the amount of water vapor in a 1 km path at sea level for $T = 15^\circ\text{C}$ and 78 percent relative humidity (see Appendix).

also appear in this region but because of a lack of reliable data have not been included here. Since the absorption coefficient due to ozone in this wavelength range is independent of pressure, it is sufficient to define the amount of ozone in an atmospheric path with a single parameter proportional to the total number of molecules in the path. Figure 23 gives the ozone amount as a function of altitude in $(\text{cm-atm})_{\text{STP}}/\text{km}$ for each of the five atmospheric models, and should be used to determine the amount of ozone in a horizontal path. Figure 24 provides total ozone amounts between the top of the atmosphere and the indicated altitudes for each model atmosphere. Ozone amounts for vertical layers within the atmosphere can be found by subtraction of values read off Figure 24 for two different altitudes. Slant path amounts are found by multiplication of the vertical amount by $\sec \theta$ or $M(\theta)$ (see Section 7). For a discussion of the unit, $(\text{cm-atm})_{\text{STP}}$, used in this section, see the Appendix.

The amount of ozone in the required atmospheric path is determined from Figures 23 and 24. Then the atmospheric transmittance through the path is found as a function of wavelength from Figure 25 obtained from Inn and Tanaka (1953). The application of this figure is identical to that described earlier for the prediction charts given in Section 5.4.

5.6 Accuracy of Low Resolution Transmittance Calculations

The overall accuracy in transmittance which this technique provides is better than 10 percent. The largest errors may occur in the distant wings of rather strongly absorbing bands. The reason for this error is that a unique spectral curve as given in Figures 16-25 cannot be defined for all possible atmospheric paths. The curves presented in these figures were constructed for moderate atmospheric paths and will tend to overestimate the transmittance for very long paths and underestimate the transmittance for very short paths.

As the transmittance approaches 1.0, the percent error in transmittance decreases toward zero, but the uncertainty in the absorptance (or emissivity) increases greatly. In fact, if the computed transmittance exceeds 0.96, the uncertainty in absorptance becomes so great that the technique should not be used for a determination of atmospheric emission or background radiation.

Error is also introduced due to the neglect of temperature dependence in the model. The spectral curves of Figs. 16-25 were constructed for a temperature of 273K and atmospheric temperatures either cooler or warmer provide some variability. This effect is not too large for normal atmospheric temperatures except in the extreme wings of bands and in bands arising from an excited lower energy state where the population of the energy states is quite temperature dependent. This is usually only true for weak bands or in weak portions of stronger absorption bands and so is not too critical for our purposes. In general, cooler

temperatures will mean somewhat higher transmittance values and higher temperatures somewhat lower transmittance values.

It cannot be emphasized enough that the results obtained from these low spectral resolution curves should never be used in the determination of atmospheric attenuation for laser propagation. Detailed, very high spectral resolution measurements or calculations such as are presented in Table 5 and elsewhere (McClatchey, 1971 and McClatchey and Selby, 1972) are required for this purpose.

6. SCATTERED SOLAR RADIATION AND INFRARED EMISSION

6.1 Transmitted and Reflected Sky Radiance in Clear and Cloudy Sky

While the energy taken out of a beam of radiation by absorption contributes to heating of the air, the energy scattered by molecules, aerosols, or cloud droplets will be redistributed in the atmosphere. We will only consider the problem of sunlight incident on a plane parallel atmosphere. As long as only single scattering is important and a homogeneous atmosphere is assumed (aerosol/air mixing ratio constant with height), the angular distribution of skylight at a specific wavelength can be obtained from

$$B(M, M', \phi) = I_0 \left(\frac{M'}{M - M'} \right) \left(e^{-tM'} - e^{-tM} \right) \frac{F(\phi)}{t_s} \quad (24)$$

where

- I_0 = extraterrestrial solar irradiance (W cm^{-2})
- B = sky radiance ($\text{W cm}^{-2} \text{sterad}^{-1}$)
- M = secant of the solar zenith angle θ
- M' = secant of the line of sight angle θ'
- t = $a_v(\sigma_a + k_a) + m_v(\sigma_m + k_m)$ = total optical thickness per unit air mass (scattering and absorption by molecules and aerosols—see Section 5.3 for a_v and m_v ; σ_a , k_a , and σ_m can be derived from Figures 21 and 22 by taking the logarithm of the transmittance). With regard to molecular absorption (k_m), Eq. 24 is only valid for monochromatic radiation (see Table 5 for k_m values)
- t_s = $a_v \sigma_a + m_v \sigma_m = t_{s,a} + t_{s,m}$
- $F(\phi)$ = angular scattering function (molecular + aerosol) per unit air mass
 $= Q_a(\phi) \tau_{s,a} + Q_m(\phi) t_{s,m}$ (see Figure 26 for $Q_a(\phi)$ and $Q_m(\phi)$).

The scattering angle ϕ is defined by $\cos \phi = \cos \theta \cos \theta' - \sin \theta \sin \theta' \cos(\Delta\Psi)$ where $\Delta\Psi$ is the angular azimuth difference between the sun direction and the line of sight.

However, if tM or tM' becomes larger than 0.10, higher order scattering can no longer be neglected; this means that illumination of the scattering volume from the sky and reflecting earth's surface becomes increasingly important. Higher order scattering becomes dominant for tM or $tM' > 0.5$, particularly for high ground albedo. This is particularly true for the radiation leaving the top of the atmosphere (radiation to space). The general radiative transfer equation has been solved analytically only for molecular scattering, and detailed tables of sky radiance, polarization (including the Stokes parameters) have been prepared by Coulson et al (1960). Skylight distributions for hazy atmospheres have been computed by de Bary et al (1965) using these tables and Eq. (24). However, computers have made possible a statistical treatment of the scattering problem in any realistic hazy or cloudy atmosphere. By this Monte Carlo method, several investigators have computed the distribution of the radiance of the hazy atmosphere, both as seen from the ground (Figure 27a) and from space (Figure 27b). The assumed aerosol size distribution and vertical distribution is essentially the same as in Table 3. Dotted curves of the radiance (per unit solid angle and unit incident solar flux) are for the sun in the zenith, and solid lines are for the sun at $\theta = 86.3^\circ$.

In Figure 27a, the downward or "transmitted" radiance generally increases with decreasing wavelength when the sun is in the zenith. Forward scattering causes the radiance to peak near the sun. Near the horizon, the radiance increases again, except at short wavelengths, and the albedo influence is large. At low solar elevations, downward radiance is generally much smaller, especially near the zenith at long wavelengths, and the albedo influence is significant only at short wavelengths. Since the sky radiance values have been averaged over intervals of 0.1 in $\cos \theta$ (that is, over angular intervals ranging from 5° to 25°), the radiance near the sun actually should be much higher than shown.

In Figure 27(b), upward or reflected radiance as seen from outside of the atmosphere is strongly dependent on the albedo of the ground. The contribution of reflected ground radiance becomes dominant, especially in the near IR and in the nadir direction where the atmospheric backscattered flux becomes small. This effect will be less pronounced in more hazy atmospheres.

The distribution of sky radiance in the ultraviolet is dominated by multiple scattering and below $0.35 \mu\text{m}$ by ozone absorption. At high solar elevations, downward as well as upward radiances at $0.30 \mu\text{m}$ are only about 1 percent of their respective values at $0.40 \mu\text{m}$, but independent of albedo.

In the case of the radiance from clouds, we present Figures 28a and 28b for a rather dense nimbostratus (Kattawar and Plass, 1968). Aerosol and molecular

scattering have been neglected in this model because they would have little effect. The strong downward radiance (Figure 28a) for high sun and low albedo is largest near the sun, but with high albedo is nearly independent of the angle of observation. At low sun, the much smaller cloud radiance is largest in the zenith. The radiance of the cloud top (Figure 28b) again is very large at high sun. At low sun there is little discrimination between a cloudy and a clear sky (see Figure 27, $\lambda = 0.7 \mu\text{m}$).

An indication of the variability of the reflectance or spectral albedo of some natural objects may be obtained from Figure 29. The data presented are typical with respect to the wavelength dependence, but absolute reflectance may vary considerably for individual objects, and generally is higher for radiation near grazing incidence.

6.2 Infrared Emission of the Atmosphere

In the infrared from 5 to 25 μm and beyond, the atmospheric emission in a collimated beam can be determined by numerical integration of the equation of radiative transfer to give the upward radiance, $I(\nu)$:

$$I(\nu) = \int_{\tau_g}^{1.0} B(\bar{\nu}, T) d\tau + B(\bar{\nu}, T_g) \tau_g \quad (25)$$

where the integral represents the atmospheric contribution and the second term is the contribution from the ground (or lower boundary) modified by the total atmospheric transmittance τ_g between the boundary and the observer; τ is the transmittance which ranges between 1.0 at the level of observation and τ_g at the lower boundary (for example, the earth's surface or cloud top); $B(\bar{\nu}, T)$ is the Planck (black body) function corresponding to frequency $\bar{\nu}$ and the temperature T of an atmospheric layer, and T_g is the ground temperature.

To obtain the downward emission from a clear sky, the second term in Eq. (25) should be omitted and τ_g is then the transmittance of the entire atmosphere. In a cloudy sky the subscript, g , refers to a cloud base.

The effects of aerosols and of molecular scattering have been neglected and the molecular absorption charts described in Section 5.2 have been applied to the water vapor, ozone, and uniformly mixed gases corresponding to the Midlatitude Winter model. Equation (25) was then applied using the derived transmittance values and performing the numerical integration according to a numerical analogue of Eq. (25).

The results are presented in Figure 30 for both downward and upward beam radiation. The downward radiation case assumes the observer to be at the ground looking up at the zenith. The upward case assumes an observation point at the top of the atmosphere viewing the nadir (that is, looking down).

It should be noted that in the upward case the major absorption features (6.3 μm H_2O , 9.6 μm O_3 , and 15 μm CO_2) appear as relative minima, whereas in the downward case these same regions appear as relative maxima. The surface temperature, T_g , was taken to be the same as the temperature of the lowest atmospheric level in the model (272K). The upper curve in Figure 30 corresponds to a black-body at this boundary temperature.

For wavelengths shorter than 5 μm , the problem of upward and downward radiance is complicated by molecular and aerosol scattering and is, therefore, a function of the solar zenith angle. Computations of radiation between 3 and 5 micrometers is particularly complicated. Some examples of measured radiation in the 1 to 5 μm region are included in Figure 31.

7. REFRACTIVE EFFECTS IN THE ATMOSPHERE

Previously (Sections 3 and 5) it was indicated that slant path length could be obtained from vertical path length through multiplication by $\sec \theta$ for $\theta < 80^\circ$. For $\theta \geq 80^\circ$, the vertical path length (or other concentration parameter), ΔL , may be converted to slant path length by

$$\Delta L \text{ (slant path)} = \Delta L \text{ (Vertical)} \times M(\theta) \quad (26)$$

where $M(\theta)$ is the relative optical path, defined as the ratio of slant path length to vertical path length between two levels. The term $M(\theta)$ always equals $\sec \theta$ for a short path near the observer, and for any path if $\theta < 80^\circ$. For a long slant path, however, $M(\theta)$ becomes smaller than $\sec \theta$ because of the curvature of the atmosphere, which is partly compensated by refraction of the beam. This implies that the vertical distribution of a scattering or absorbing atmospheric constituent also influences the optical path, and the slant path length may have to be derived from Eq. (26) if high accuracy is warranted.

If curvature and refraction are considered, the general equation for the optical path between altitudes z_0 and z_1 of a constituent of density ρ at z and scale height

$$H = (z_1 - z_0) / \log_e [\rho(z_0) / \rho(z_1)] \text{ may be written}$$

$$M(\theta) = \left[\frac{\rho(z_0) - \rho(z_1)}{\rho(z_0)} H \right]^{-1} \int_{z_0}^{z_1} \left[1 - \frac{(r+z_0)^2}{(r+z)^2} \left(\frac{n_0}{n(z)} \sin \theta \right)^2 \right]^{-1/2} \rho(z) dz \quad (27)$$

where n is the refractive index of air and the (o) subscript refers to the lower reference level, and r is the radius of the earth.

For the molecular atmosphere and uniformly mixed atmospheric constituents, the air mass relative to the vertical air mass of the entire atmosphere measured from the ground, $M(\theta)$, as computed by Kasten (1967) is presented in Figure 32. These data are based on the ARDC Model Atmosphere of Minzner et al (1959) and a refractive index of air corresponding to a wavelength of $0.7 \mu\text{m}$. Earlier values of $M(\theta)$ of which the data by Bemporad (1907) are most often used, are in fair agreement. Kasten (1967) has shown that the average influence of latitude and season on $M(\theta)$ is less than 2 percent but abnormal tropospheric density profiles may have larger effects. Figure 32 compares $M(\theta)$ values for dry air with $M_w(\theta)$ values for an atmosphere containing water vapor with a distribution according to Schnaidt (1938). Values of $\sec \theta$ are included for comparison

The angular deviation between the actual and apparent solar zenith angles, $\Delta\theta$, due to refractive effects is presented in Table 6.

Table 6. Difference between Actual and Apparent Zenith Angle as a Function of Apparent Zenith Angle

θ_{app} (DEG)	75	80	83	85	86	87
$\Delta\theta$ (DEG)	0.061	0.090	0.124	0.167	0.199	0.248
θ_{app} (DEG)	88	88.5	89	89.5	90	
$\Delta\theta$ (DEG)	0.311	0.358	0.417	0.497	0.570	

Table 7. Relative Optical Path of a Thin, High Altitude Layer as a Function of Zenith Angle θ

θ	Height of Layer (km) Above Surface					
	10	20	30	40	50	60
70	2.89	2.86	2.83	2.80	2.77	2.74
75	3.78	3.71	3.63	3.57	3.50	3.44
80	5.49	5.26	5.05	4.87	4.70	4.56
85	9.66	8.51	7.70	7.08	6.60	6.20
87	13.07	10.56	9.11	8.13	7.41	6.86
88	15.17	11.58	9.74	8.57	7.74	7.12
89	17.08	12.37	10.19	8.87	7.96	7.28
89.5	17.66	12.58	10.30	8.94	8.01	7.33
90	17.88	12.66	10.35	8.97	8.03	7.34

For thin atmospheric layers (10 km or less) at high altitudes (where refractive effects can be neglected), Table 7 provides the geometric portion (that is, the effect is due to curvature only) of the slant path correction. For example, the geometric path through a thin layer at 30 km viewed at a zenith angle of 90° is 10.36 times the geometric path in the vertical. However, the optical path through a uniformly mixed atmospheric constituent at the same viewing angle would be 36.3 (see Figure 32). This situation may occur in the treatment of transmittance through the ozone layer or stratospheric dust layers.

8. EFFECT OF CLOUDS AND FOG ON ATMOSPHERIC RADIATION

As in the case of aerosol extinction (Section 3.2) when a beam of radiation is intercepted by a cloud or fog layer, some of the incident radiation may be absorbed and some may be scattered out of this beam with both effects thereby causing a net attenuation of the original radiation. The magnitude of the attenuation depends on the number, size distribution and refractive index of the suspended droplets and on the thickness of the layer. Since the radiation may be scattered in all directions, including those close to that of the original beam, the resulting attenuation may also depend on the acceptance angle of the receiver.

Natural fogs and low level clouds are composed of spherical water droplets, the refractive properties of which have been fairly well documented in the spectral region of interest here (Kislovskii, 1959; and Irvine and Pollack, 1968). However, in the case of cirrus clouds the particles consist of ice crystals of various shapes (hexagonal or cylindrical crystals) which, when mutually oriented, can give rise to anomalous scattering and polarization phenomena when radiation is propagated through them.

In this section we will restrict ourselves to the propagation of a collimated beam of radiation. Generally, fogs and clouds show only a small increase in transmittance with wavelengths from the visible to about $6 \mu\text{m}$. Beyond $6 \mu\text{m}$, a greater increase is observed. However, certain infrequently occurring types of fog characterized by a sharply peaked distribution of small droplets (this phenomenon is also found near the base of stratus and cumulus clouds), show a significant increase in infrared transmittance.

These general effects can be seen from Figure 33, which shows the wavelength variation of the extinction coefficient for a drop size distribution representative of fair weather cumulus cloud after Deirmendjian (1964 and 1969). The model drop size distribution (shown in Figure 34), which is given by

$$n(r) = 2.373 r^6 e^{-1.5r} \text{ cm}^{-3} \mu\text{m}^{-1}, \quad (28)$$

has a maximum corresponding to a radius of $4 \mu\text{m}$ and is normalized to $100 \text{ drops cm}^{-3}$

Figure 33 was calculated and based on single scattering theory, using the complex refractive index values for water given by Kislovskii (1959) and Eq. (28).

It will be seen from Figure 33 that the attenuation due to this fairly thin model cloud is rather severe; for example, for a 100m path length the transmittance is approximately 0.3 and 0.15 at $10 \mu\text{m}$ and $1 \mu\text{m}$ respectively.

Some mention should be made, at this point, of the validity of using single scattering theory to account for the attenuation of radiation in cloud.

It has generally been assumed that calculations of attenuation based on single scattering theory are valid for an optical thickness of less than 0.03 (van de Hulst's criterion) and that for values of optical thickness in excess of unity, secondary and multiple scattering effects become important. However, this applies to the propagation of diffuse radiation. For a narrow beam of collimated radiation (or laser beam propagation) it has been found (Zuev et al, 1967) that single scattering theory can account for the observed attenuation for values of optical thickness of up to 25. In this context optical thickness is defined as the product of the extinction coefficient and path length.

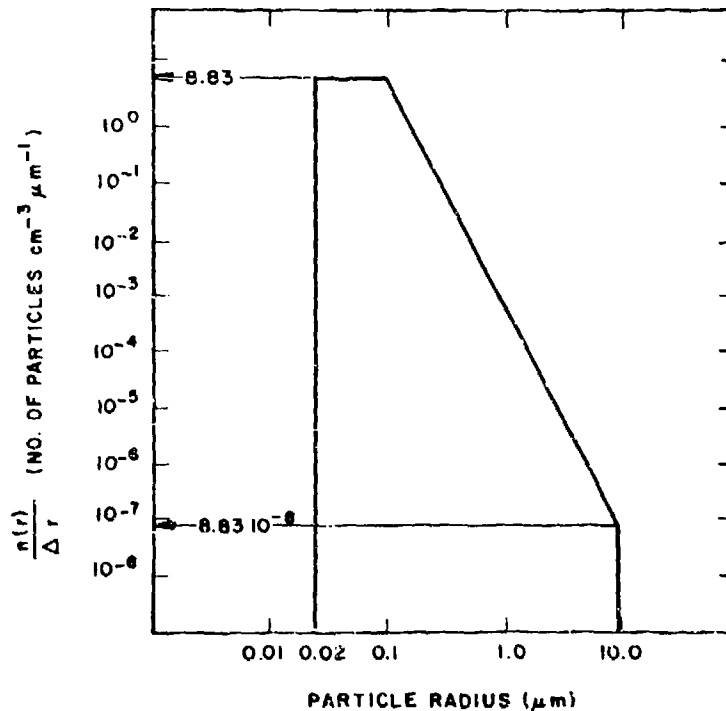


Figure 1. Normalized Particle Size Distribution for Aerosol Models

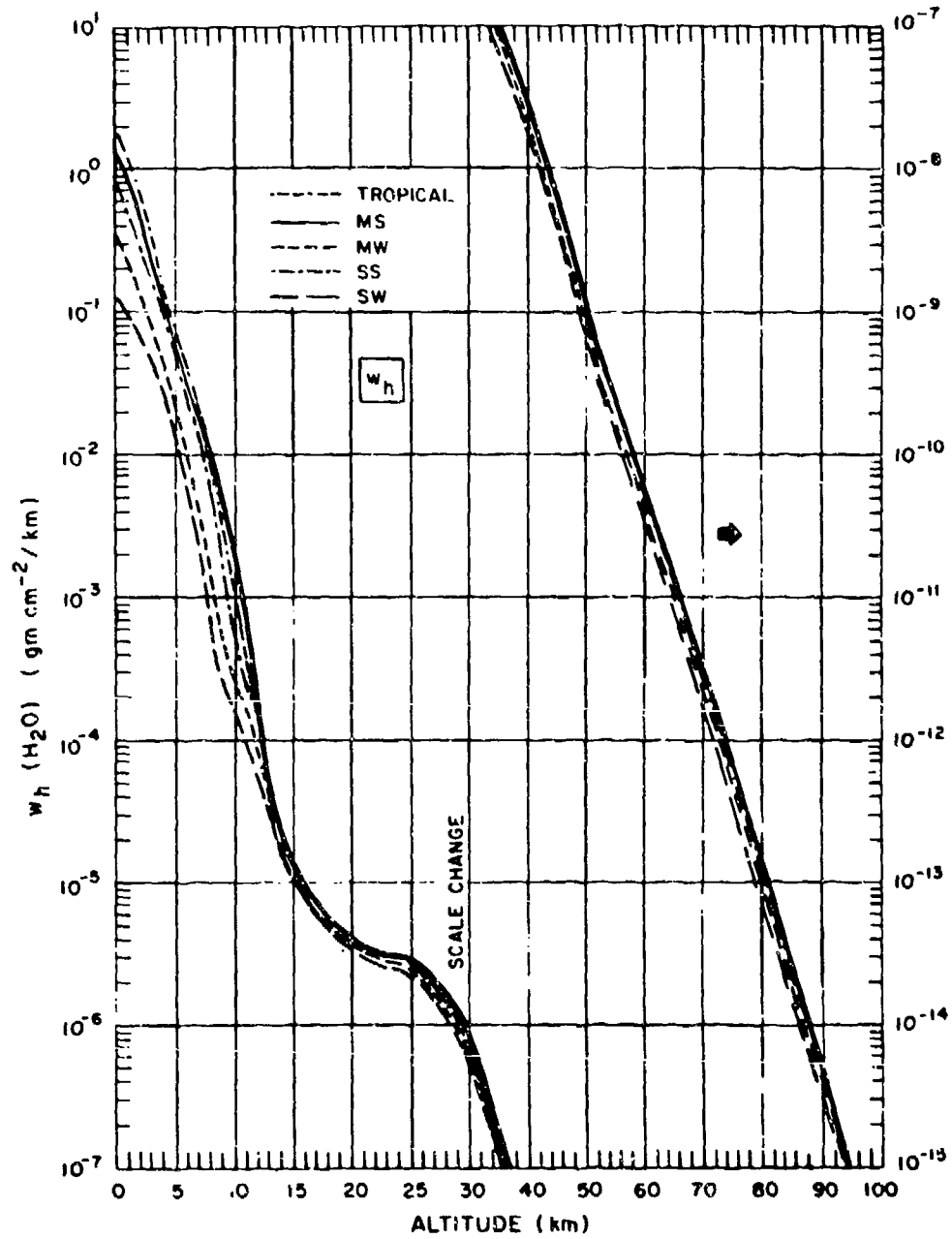


Figure 2. Equivalent Sea Level Path Length of Water Vapor as a Function of Altitude for Horizontal Atmospheric Paths

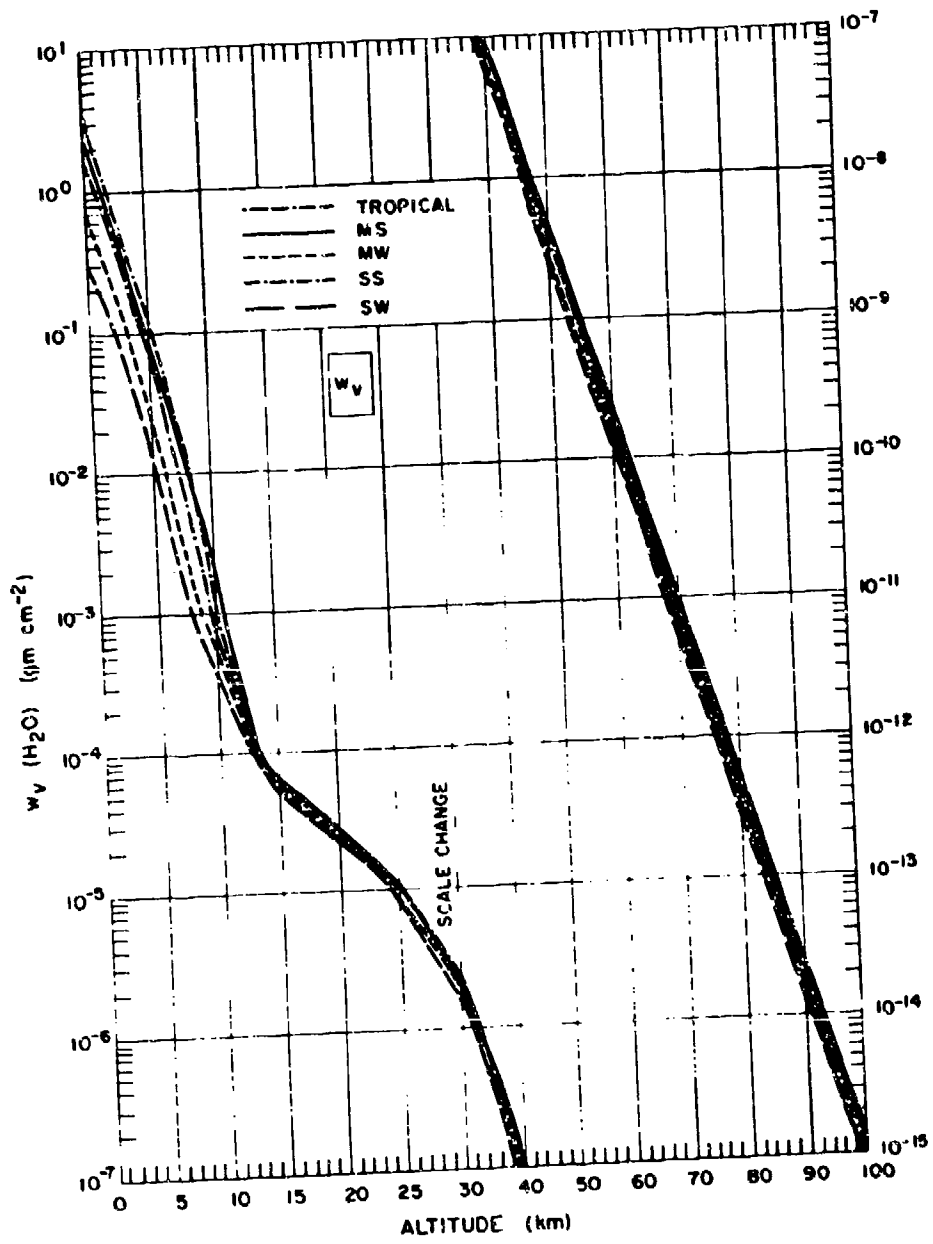


Figure 3. Equivalent Sea Level Path Length of Water Vapor as a Function of Altitude for Vertical Atmospheric Paths

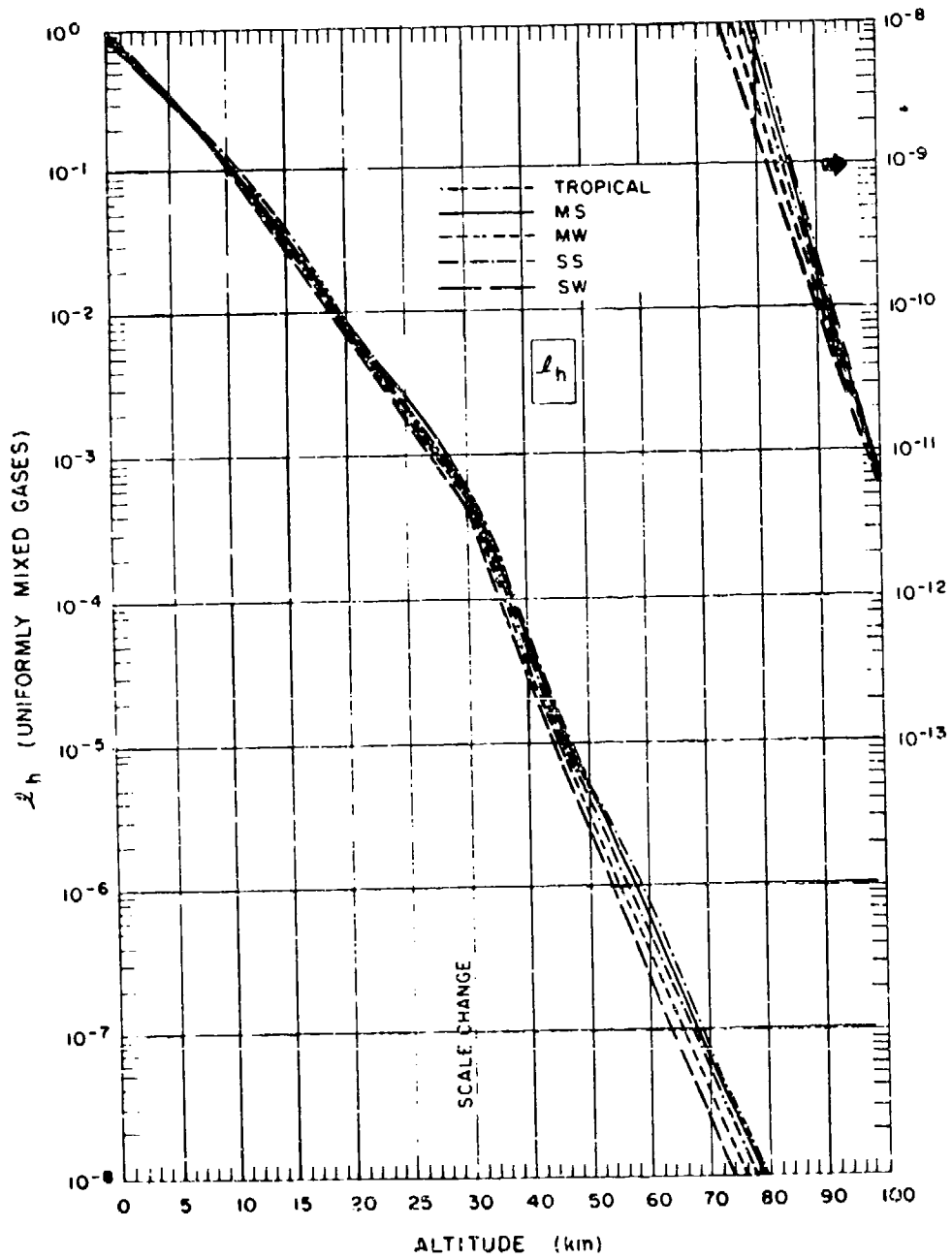


Figure 4. Equivalent Sea Level Path Length of Uniformly Mixed Gases as a Function of Altitude for Horizontal Atmospheric Paths

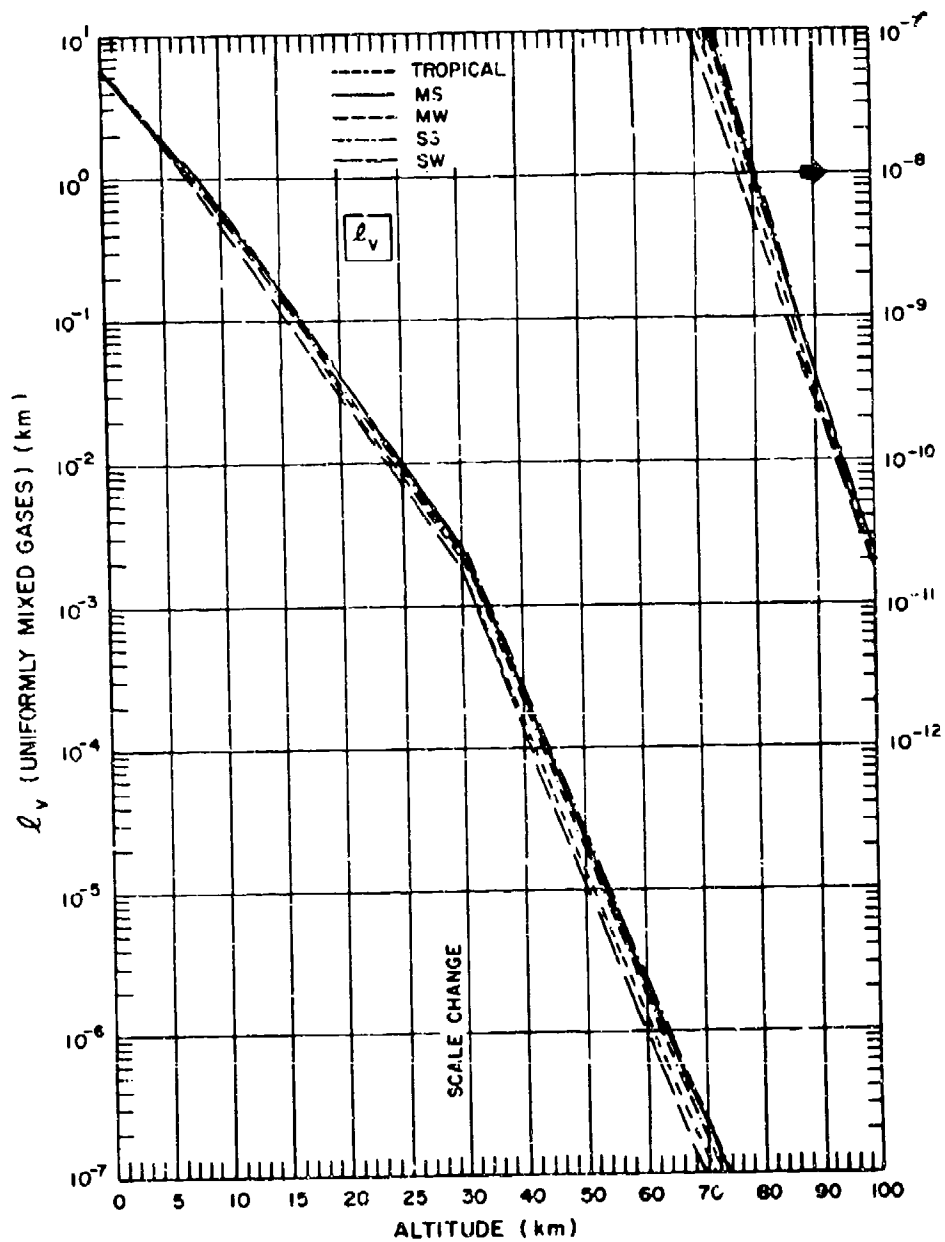


Figure 5. Equivalent Sea Level Path Length of Uniformly Mixed Gases as a Function of Altitude for Vertical Atmospheric Paths

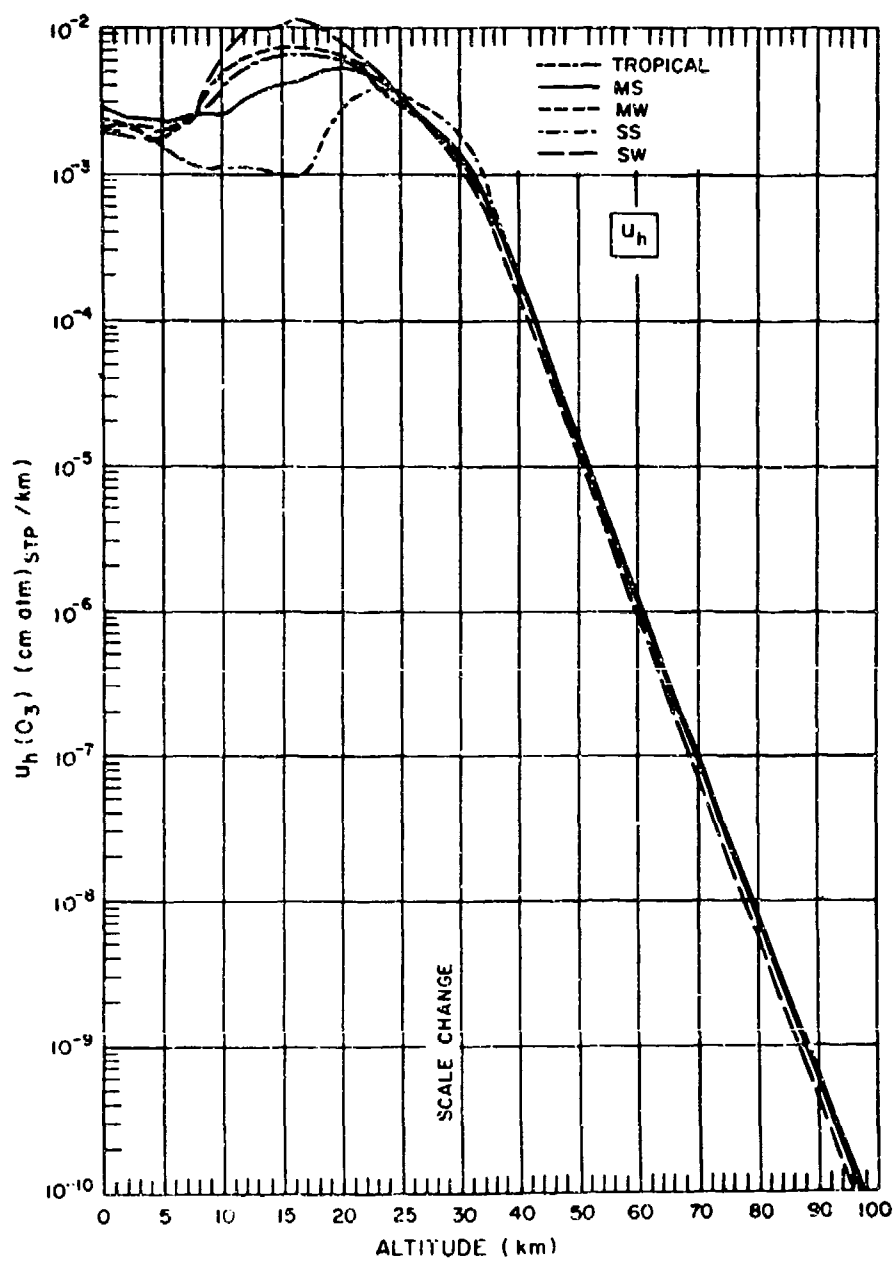


Figure 6. Equivalent Sea Level Path Length of Ozone as a Function of Altitude for Horizontal Atmospheric Paths

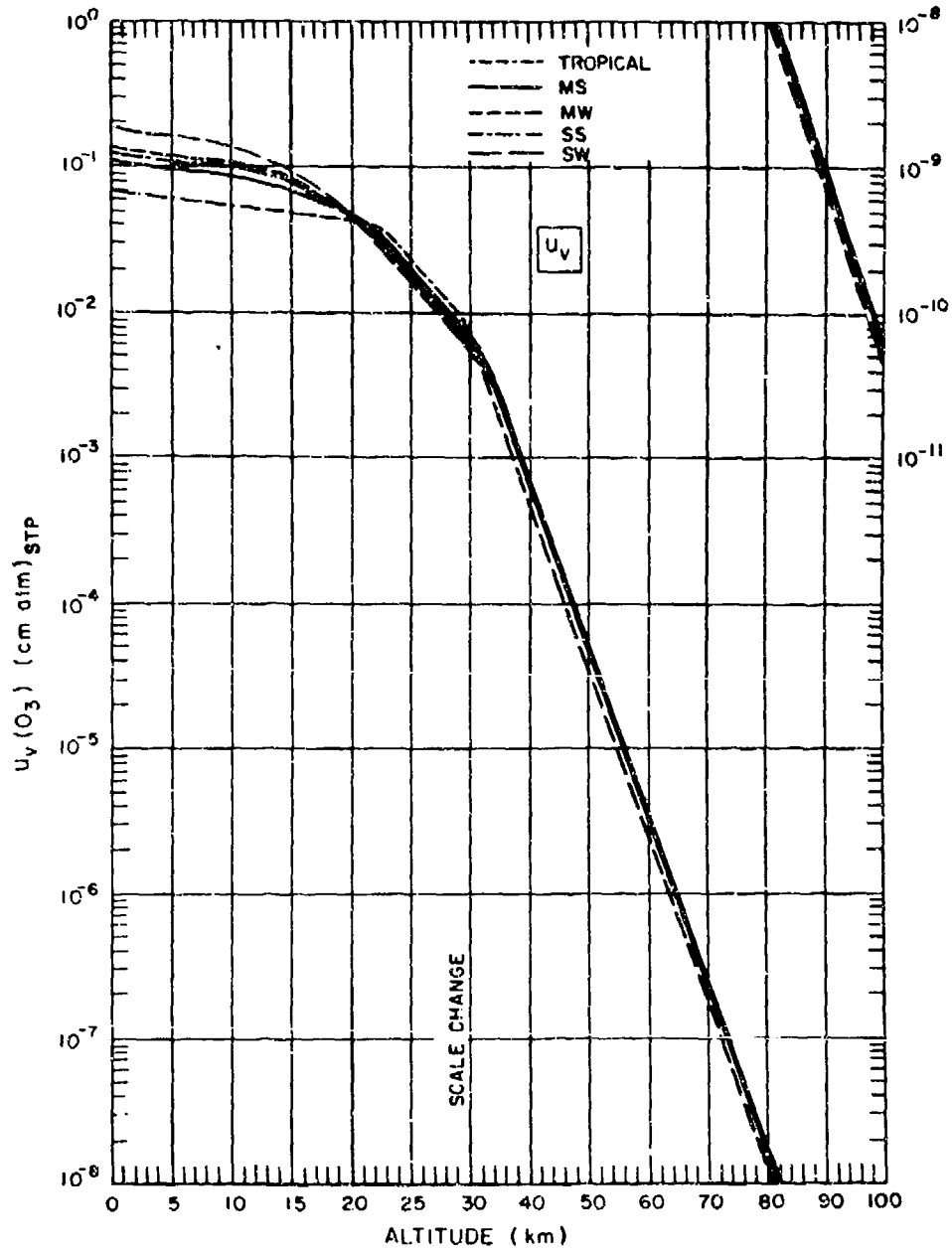


Figure 7. Equivalent Sea Level Path Length of Ozone as a Function of Altitude for Vertical Atmospheric Paths

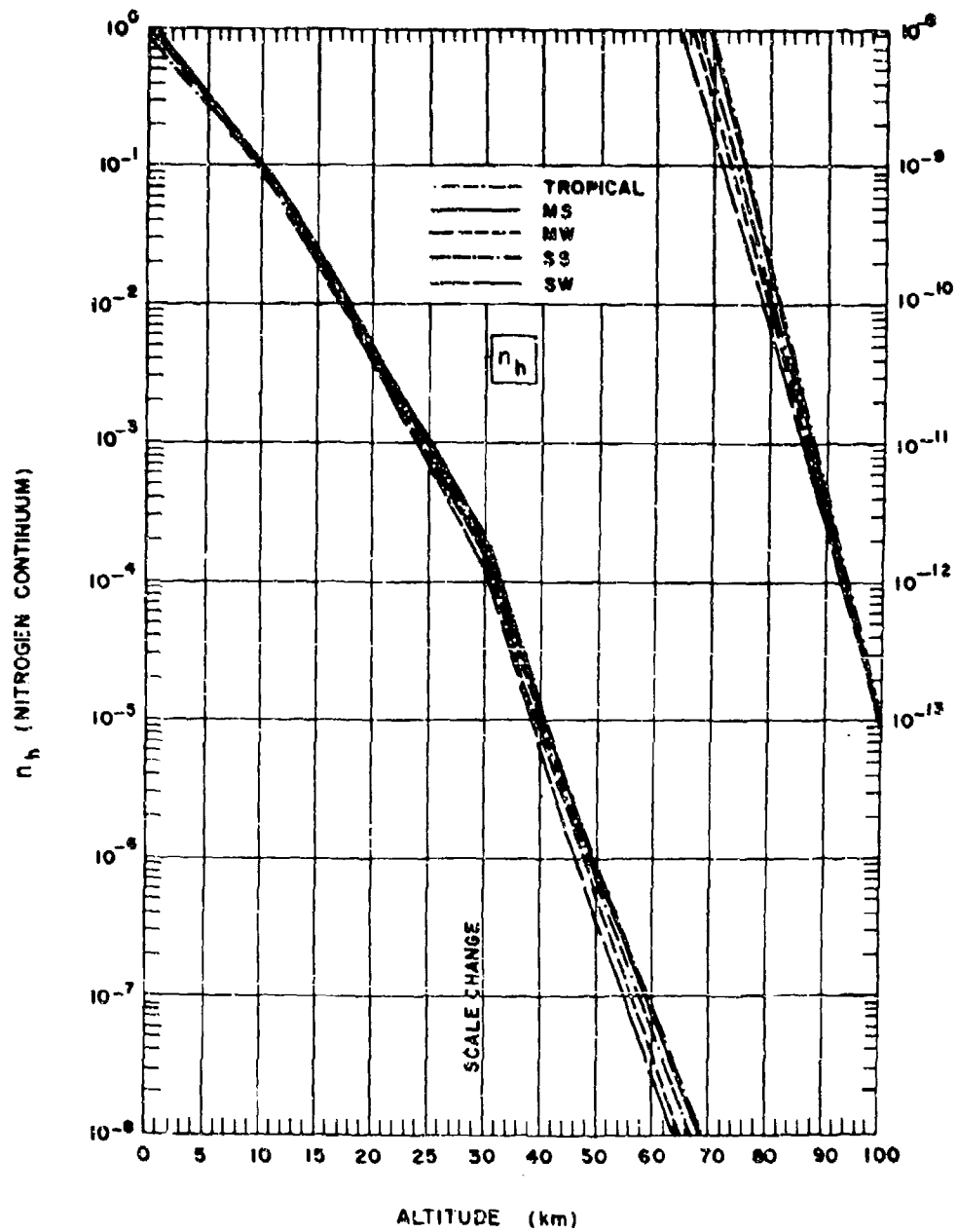


Figure 8. Equivalent Sea Level Path Length of Nitrogen as a Function of Altitude for Horizontal Atmospheric Paths

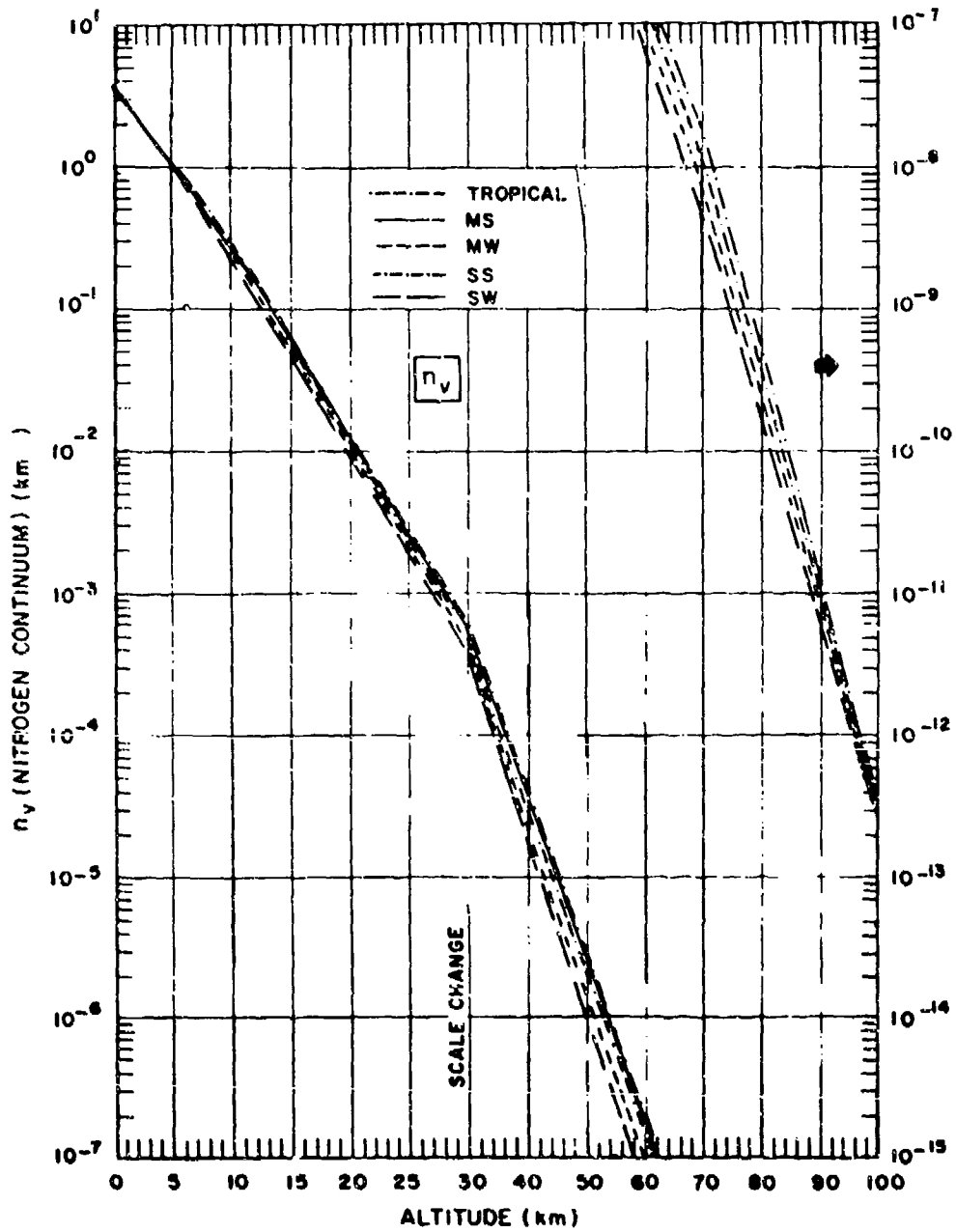


Figure 9. Equivalent Sea Level Path Length of Nitrogen as a Function of Altitude for Vertical Atmospheric Paths

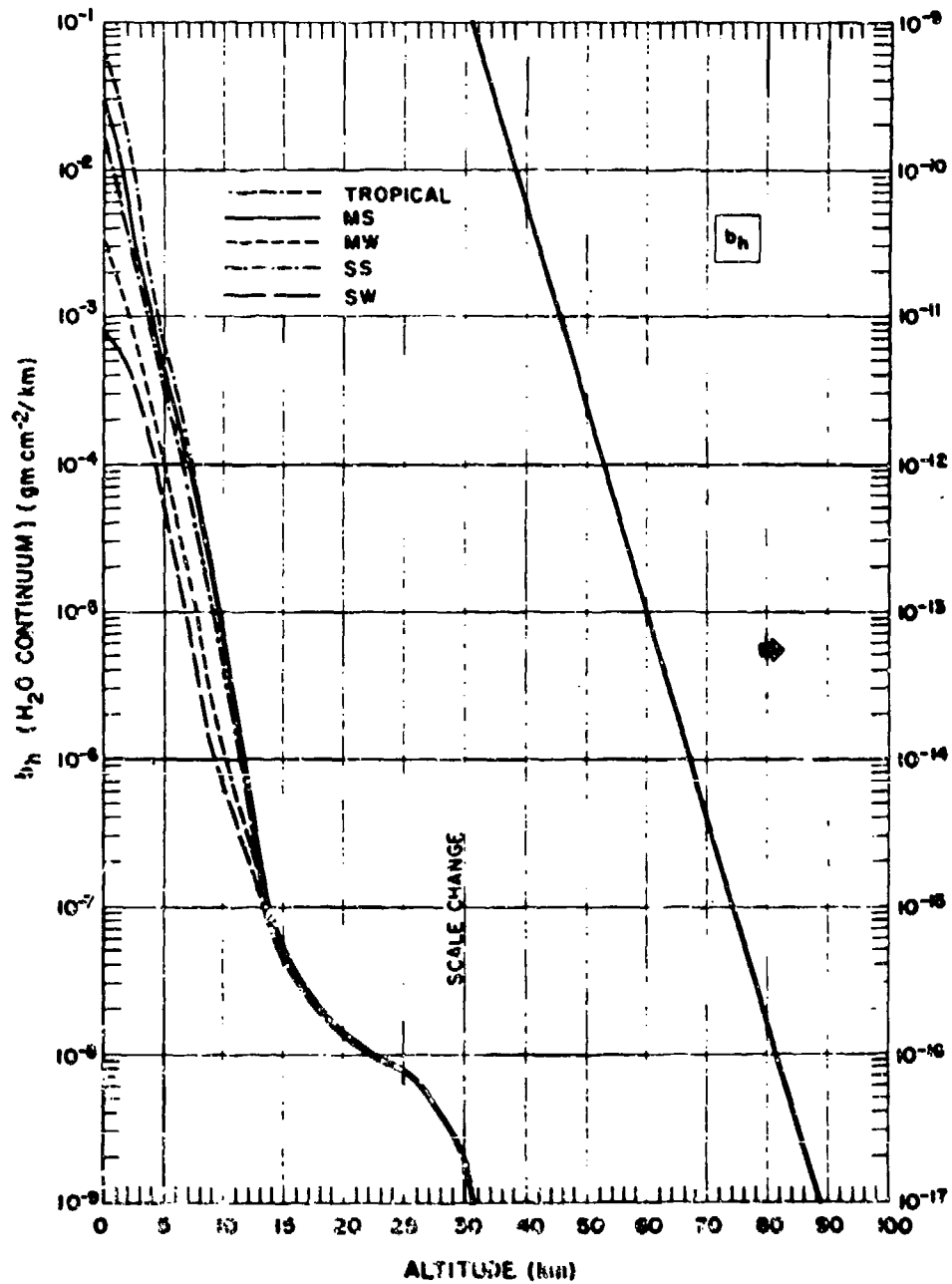


Figure 10. Equivalent Sea Level Path Length for Water Vapor Continuum as a Function of Altitude for Horizontal Atmospheric Paths

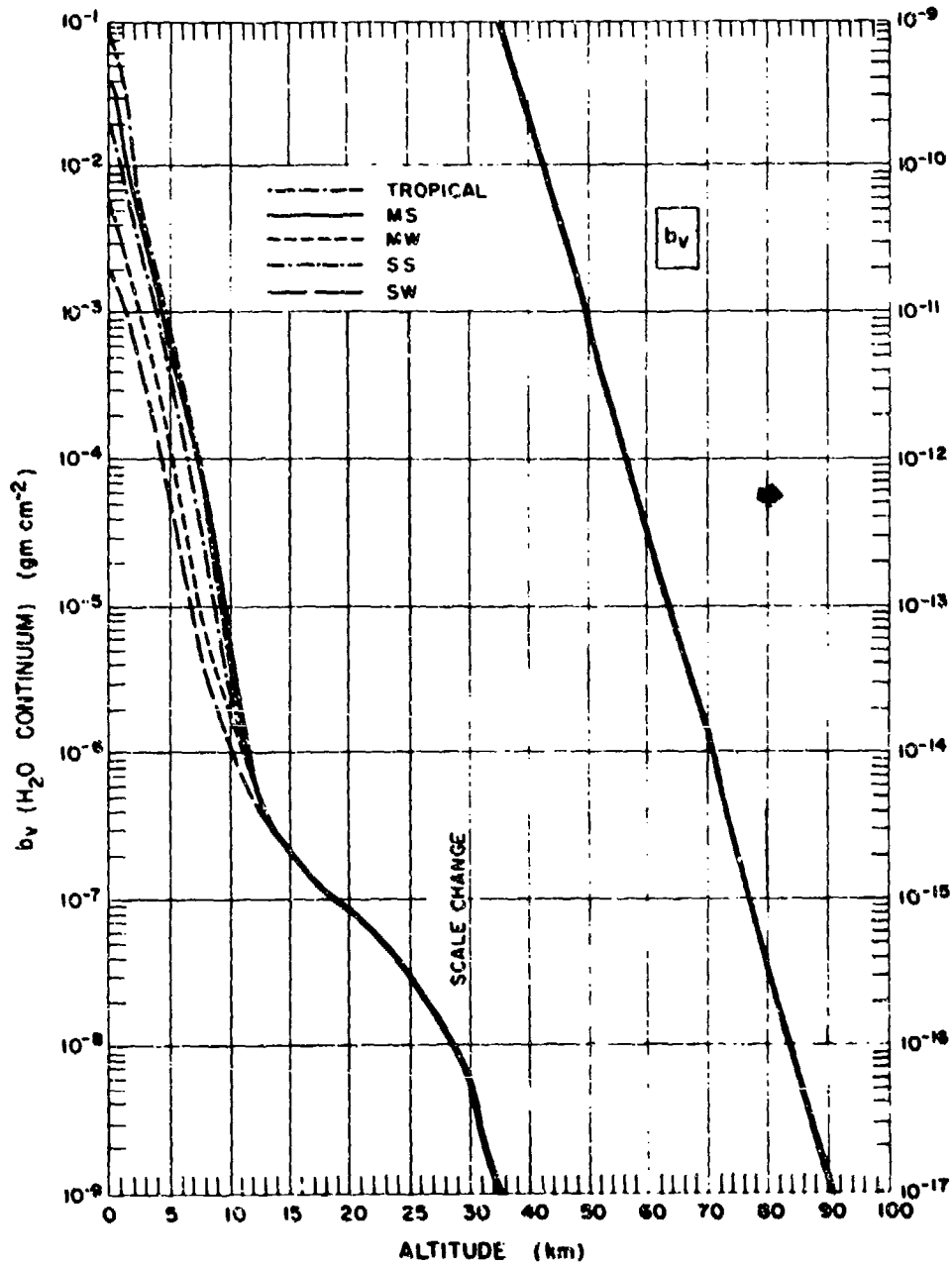


Figure 11. Equivalent Sea Level Path Length for Water Vapor Continuum as a Function of Altitude for Vertical Atmospheric Paths

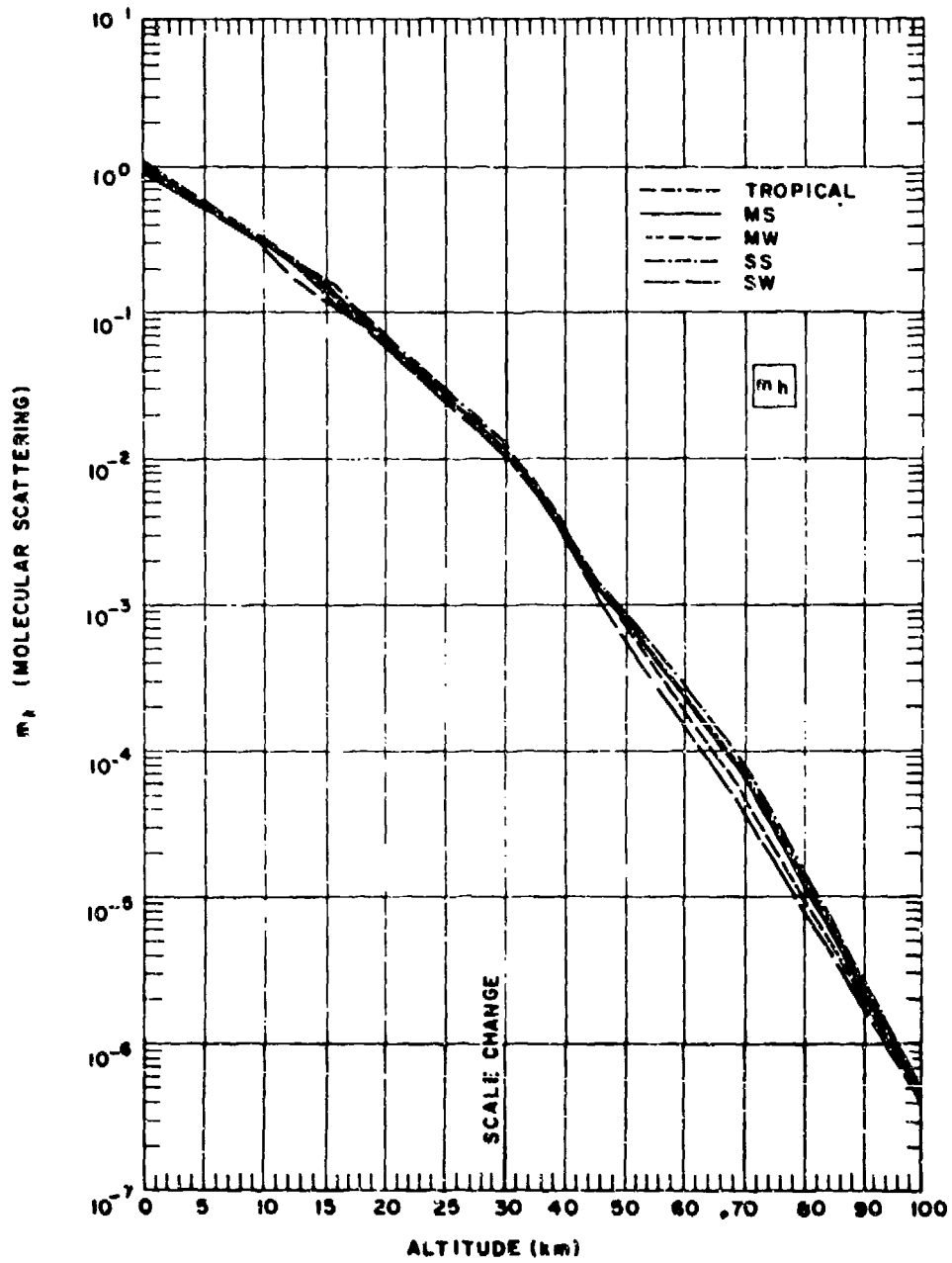


Figure 12. Equivalent Sea Level Path Length for Molecular Scattering as a Function of Altitude for Horizontal Atmospheric Paths

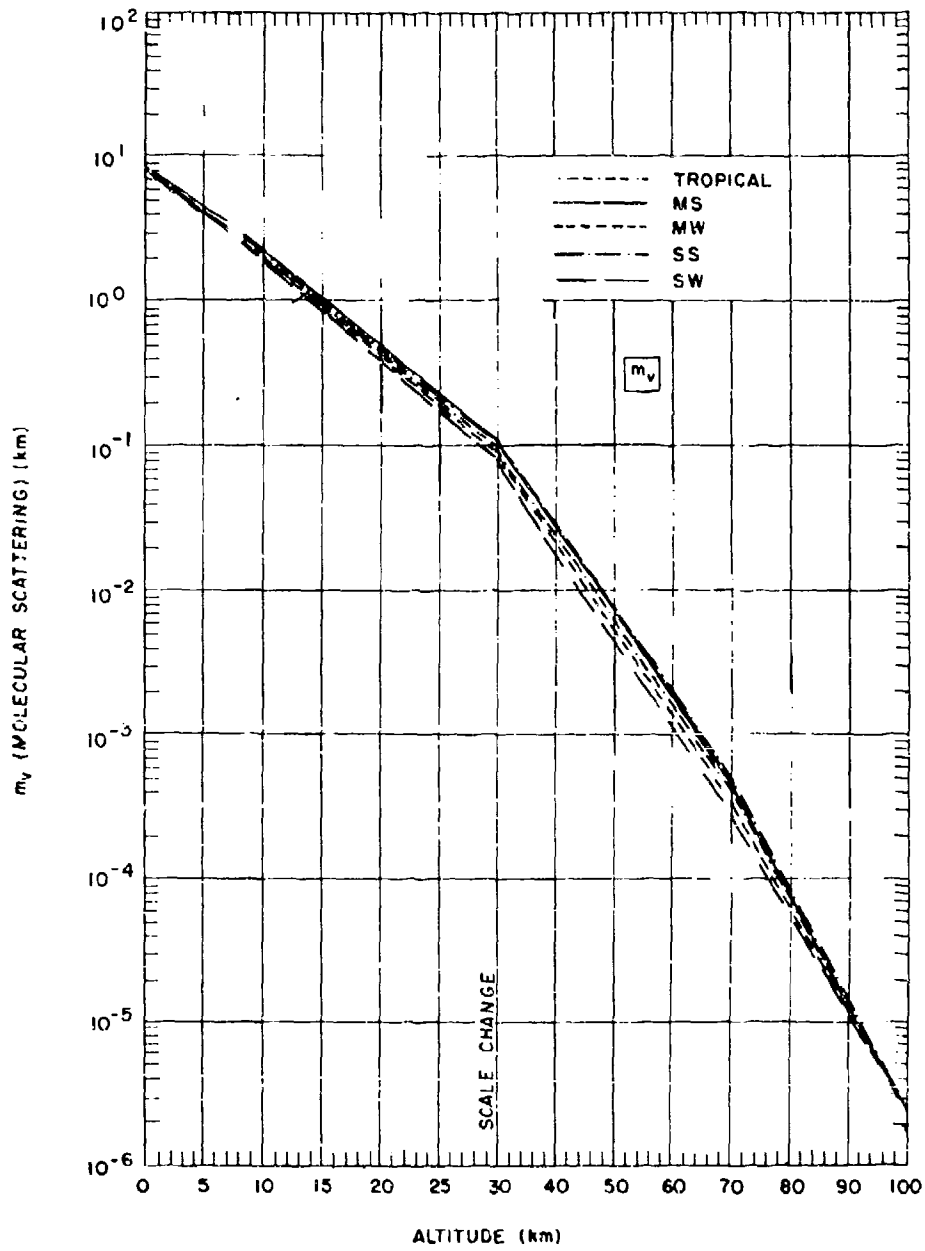


Figure 13. Equivalent Sea Level Path Length for Molecular Scattering as a Function of Altitude for Vertical Atmospheric Paths

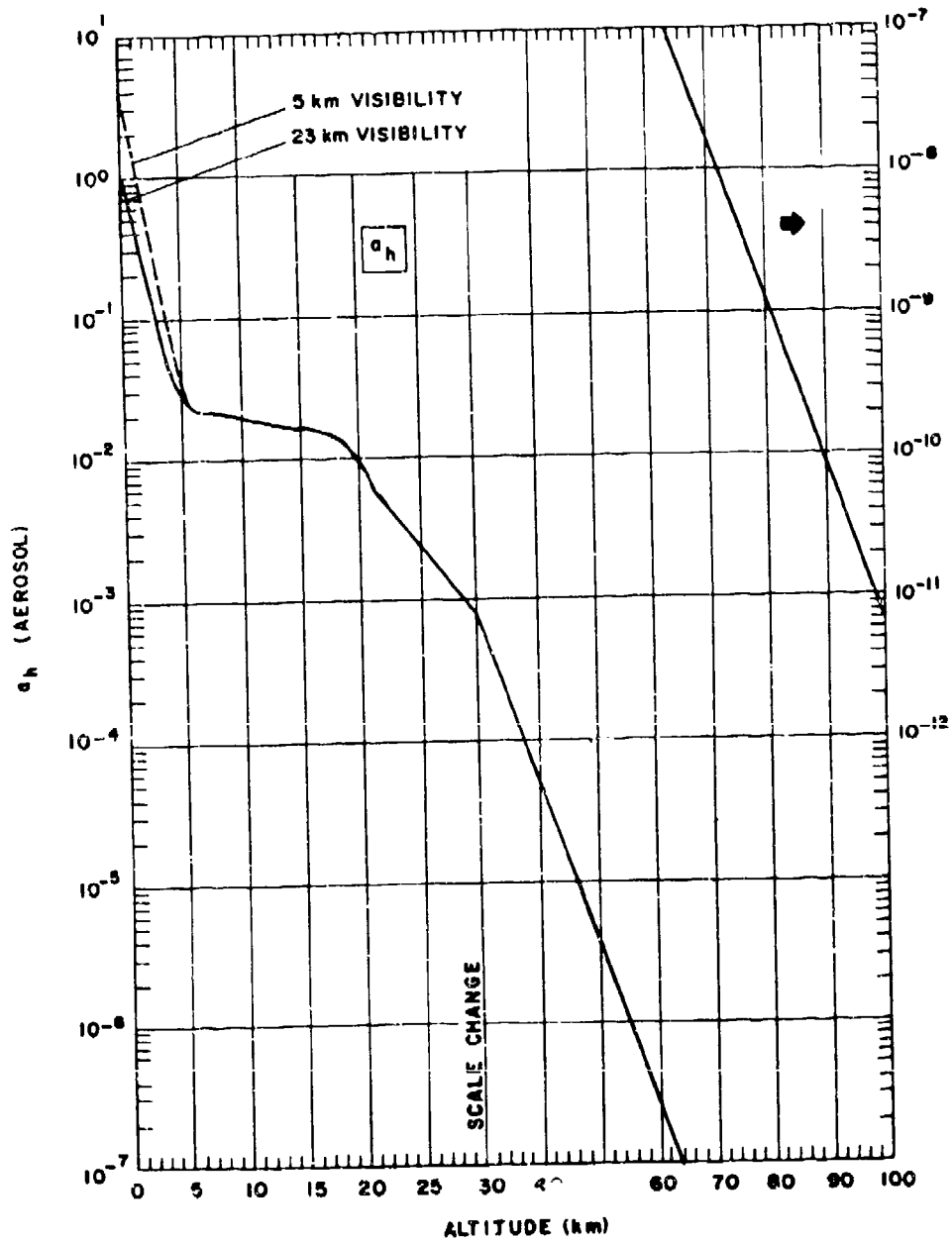


Figure 14. Equivalent Sea Level Path Length for Aerosol Extinction as a Function of Altitude for Horizontal Atmospheric Paths

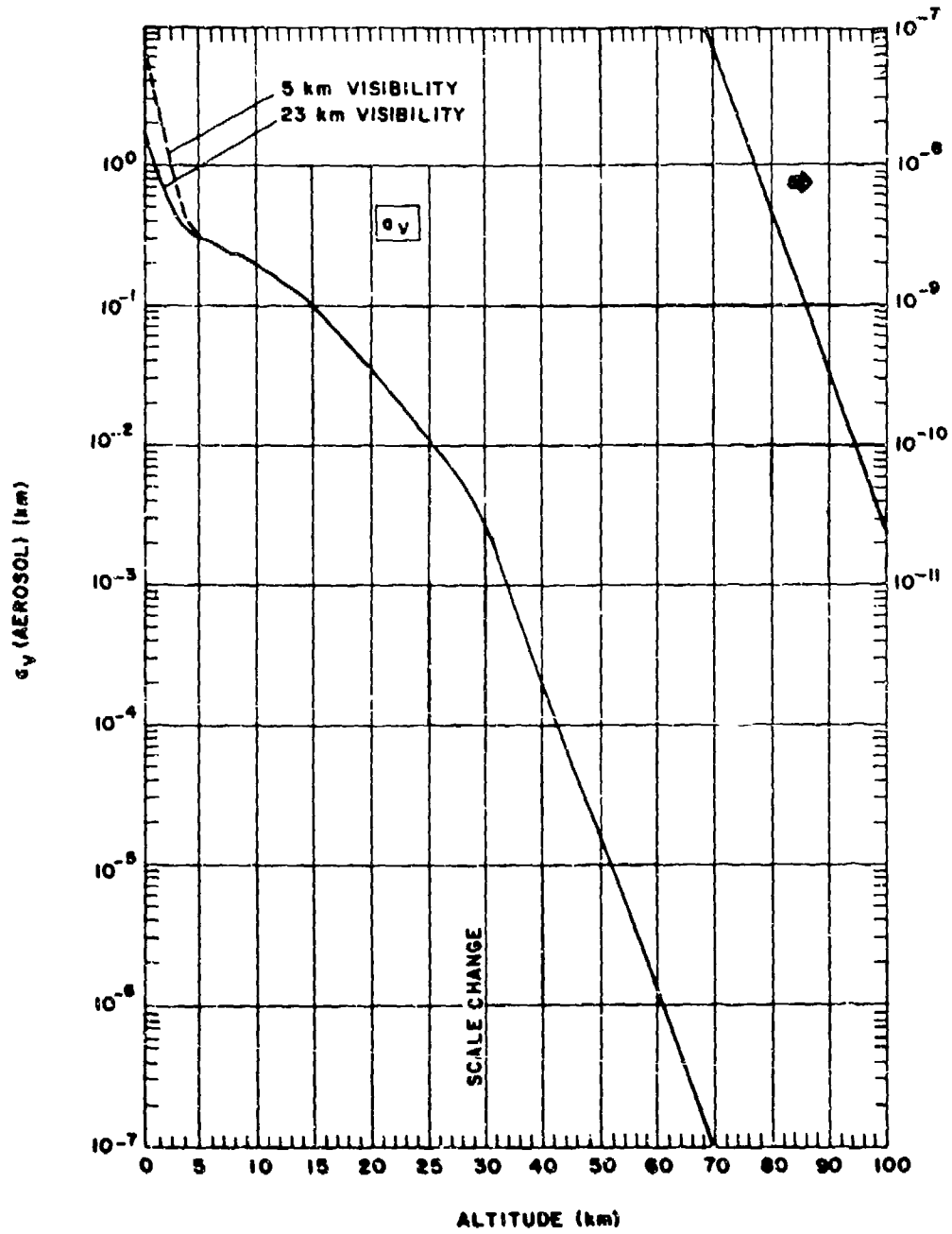


Figure 15. Equivalent Sea Level Path Length for Aerosol Extinction as a Function of Altitude for Vertical Atmospheric Paths

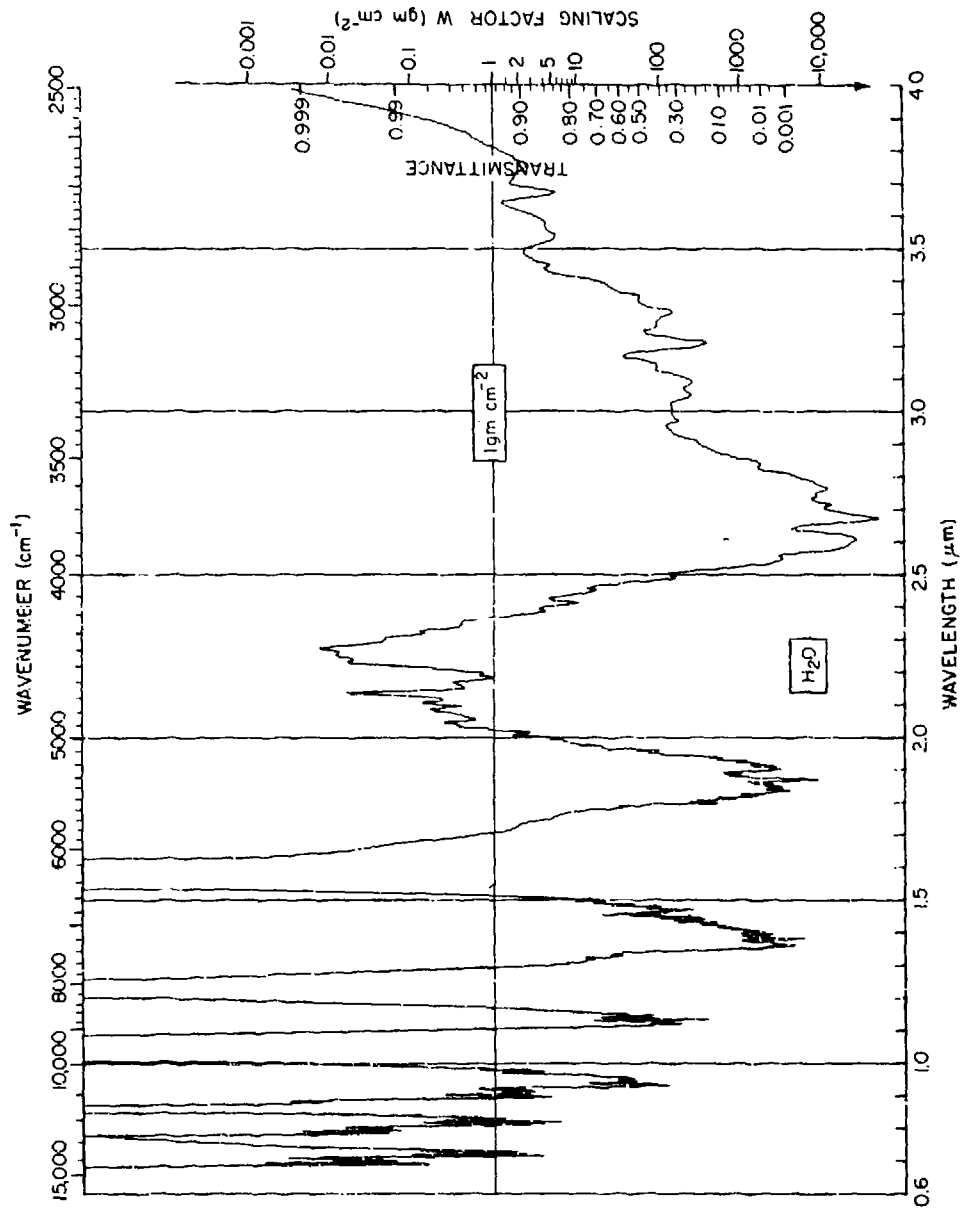


Figure 16a. Prediction Chart for Water Vapor Transmittance (0.6-4.0 μm)

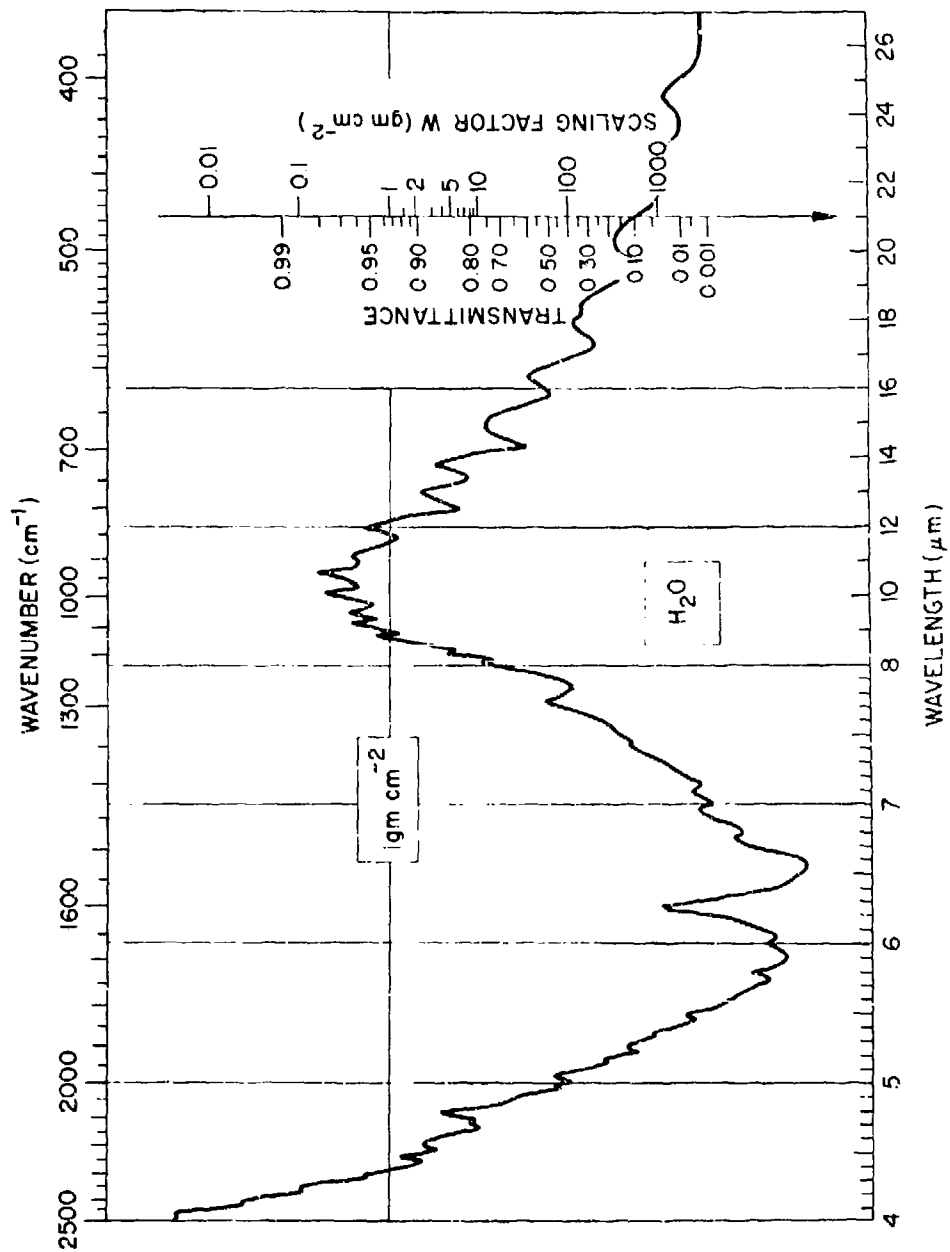


Figure 16b. Prediction Chart for Water Vapor Transmittance (4-26 μm)

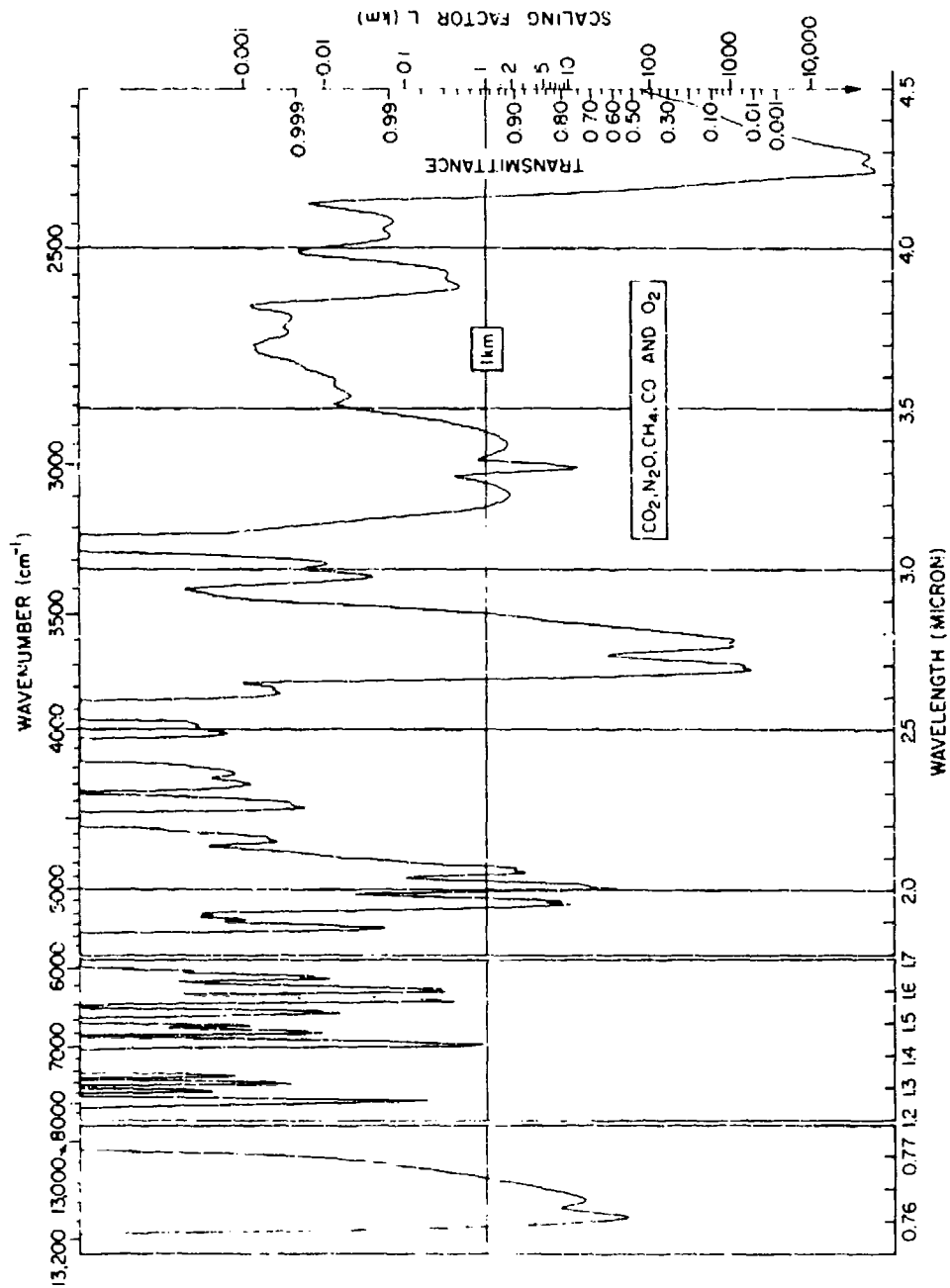


Figure 17a. Prediction Chart for the Transmittance of Uniformly Mixed Gases (CO_2 , N_2O , CO , CH_4 , O_2) (0.76-4.5 μm)

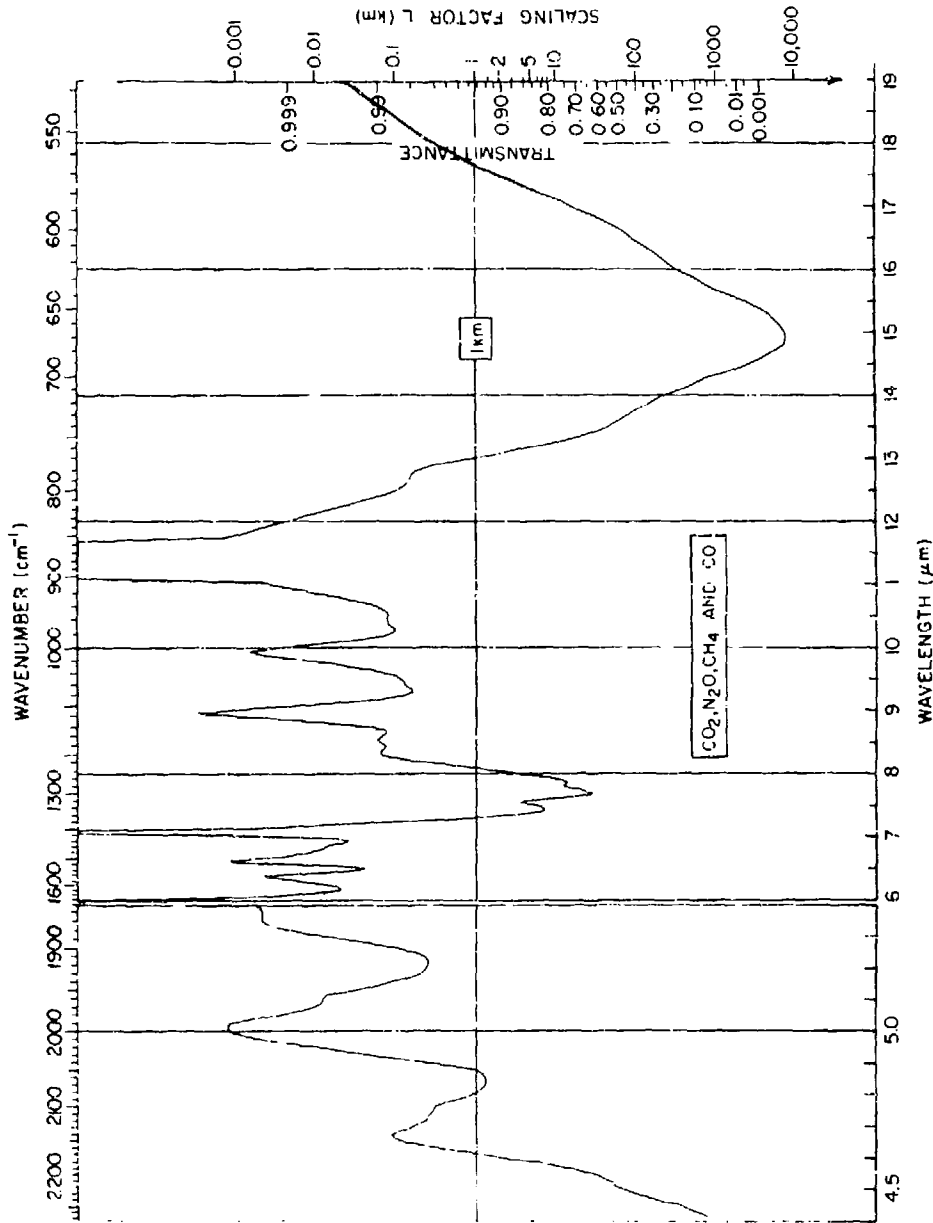


Figure 17b. Prediction Chart for the Transmittance of Uniformly Mixed Gases (CO₂, N₂O, CO, CH₄) (4.5-19 μm)

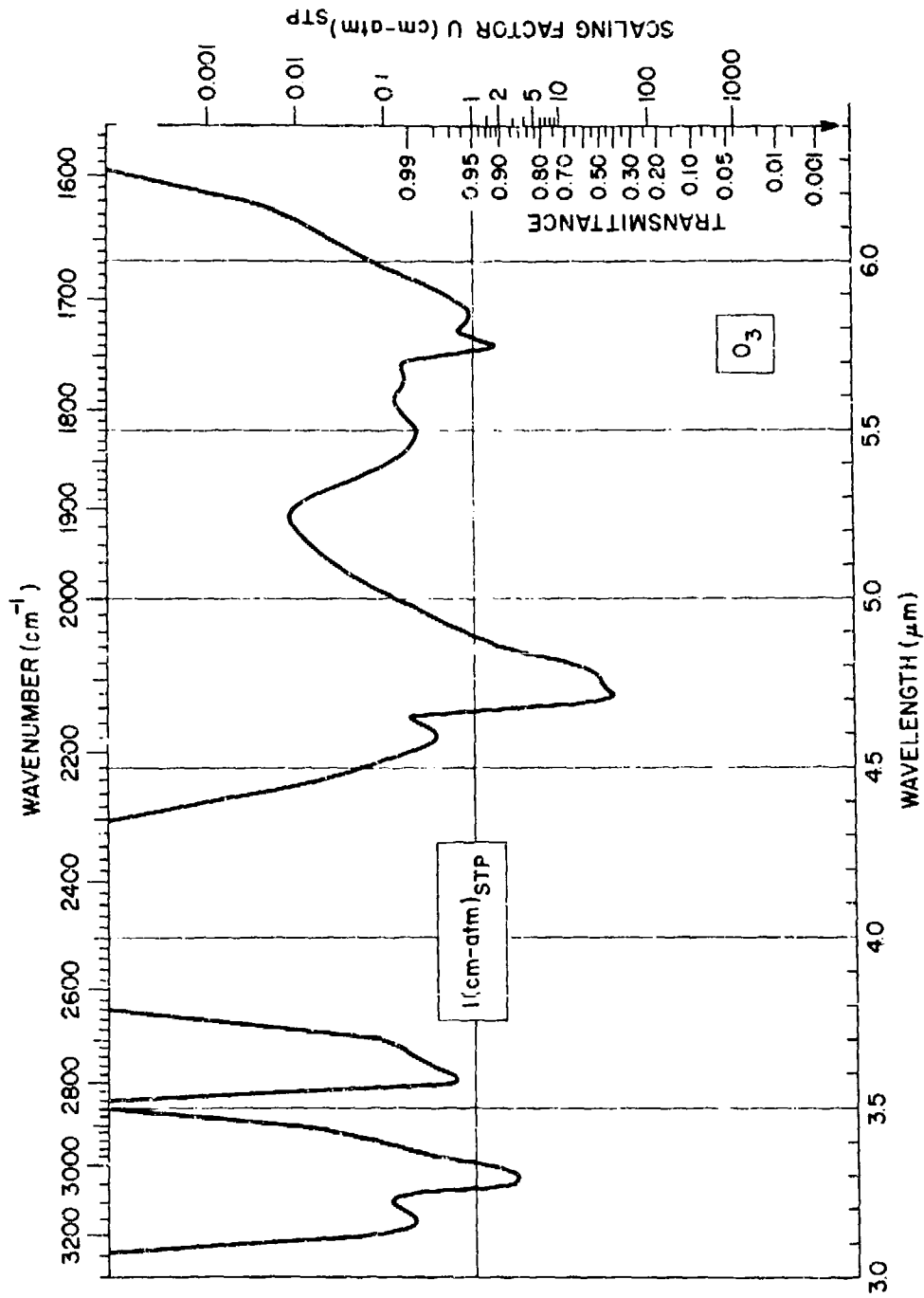


Figure 18a. Prediction Chart for Ozone Transmittance (3-6.4 μm)

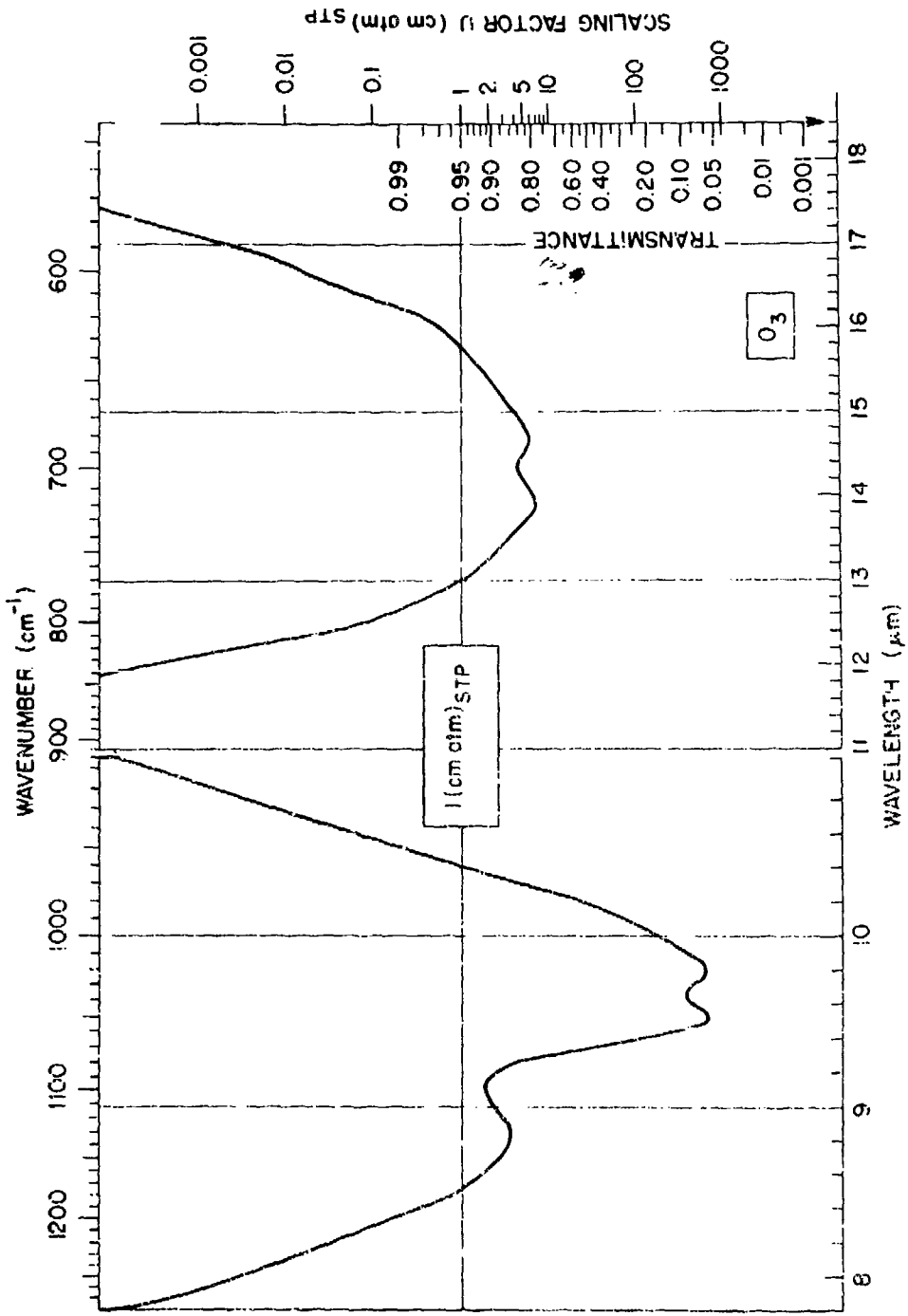


Figure 18b. Prediction Chart for Ozone Transmittance (8-18 μm)

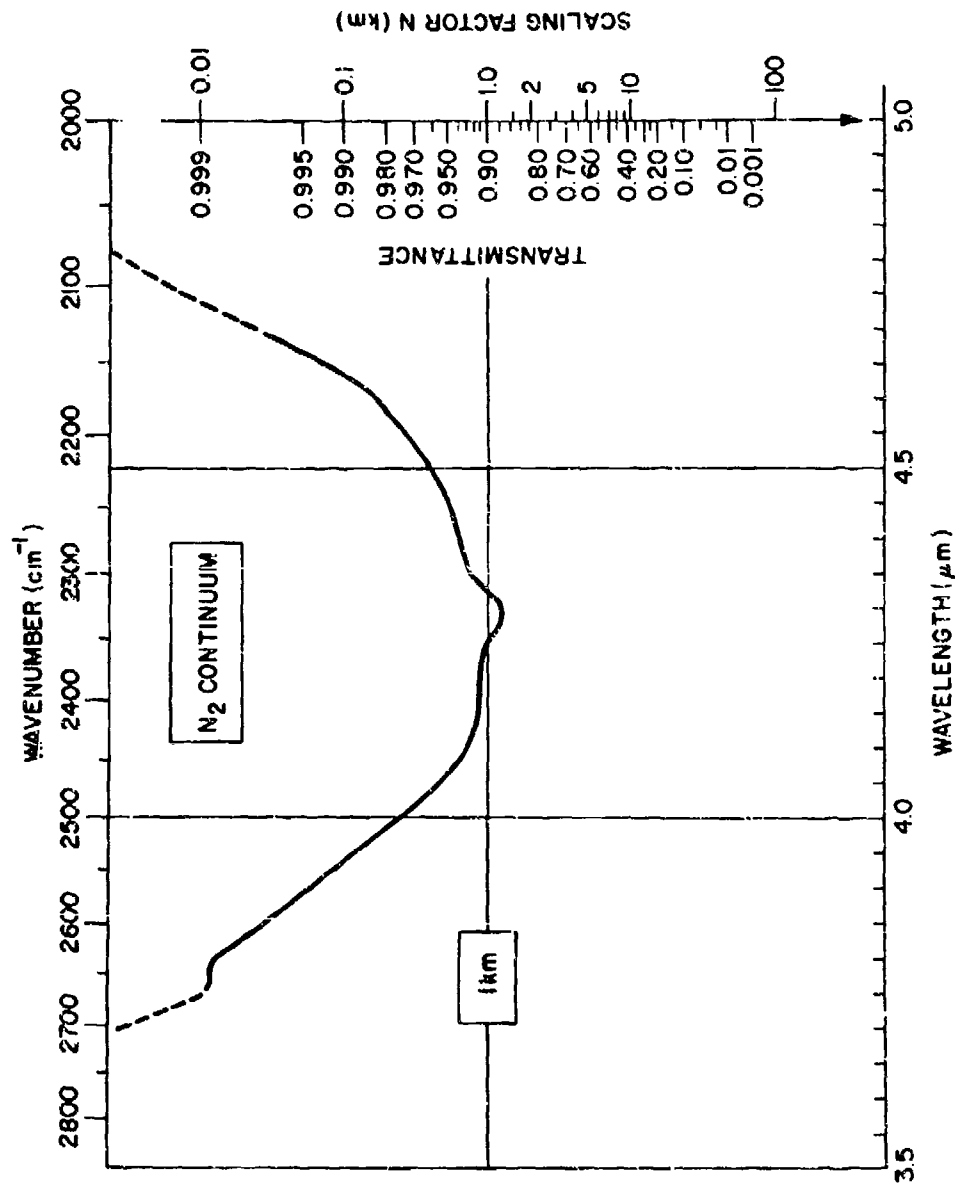


Figure 19. Prediction Chart for Nitrogen Transmittance

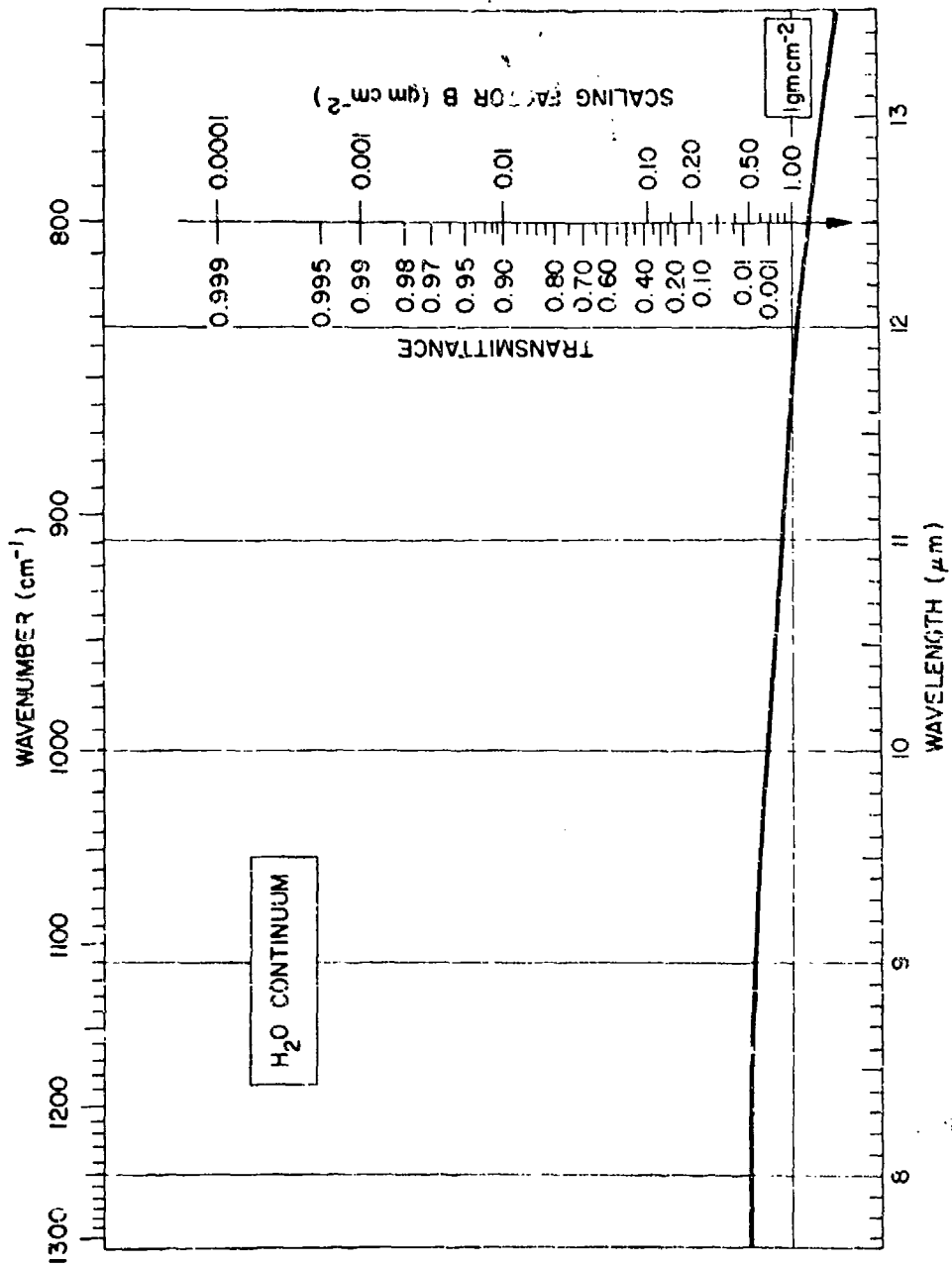


Figure 20. Prediction Chart for Transmittance Due to Water Vapor Continuum

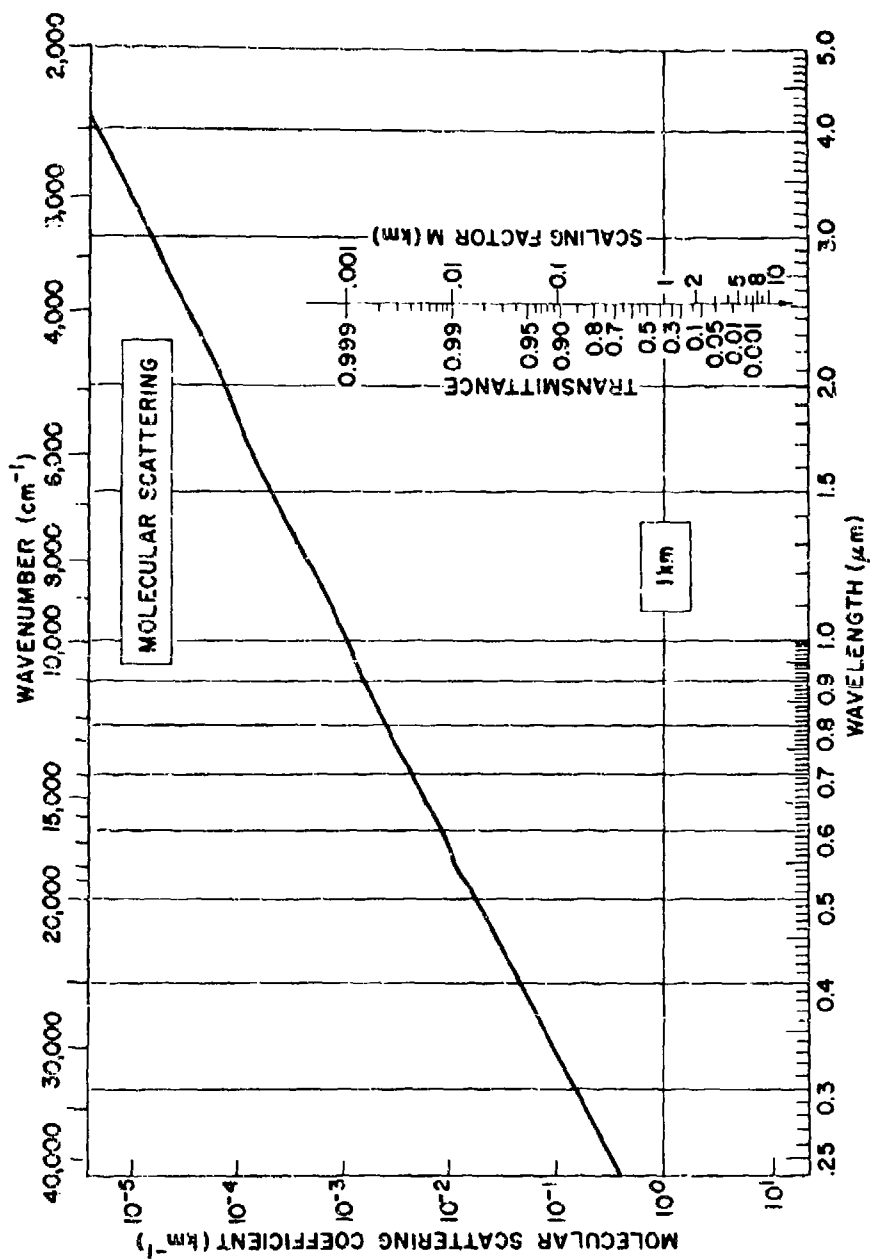


Figure 21. Prediction Chart for Transmittance Due to Molecular Scattering

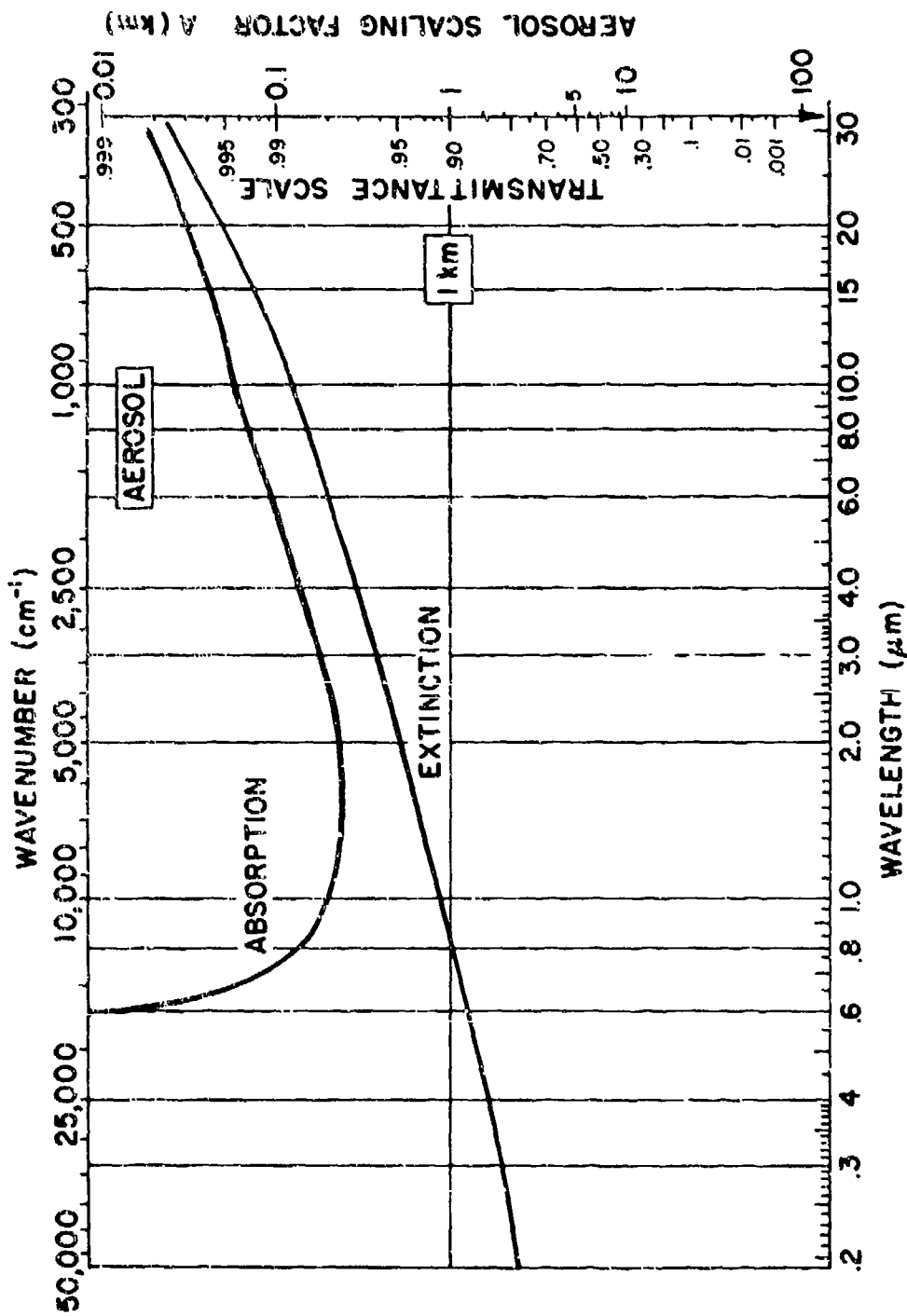


Figure 22. Prediction Chart for Aerosol Transmittance (Scattering and Absorption)

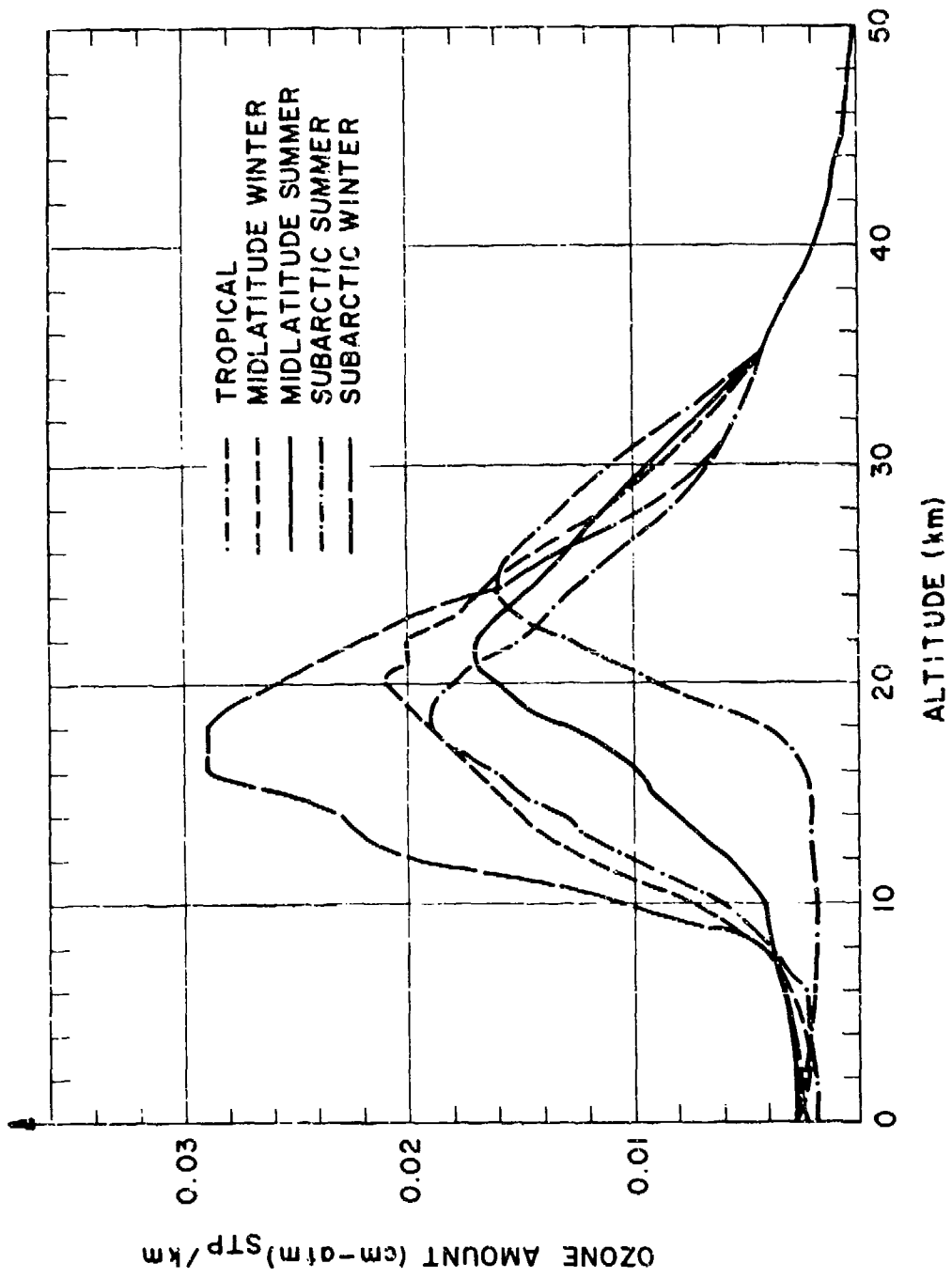


Figure 23. Equivalent Sea Level Path Length for Ozone (0.25-0.75 μm) as a Function of Altitude for Horizontal Atmospheric Paths

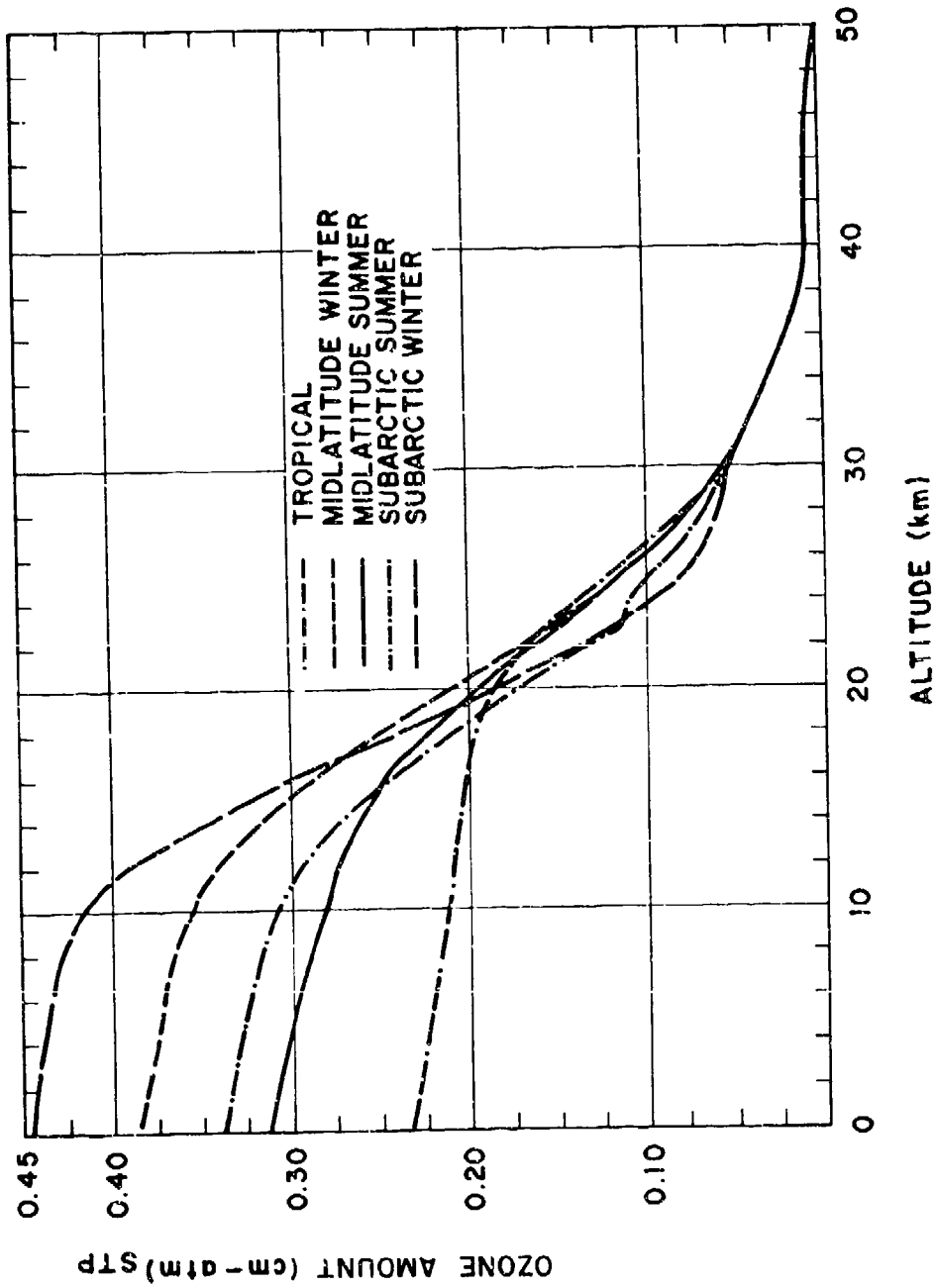


Figure 24. Equivalent Sea Level Path Length for Ozone (0.25-0.75 μm) as a Function of Altitude for Vertical Atmospheric Paths

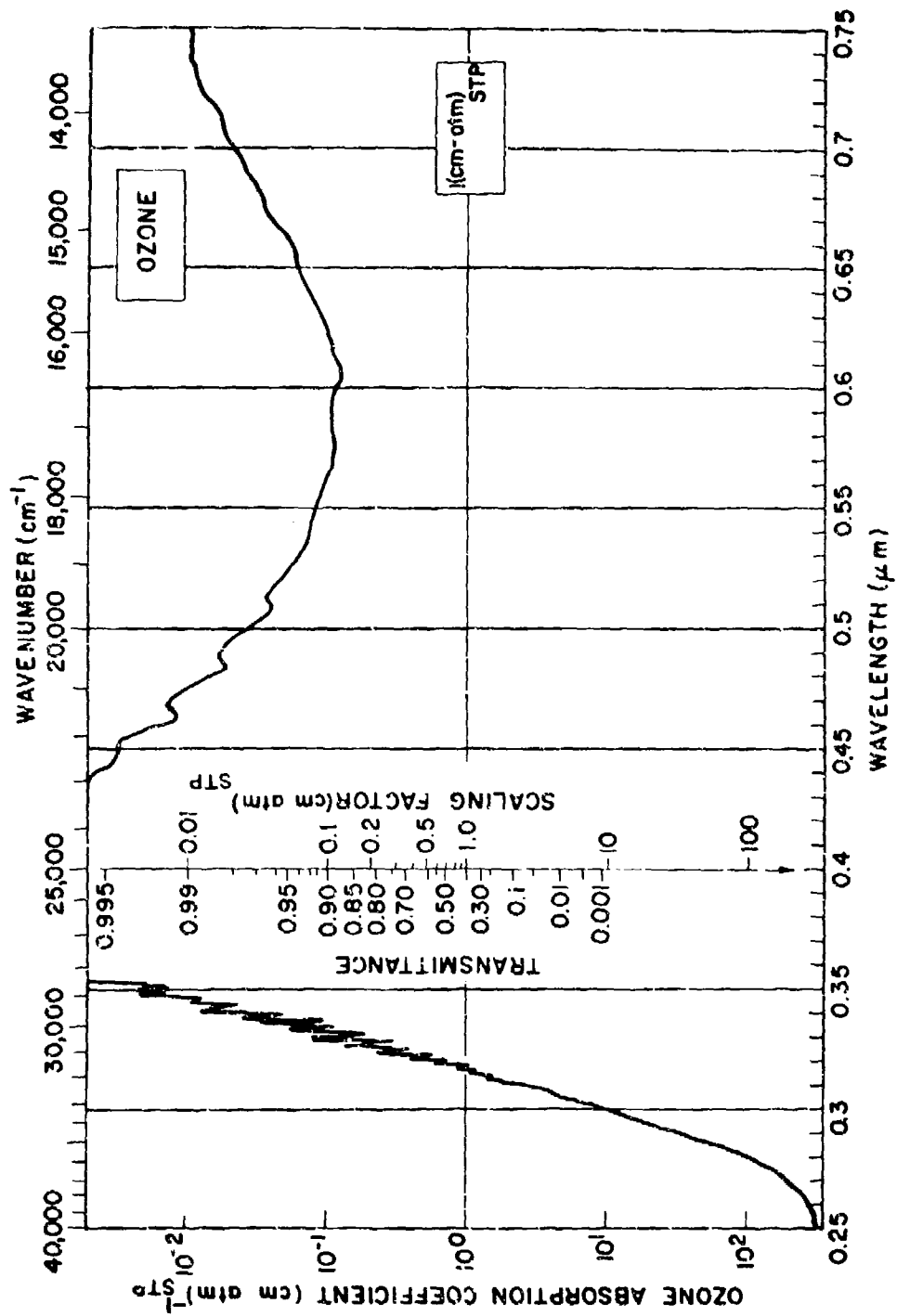


Figure 25. Prediction Chart for Ozone Transmittance (0.25-0.75 μm)

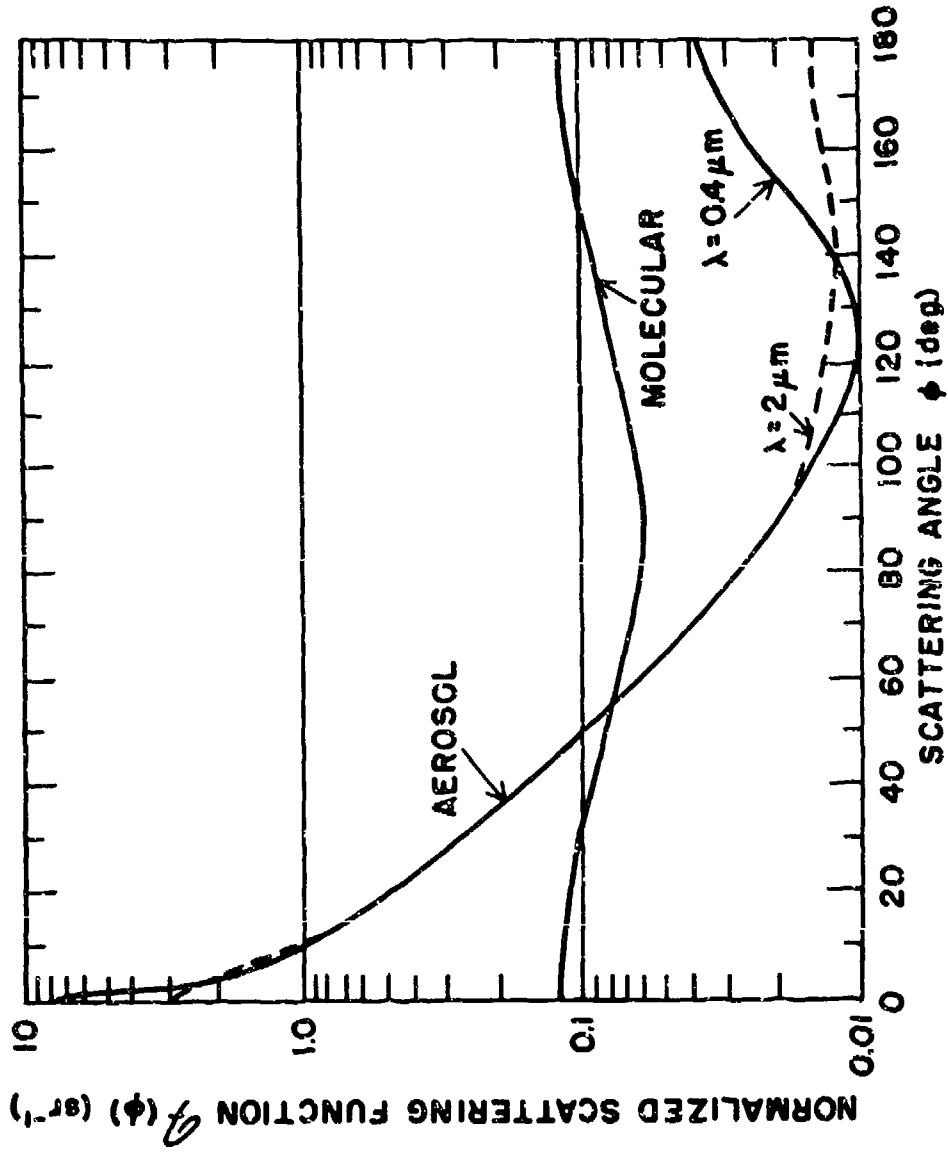


Figure 26. Normalized Scattering Phase Function of Aerosol and Air
Based on the Model Described in Section 2.3

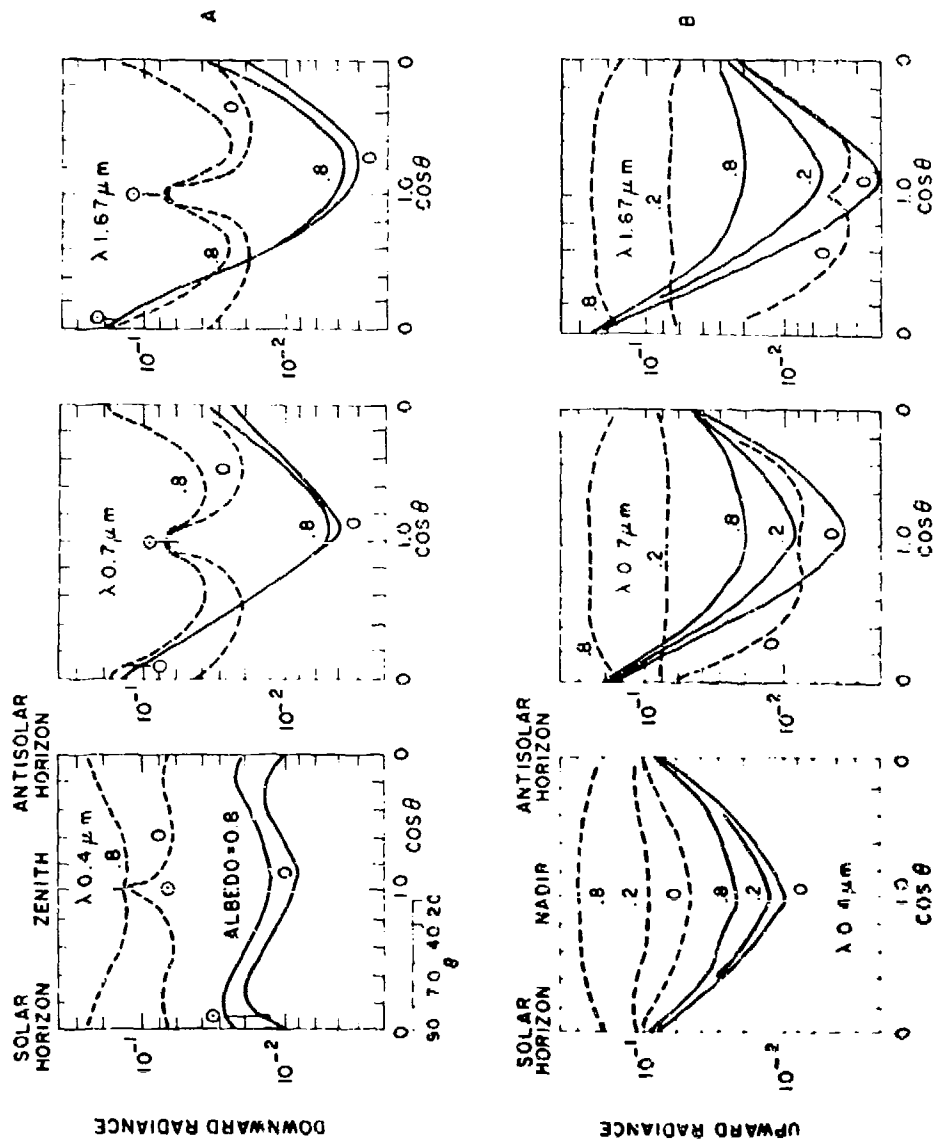
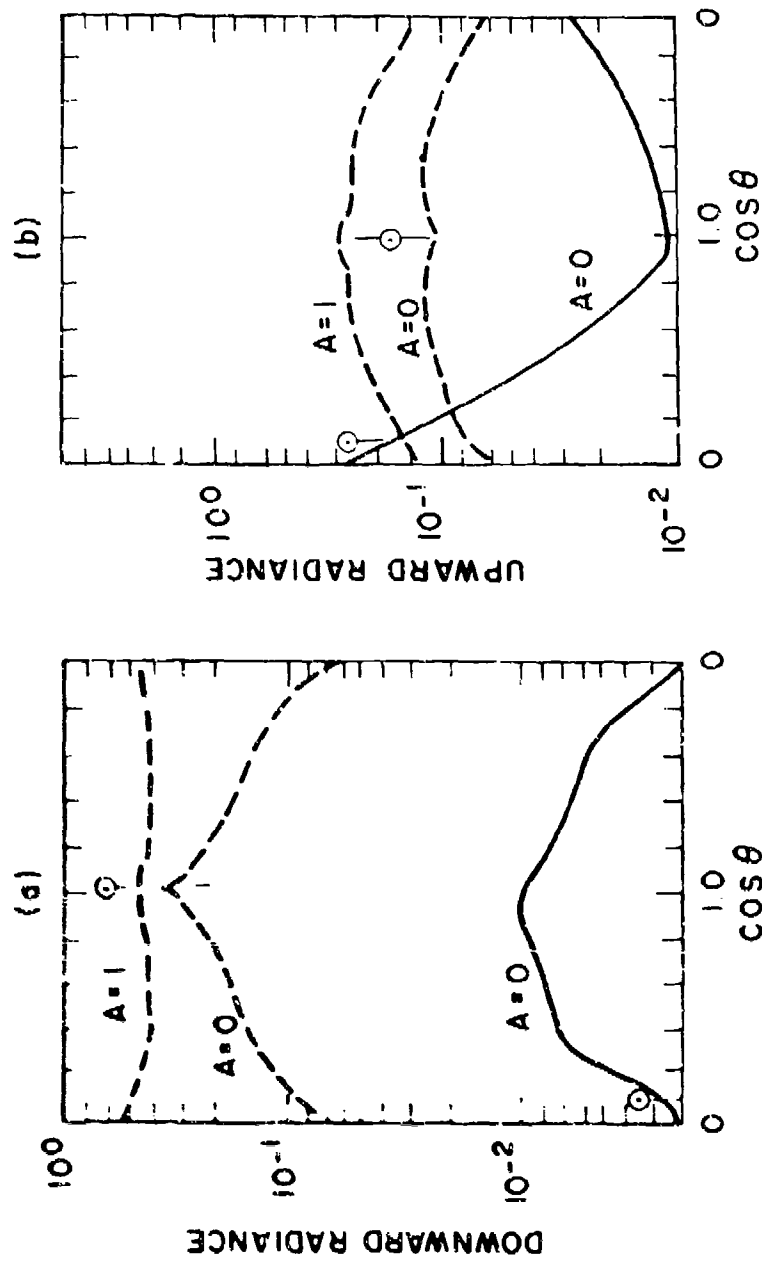


Figure 27. Downward (a) and Upward (b) Radiance Computed by Monte Carlo Techniques. Dashed curves are for sun in the zenith. Solid curves are for the sun at $\theta = 86.30^\circ$. The indicated parameter is the surface albedo and t is the total scattering optical thickness.



NIMBOSTRATUS $\tau = 10$, $\lambda = 0.7 \mu\text{m}$

Figure 28. Downward (a) and Upward (b) Radiance Computed for a Dense Nimbostratus Cloud. Dashed curves are for the sun in the zenith. Solid curves are for the sun at $\theta = 86.30$

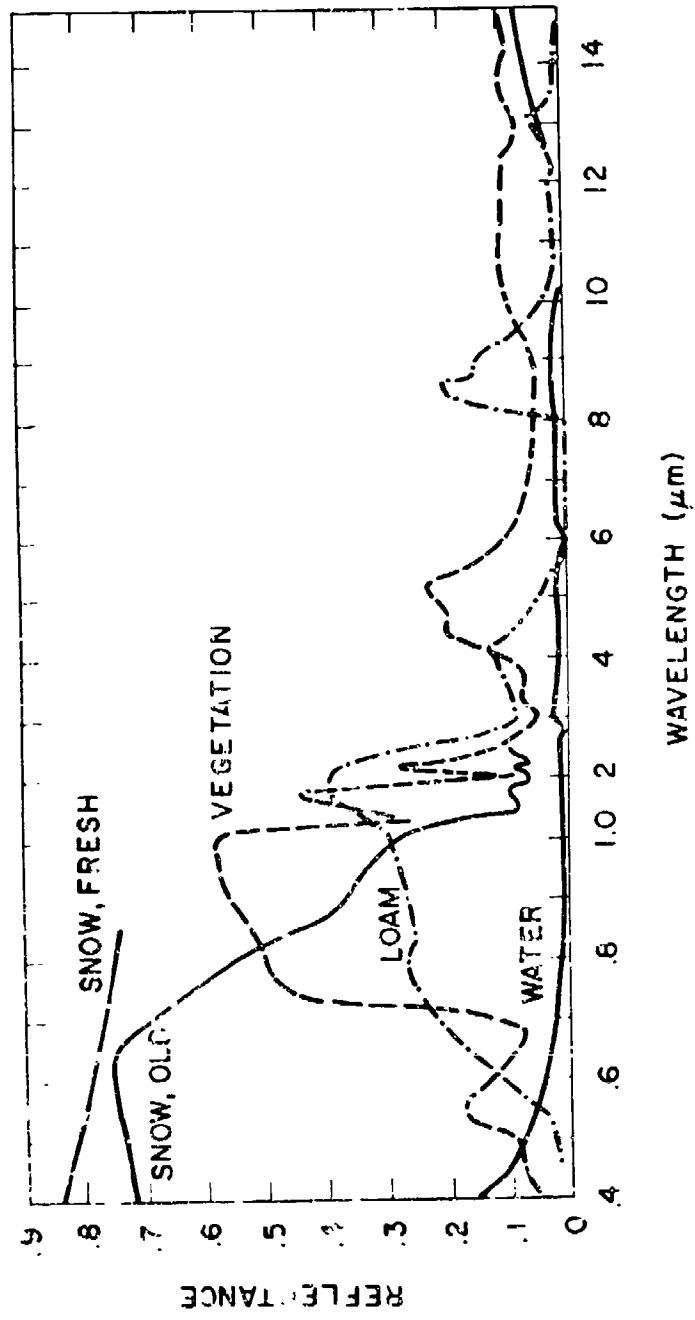


Figure 29. Typical Reflectance of Water Surface. Snow, Dry Soil and Vegetation (see Krinov, 1953; Penndorf, 1956; and Earling and Smith, 1956)

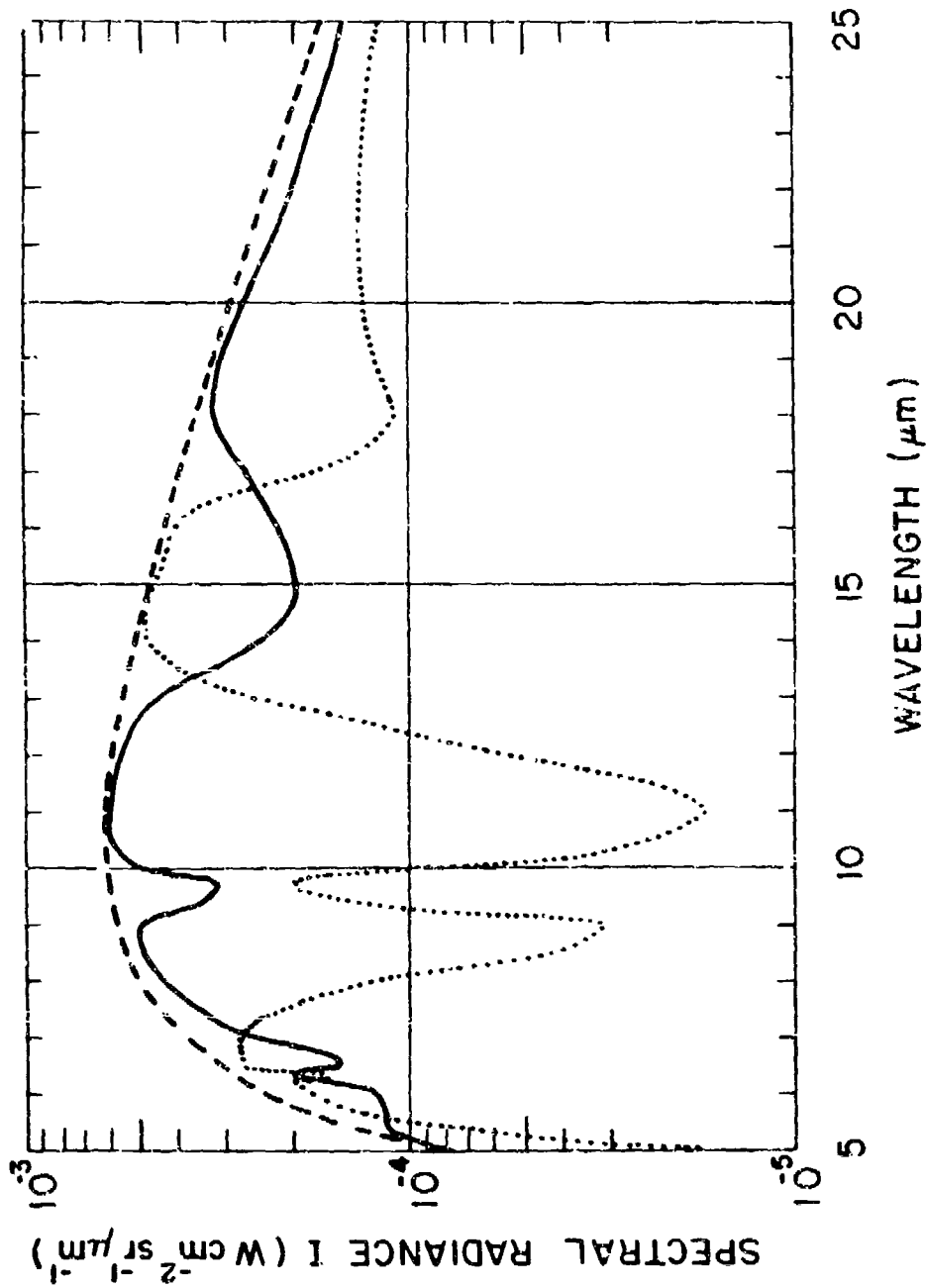


Figure 30. Radiance as a Function of Wavelength Computed for Temperature Distribution Corresponding to the Midlatitude Winter Model. Transmittance calculations are based on molecular absorption prediction charts described in Section 5. Upper curve is the radiance corresponding to a black body at 272K. Solid line spectrum is the computed upward radiance. Dashed spectrum is the computed downward radiance.

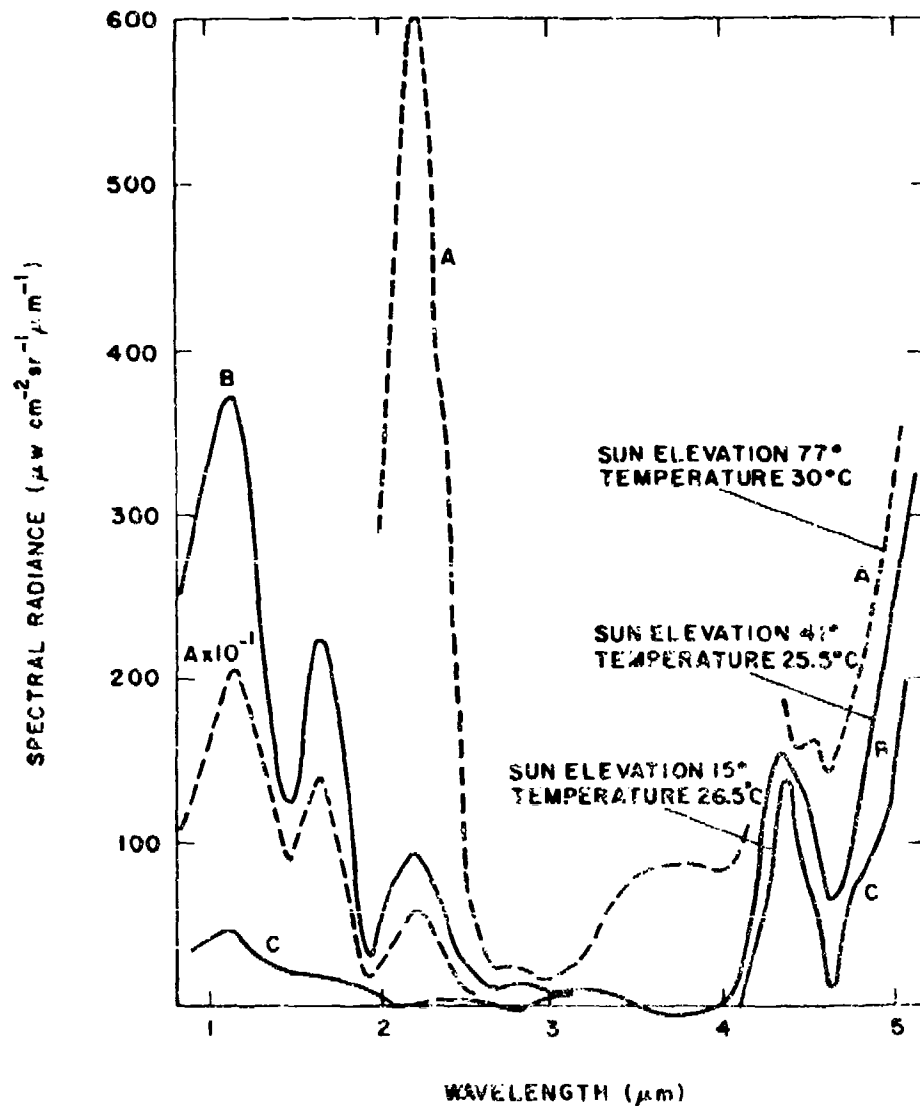


Figure 31. Spectral Radiance of a Clear Zenith Sky Showing the Effect of the Position of the Sun on the Radiation Scattered Below $3 \mu\text{m}$ and the Effect of Thermal Emission at Longer Wavelengths. Measured at Cocoa Beach, Florida (see Bell et al, 1960)

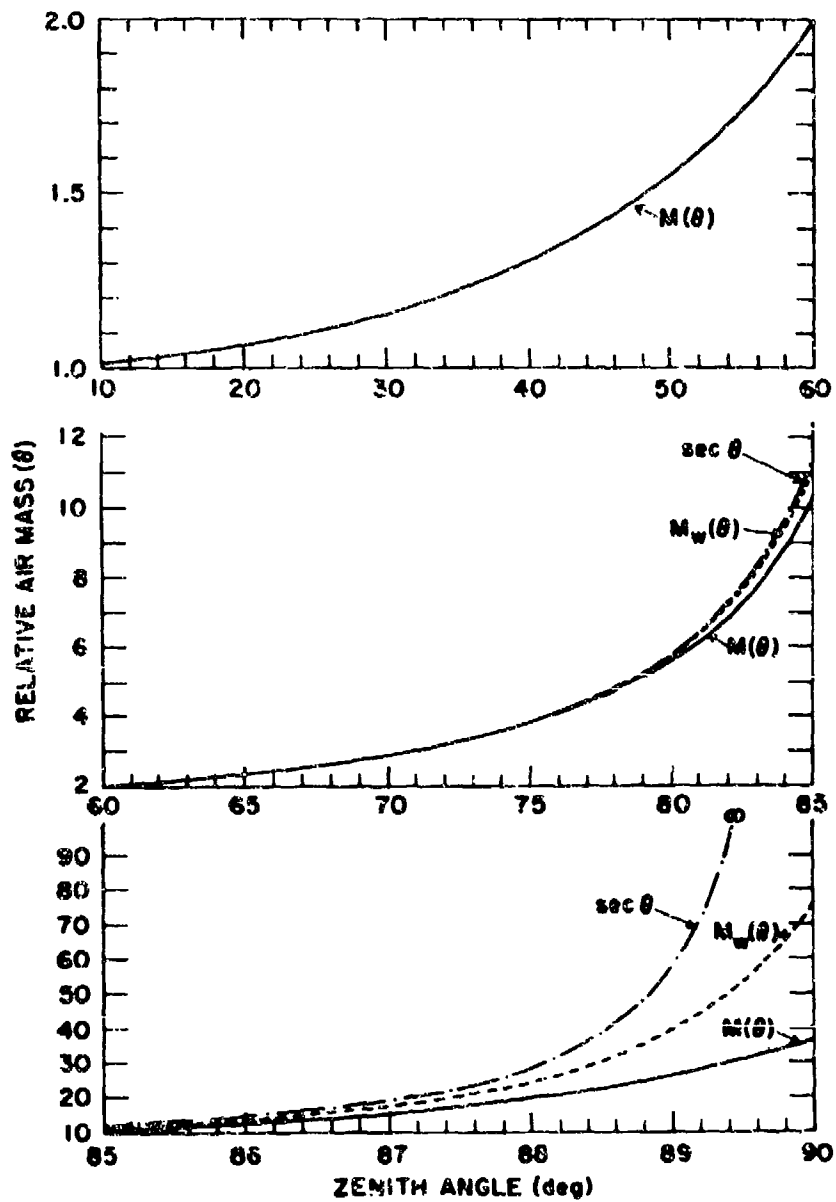


Figure 32. Comparison of the Relative Air Mass [$M(\theta)$] Computed by Kasten (1967) as a Function of Apparent Zenith Angle, θ , Based on the ARDC Model Atmosphere (Minzner et al, 1959) With a Similar Quantity [$M_w(\theta)$] Based on a vertical Water Vapor Distribution According to Schnaidt (1938) and for $\sec \theta$ (Note that for $\theta < 60^\circ$, $m(\theta) = M_w(\theta) = \sec \theta$.)

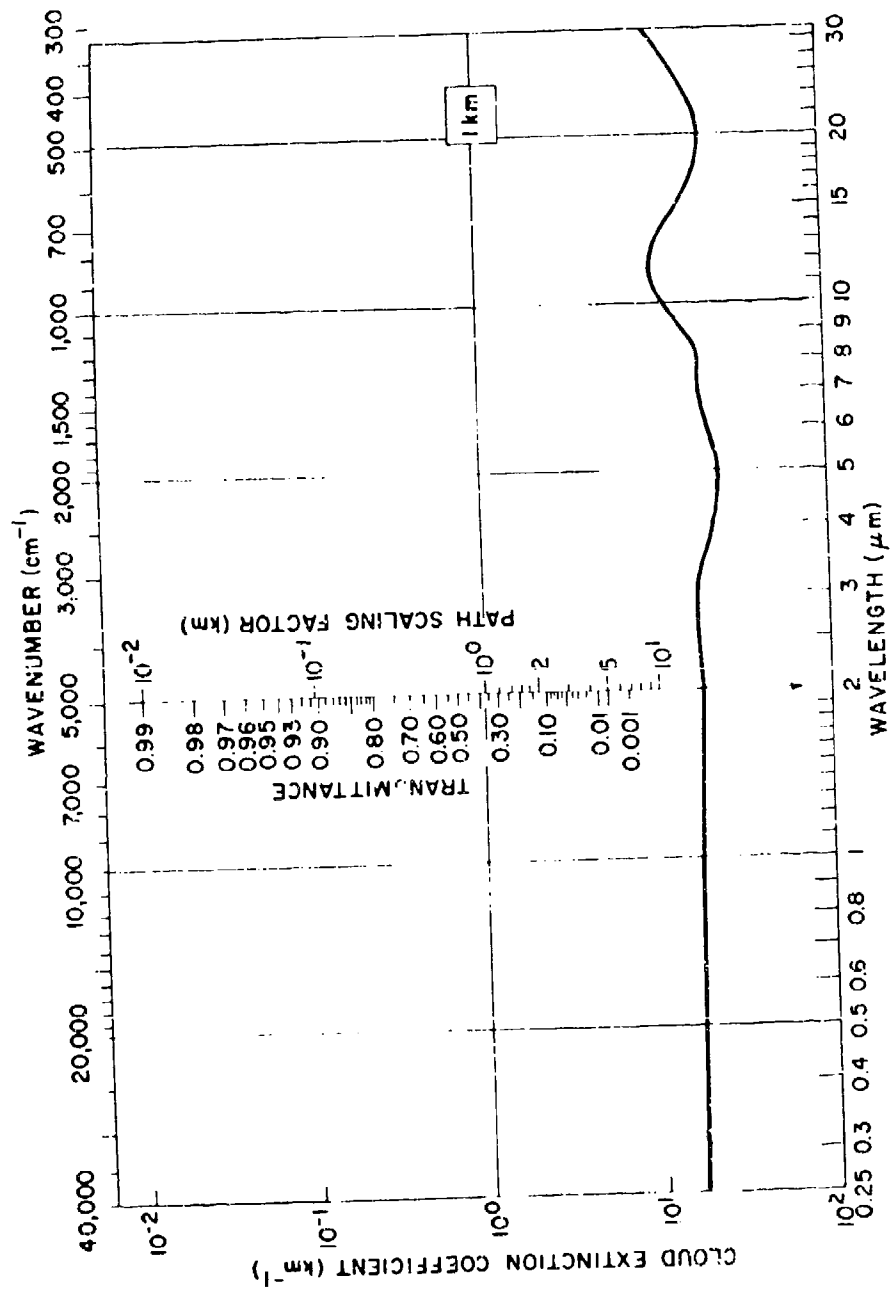


Figure 33. The Attenuation as a Function of Wavelength Due to Fair-weather Cumulus Cloud

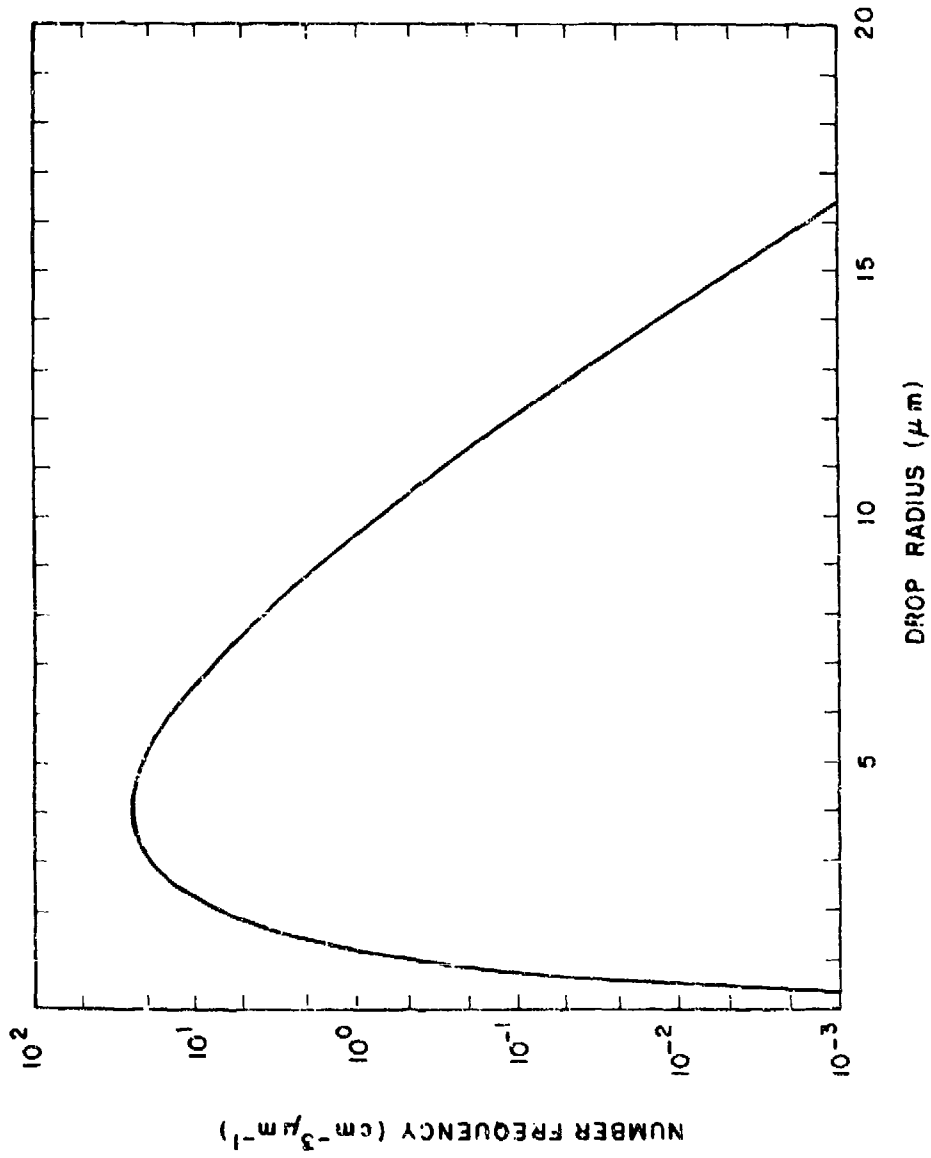


Figure 34. Particle Size Distribution for Fair-weather Cumulus Cloud Model

Acknowledgment

We wish to acknowledge the many helpful suggestions made by Dr. Darrell F. Burch as a result of careful reading of the manuscript.

References

- Altshuler, T. L. (1961) Infrared Transmission and Background Radiation by Clear Atmospheres, GE Report 61 SD 159, AD-401933.
- Bell, E. E., Eisner, L., Young, J., and Oetjen, R. (1960) J. Opt. Soc. Am., 50:1313.
- Bemporad, A. (1907) Meteorol Z. 24:306.
- Birkland, J. W. and Shaw, J. H. (1959) J. Opt. Soc. Am. 49:637.
- Bullrich, K. (1964) Advances in Geophysics 10:99.
- Burch, D. E. (1970) Semi-Annual Technical Report, Investigation of the Absorption of Infrared Radiation by Atmospheric Gases, Philco Ford Corp., Aeronutronic Report U4784, Contract No. F15628-69-C-0263.
- Burch, D. E. and Gryvna, D. A. (1966) Absorption by H₂O Between 5045 and 14,485 cm⁻¹ (0.69 to 1.98 μm Region), Aeronutronic Report U-3704.
- Burch, D. E. and Gryvna, D. A. (1967) Strengths, Widths and Shapes of the Oxygen Lines Near 7600 Angstroms, Aeronutronic Report U-4076.
- Burch, D. E., Gryvna, D. A., and Patty, R. R. (1964) Absorption by CO₂ Between 4500 and 5400 cm⁻¹ (2 μm Region), Aeronutronic Report U-2955.
- Burch, D. E., Gryvna, D. A., and Patty, R. R. (1965a) Absorption by CO₂ Between 6600 and 7125 cm⁻¹ (1.4 μm Region), Aeronutronic Report U-3127.
- Burch, D. E., Gryvna, D. A., and Patty, R. R. (1965b) Absorption by CO₂ Between 8000 and 10,600 cm⁻¹ (1 to 1.25 μm Region), Aeronutronic Report U-3200.
- Burch, D. E., Gryvna, D. A., and Patty, R. R. (1965c) Absorption by CO₂ Between 5400 and 6600 cm⁻¹ (1.6 μm Region), Aeronutronic Report U-3201.
- Burch, D. E., Gryvna, D. A., and Patty, R. R. (1965d) Absorption by H₂O Between 2800 and 4500 cm⁻¹ (2.7 μm Region), Aeronutronic Report U-3262.
- Burch, D. E., Gryvna, D. A., and Patty, R. R. (1967) Absorption by CO₂ Between 7125 and 8000 cm⁻¹ (1.25 to 1.4 μm Region), Aeronutronic Report U-3930.

- Burch, D. E., Gryvnak, D. A. and Patty, R. R. (1968) Absorption by CO₂ Between 3100 and 4100 cm⁻¹ (2.44 to 3.22 μm Region), Aeronutronic Report U-4132.
- Burch, D. E., Gryvnak, D. A., Singleton, E. B., France, W. F. and Williams, D. (1962) Infrared Absorption by Carbon Dioxide, Water Vapor and Minor Atmospheric Constituents, AFCRL, Research Contract AF19(604)-2633, Ohio State Univ.
- Coulson, K. L., Dave, J. V. and Sekera, Z. (1960) Tables Related to Radiation Emerging from a Planetary Atmosphere with Rayleigh Scattering, Univ. of California Press, Los Angeles.
- de Bary, E., Braun, B. and Bullrich, K. (1965) Tables Related to Light Scattering in a Turbid Atmosphere, Special Report No. 33, I-III, AFCRL.
- Deirmendjian, D. (1963) Scattering and Polarization Properties of Polydispersed Suspensions with Partial Absorption, Proc. of the Interdisciplinary Conf. on Electromagnetic Scattering, Potsdam, New York, Milton Kerker, Ed., Pergamon Press.
- Deirmendjian, D. (1964) Appl. Opt. 3:187.
- Deirmendjian, D. (1969) Electromagnetic Scattering on Spherical Polydispersions, American Elsevier Pub. Co., N. Y.
- Earing, D. G. and Smith, J. A. (1966) Target Signatures Analysis Center: Data Compilation, AFAL, AD 489-968.
- Elsasser, W. M. (1938) Phys. Rev. 54:126; also Harvard Meteorological Studies, No. 6, 1942.
- Elterman, L. (1968) UV, Visible, and IR Attenuation for Altitudes up to 50 KM, 1968, AFCRL, Environmental Res. Paper No. 285, AFCRL-68-0153.
- Elterman, L. (1970) Vertical-Attenuation Model with Eight Surface Meteorological Ranges 2 to 13 Kilometers, 1970, AFCRL, Environmental Research Paper No. 310, AFCRL-70-0200.
- Fink, U., Rank, D. H. and Wiggins, T. A. (1964) J. Opt. Soc. Am. 54:472.
- Goody, R. M. (1952) Quart. J. Roy. Meteorol Soc. 78:165.
- Goody, R. M. (1964) Atmospheric Radiation, Vol. I Theoretical Basis, Oxford University Press, London.
- Gryvnak, D. A., Patty, R. R., Burch, D. E. and Miller, E. E. (1966) Absorption by CO₂ Between 1800 and 2850 cm⁻¹ (3.5-5.6 μm Region), Aeronutronic Report U-3857.
- Hering, W. S., and Borden, T. R. (1964) Ozone Observations Over North America, OAR Research Report, AFCRL-64-30, Vol. 2, 1964.
- Inn, F. C. Y. and Tanaka, Y. (1953) J. Opt. Soc. Am. 43:870-873.
- Irvine, W. M. and Pollack, J. B. (1968) Icarus 8:324.
- Kasten, F. (1967) Arch. Meteorol Geophys. Bioklim. B15:62.
- Kattawar, G. W. and Plass, G. N. (1968) Appl. Opt. 7:869.
- King, J. I. F. (1959) Proc. IRIS 4 (No. 1):164.
- King, J. I. F. (1964) JQSRT 4:705.
- Kislovskii, D. L. (1959) Optics Spectry 7:201.
- Krinov, E. L. (1953) Spectral Reflectance Properties of Natural Formations (in Russian 1947), National Research Council of Canada (Ottawa) Technical Translations TT-439.
- McCaa, D. J. and Shaw, J. H. (1967) Infrared Absorption Bands of Ozone, Report AFCRL-67-0237, Ohio State Univ.
- McClatchey, R. A., Fenn, R. W., Selby, J. E. A., Volz, F. E., Garing, J. S. (1970) Optical Properties of the Atmosphere, 1970, AFCRL Environmental Research Paper, No. 331, AFCRL-70-0527.

- McClatchey, R. A., Fenn, R. W., Selby, J. E. A., Volz, F. E., Garing, J. S. (1971) Optical Properties of the Atmosphere (Revised), 1971, AFCRL, Environmental Research Paper, No. 354, AFCRL-71-0279.
- McClatchey, R. A. (1970) Atmospheric Attenuation of CO Laser Radiation, Environmental Research Paper, No. 357, AFCRL-71-0370.
- McClatchey, R. A., and Selby, J. E. A. (1972) Atmospheric Attenuation of HF and DF Laser Radiation, Environmental Research Paper, No. 400, AFCRL-72-0312.
- McCoy, J. H., Rensch, D. B., Long, R. K. (1969) Appl. Opt. 8:1471.
- Mie, G. (1908) Ann d. Phys. 25:377.
- Minzner, R. A., Champion, K. S. W. and Pond, H. L. (1959) The ARDC Model Atmosphere, 1959, Air Force Surveys in Geophysics, No. 115, (AFCRL-TN-59-267).
- Penner, S. S. (1959) Quantitative Molecular Spectroscopy and Gas Emissivities, Addison-Wesley, Reading, Massachusetts.
- Penndorf, R. (1956) Luminous and Spectral Reflectance as Well as Colors of Natural Objects, Geophysical Research Paper No. 44, AFCRL-TR-56-203.
- Plass, G. N. (1958) J. Opt. Soc. Am 48:690.
- Plass, G. N. and Kattawar, G. W. (1968) Appl. Opt. 7:1129.
- Reddy, S. R., and Cho, C. W. (1965) Can. J. Phys. 43:2331.
- Schnaidt, F. (1938) Meteorol Z. 55:296.
- Shaw, J. H. (1959) A Determination of the Abundance of N₂O, CO, and CH₄ in Ground Level Air at Several Locations Near Columbus, Ohio, Sci. Report No. 1, Contract AF19(604)-2259, AFCRL.
- Shaw, J. H. (1968) Monthly Report on Infrared Temperature Sounding, The Ohio State University, RF Project 2469, Report No. 16, October 1968.
- Sissenwine, N., Grantham, D. D., Salmela, H. A. (1968) Humidity Up to the Mesopause, AFCRL-68-0550.
- Smithsonian Meteorological Tables (1963), 6th Revised Edition, List, R. J., Ed., Smithsonian Institution, Washington, D. C.
- Streete, J. L. (1968) Appl. Opt. 7:1545.
- Valley, S. L., Ed., (1965) Handbook of Geophysics and Space Environments, AFCRL.
- Van de Hulst, H. C. (1957) Light Scattering by Small Particles, John Wiley and Sons, Incorporated.
- Volz, F. E. (1957) Ann. Meteorol. 8:34.
- Wyatt, P. J., Stull, V. R., and Plass, G. N. (1964) Appl. Opt. 3:229.
- Yates, H. W. and Taylor, J. H. (1960) Infrared Transmission of the Atmosphere, NRL Report 5453.
- Zuev, V. E., Kabanov, M. V., and Savel'ev, B. A. (1967) Izv. Akad. Nauk, SSSR, Fiz. Atmos. i. Okeana 3:724.

Appendix A

Units and Conversion Factors

1. INTRODUCTION

Throughout this report we have used the term "frequency" rather loosely to signify spectral variation. In general, frequency is assumed to be synonymous with wavenumber, ν (cm^{-1}), which is given by $\nu = 10^4/\lambda$ where the wavelength λ is given in units of μm (that is, 10^{-6} meter).

The subject of units used in atmospheric physics is rather confusing to the beginner. This is particularly true where units of absorber concentration or amount are concerned. In this Appendix we will show the reader how to derive the absorber concentrations for use with the prediction charts given in Section 5, on the assumption that one has the relevant meteorological data available. We will then discuss the units of absorber concentration and indicate how to make the appropriate conversions.

2. ABSORBER CONCENTRATION

For most gases absorber concentration denoted here by ΔL is generally measured by the equivalent length of pure absorber in the path under the existing conditions of pressure, P , and temperature, T . The unit, centimeter atmospheres, (cm-atm) is given by $\Delta L = cRP$ where c is the fractional concentration of the absorber (see Table 2), R is the path length (cm) and the P is the pressure in atmospheres. More often ΔL_0 is quoted as the absorber concentration reduced to STP

conditions, which is a more meaningful quantity where vertical or slant atmospheric paths are concerned. Thus, for a horizontal path at altitude, z , we have

$$\Delta L_o = cR \frac{P(z)}{P_o} \left(\frac{T_o}{T(z)} \right) (\text{cm-atm})_{\text{STP}} \quad (\text{A1})$$

where $T_o = 273\text{K}$, and $P_o = 1 \text{ atm}$. If c is given in parts per million (ppm), (see Table 2), and R is given in km, the following expression can be used.

$$\Delta L_o (\text{cm-atm})_{\text{STP}} = 10^{-1} c R \frac{P}{P_o} \left(\frac{T_o}{T} \right) \quad (\text{A2})$$

For a uniformly mixed gas of fractional concentration by volume, c , the number of centimeter atmospheres at STP in a slant path from any altitude z to the limit of the atmosphere is given by

$$\Delta L_o (\theta, z \rightarrow \infty)_{\text{STP}} = c H(z) \sec \theta \frac{P(z)}{P_o} \left(\frac{T_o}{T(z)} \right) = c H(z) \sec \theta \rho(z) / \rho_o \quad (\text{A3})$$

where $H(z)$ is called the scale height of the atmosphere above altitude z , θ is the zenith angle and $\rho(z)$ and ρ_o are the atmospheric density at altitude z and STP, respectively. For $\theta > 70^\circ$, see Section 7. From the hydrostatic equation, $H(z)$ can be defined as follows:

$$P(z) = g \rho(z) H(z) \quad (\text{A4})$$

where $P(z)$ is the pressure at altitude z , and g is the acceleration due to gravity (981 cm sec^{-2}). Thus, for a vertical column of air at STP, $H(o) = 7.99 \times 10^5 \text{ cm}$ (that is, approximately 8 km). If the scale height in cm is required at another altitude, z , it can be determined from

$$H(z) = 1.02 \times 10^6 \times [P(z) / \rho(z)] \quad (\text{A5})$$

where $P(z)$ is given in millibars and $\rho(z)$ is given in gm/m^3 (see Table 1). Note from Eq. (A5) that the quantity $H(z) \rho(z)$ is directly proportional to $P(z)$ and is independent of temperature. Thus, inserting $H(z) \rho(z)$ into Eq. (A3), we have

$$\Delta L_o (\theta, z \rightarrow \infty)_{\text{STP}} = c \times 1.02 \times 10^6 P(z) \sec \theta / \rho_o \quad (\text{A6})$$

and for the amount of absorber between levels z_1 and z_2 (see Table 2):

$$\Delta L_o (\theta, z_1 \rightarrow z_2)_{STP} = c \times 1.02 \times 10^6 [P(z_1) - P(z_2)] \sec \theta / \rho_o. \quad (A7)$$

For condensible vapors (for example, water vapor) it is more convenient to measure the total length of liquid (in cms) which may be precipitated out of the path (per unit area). The number of precipitable centimeters (abbreviated pr cm) of water vapor in a given path of length R (cm) is given by, $w = \rho(T) \mathcal{H} R$ where $\rho(T)$ is the saturation vapor density of water at temperature T (gm cm^{-3}) and \mathcal{H} is the fractional relative humidity. It will be noted that the units of pr cm and gm cm^{-2} are equivalent.

Figure A1 will enable the reader to calculate the number of pr cms of water vapor per km path length, for a given temperature and relative humidity. For temperatures below -40°C the reader should use density values of water vapor measured over ice for determining water vapor concentrations for atmospheric paths (see Smithsonian Meteorological Tables, 1963).

In Table 1, water vapor densities are given in units gm m^{-3} as a function of altitude for the 5 model atmospheres. It may be useful to remember that for water vapor,

$$1 \text{ gm m}^{-3} = 0.1 \text{ gm cm}^{-2}/\text{km (or } 0.1 \text{ pr cm/km)}.$$

3. UNIT CONVERSION FACTORS

According to Avogadro's hypothesis the molecular weight, M , in gms., or any gas occupies 22.4 liters at STP. Hence one cubic centimeter of gas at STP weighs $(M/2.24 \cdot 10^4)$ gms. Since 1 (cm-atm)_{STP} is equivalent to a length of 1 cm of gas at STP per cm^2 , we can write the following:

$$1 \text{ cm-atm of gas} = \frac{M}{2.24 \times 10^4} \text{ gm cm}^{-2} \quad (A8)$$

where M is the molecular weight of the gas (see Table 2).

Also since 1 cm^3 of gas at STP contains $1/2.24 \times 10^4$ moles and one mole of gas contains the same number (\mathcal{R}) of molecules (where \mathcal{R} is Avogadro's Number) we can write that 1 cm^3 of gas at STP contains $6.06 \times 10^{23}/2.24 \times 10^4 = 2.69 \times 10^{19}$ molecules or

$$1 \text{ (cm-atm)}_{STP} = 2.69 \times 10^{19} \text{ molecules/cm}^2. \quad (A9)$$

Note that Eq. (A9) is valid independent of the gas. Since for water vapor one can write 1 gm cm^{-2} in terms of $(\text{cm-atm})_{\text{STP}}$, using Eq. (A8) it will also be seen that for water vapor:

$$1 \text{ pr cm (H}_2\text{O)} = 3.34 \times 10^{22} \text{ molecules/cm}^2. \quad (\text{A10})$$

Thus the unit, molecule/cm², is independent of the nature of the absorbing gas and basic to all gases. It is hoped that this unit will become more widely used and thereby help to unify absorber concentration units for all the atmospheric constituents.

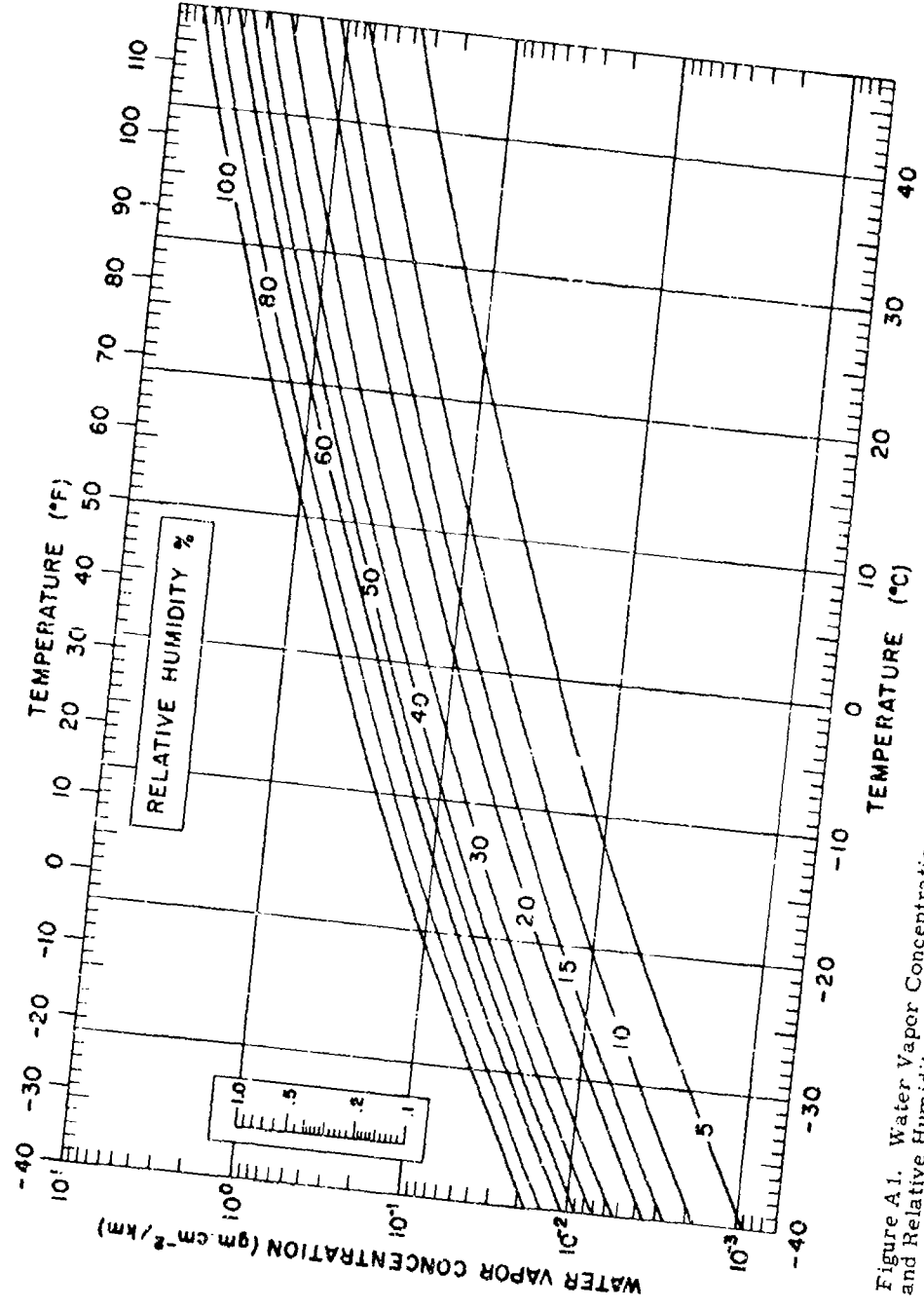


Figure A.1. Water Vapor Concentration per Kilometer Path Length as a Function of Temperature and Relative Humidity

Preceding page blank

Appendix B

Equivalent Sea Level Path Charts for U.S. Standard Atmosphere, 1962

In both the original version of this report (McClatchey, et al, 1970) and in the revised version (McClatchey, et al, 1971), it was decided to provide explicit computational capability for five atmospheric molecular models and two aerosol models. The inclusion of water vapor models in the U.S. Standard Atmosphere Supplements, 1966 as provided in the AFRL Handbook of Geophysics and Space Environments (Valley, 1965), provided an appropriate set of models for this purpose. The U.S. Standard Atmosphere, 1962 does not provide an accompanying water vapor distribution and so this model was initially omitted.

Within the meteorology and atmospheric physics community, there is a need to intercompare calculations for a single appropriate atmospheric model. It is felt that the best model for this purpose is the U.S. Standard Atmosphere, 1962 with an appropriate water vapor and ozone distribution. The U.S. Standard Atmosphere Supplements, 1966 provides an appropriate ozone distribution utilizing the experimental work of Hering and Borden, 1964 and calculations. The model specified there is given below in Table B1. An appropriate water vapor distribution (Sissenwine, 1968) has also been included in Table B1 together with the temperature, pressure and density results from the U.S. Standard Atmosphere, 1962.

Using the model atmosphere parameters from Table B1 and the equivalent sea level path relations from Section 5.3, Figures B1 - B14 have been constructed. These figures should be used to determine the equivalent sea level path lengths for the Standard Atmosphere and the results used with Figures 16a through Figure 25 as described in Section 5.4.

Table B1. Model Atmosphere Used as a Basis for the Computation of Atmospheric Optical Properties

U. S. STANDARD ATMOSPHERE, 1962					
Ht. (km)	Pressure (mb)	Temp. (°K)	Density (g/m ³)	Water Vapor (g/m ³)	Ozone (g/m ³)
0	1.013E+03	288.1	1.225E+03	5.9E+00	5.4E-05
1	8.986E+02	281.6	1.111E+03	4.2E+00	5.4E-05
2	7.950E+02	275.1	1.007E+03	2.9E+00	5.4E-05
3	7.012E+02	268.7	9.093E+02	1.8E+00	5.0E-05
4	6.1C6E+02	262.2	8.193E+02	1.1E+00	4.6E-05
5	5.405E+02	255.7	7.364E+02	6.4E-01	4.5E-05
6	4.722E+02	249.2	6.601E+02	3.8E-01	4.5E-05
7	4.111E+02	242.7	5.900E+02	2.1E-01	4.8E-05
8	3.565E+02	236.2	5.258E+02	1.2E-01	5.2E-05
9	3.080E+02	229.7	4.671E+02	4.6E-02	7.1E-05
10	2.650E+02	223.2	4.135E+02	1.8E-02	9.0E-05
11	2.270E+02	216.8	3.648E+02	8.2E-03	1.3E-04
12	1.940E+02	216.6	3.119E+02	3.7E-03	1.6E-04
13	1.658E+02	216.6	2.666E+02	1.8E-03	1.7E-04
14	1.417E+02	216.6	2.279E+02	8.4E-04	1.9E-04
15	1.211E+02	216.6	1.948E+02	7.2E-04	2.1E-04
16	1.035E+02	216.6	1.665E+02	6.1E-04	2.3E-04
17	8.850E+01	216.6	1.423E+02	5.2E-04	2.8E-04
18	7.565E+01	216.6	1.216E+02	4.4E-04	3.2E-04
19	6.467E+01	216.6	1.040E+02	4.4E-04	3.5E-04
20	5.529E+01	216.6	8.891E+01	4.4E-04	3.8E-04
21	4.729E+01	217.6	7.572E+01	4.8E-04	3.8E-04
22	4.047E+01	218.6	6.451E+01	5.2E-04	3.9E-04
23	3.467E+01	219.6	5.500E+01	5.7E-04	3.8E-04
24	2.972E+01	220.6	4.694E+01	6.1E-04	3.6E-04
25	2.549E+01	221.6	4.008E+01	6.6E-04	3.4E-04
30	1.197E+01	226.5	1.841E+01	3.8E-04	2.0E-04
35	5.746E+00	236.5	8.463E+00	1.3E-04	1.1E-04
40	2.871E+00	250.4	3.996E+00	6.7E-05	4.9E-05
45	1.491E+00	264.2	1.966E+00	3.2E-05	1.7E-05
50	7.978E-01	270.6	1.027E+00	1.2E-05	4.0E-06
70	5.520E-02	219.7	8.754E-02	1.5E-07	8.3E-08
100	3.008E-04	210.0	4.989E-04	1.0E-09	4.3E-11

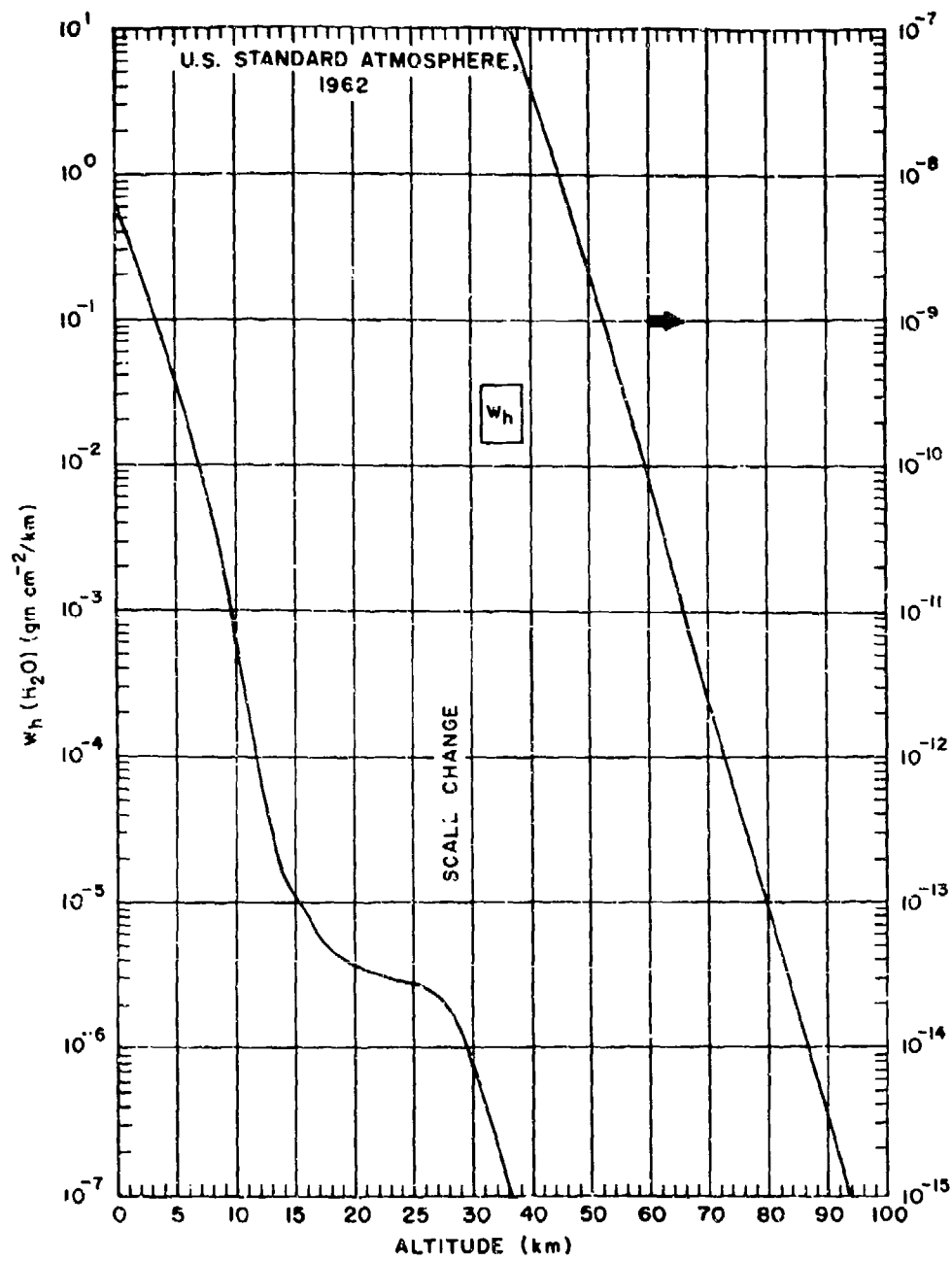


Figure B1. Equivalent Sea Level Path Length of Water Vapor as a Function of Altitude for Horizontal Atmospheric Paths

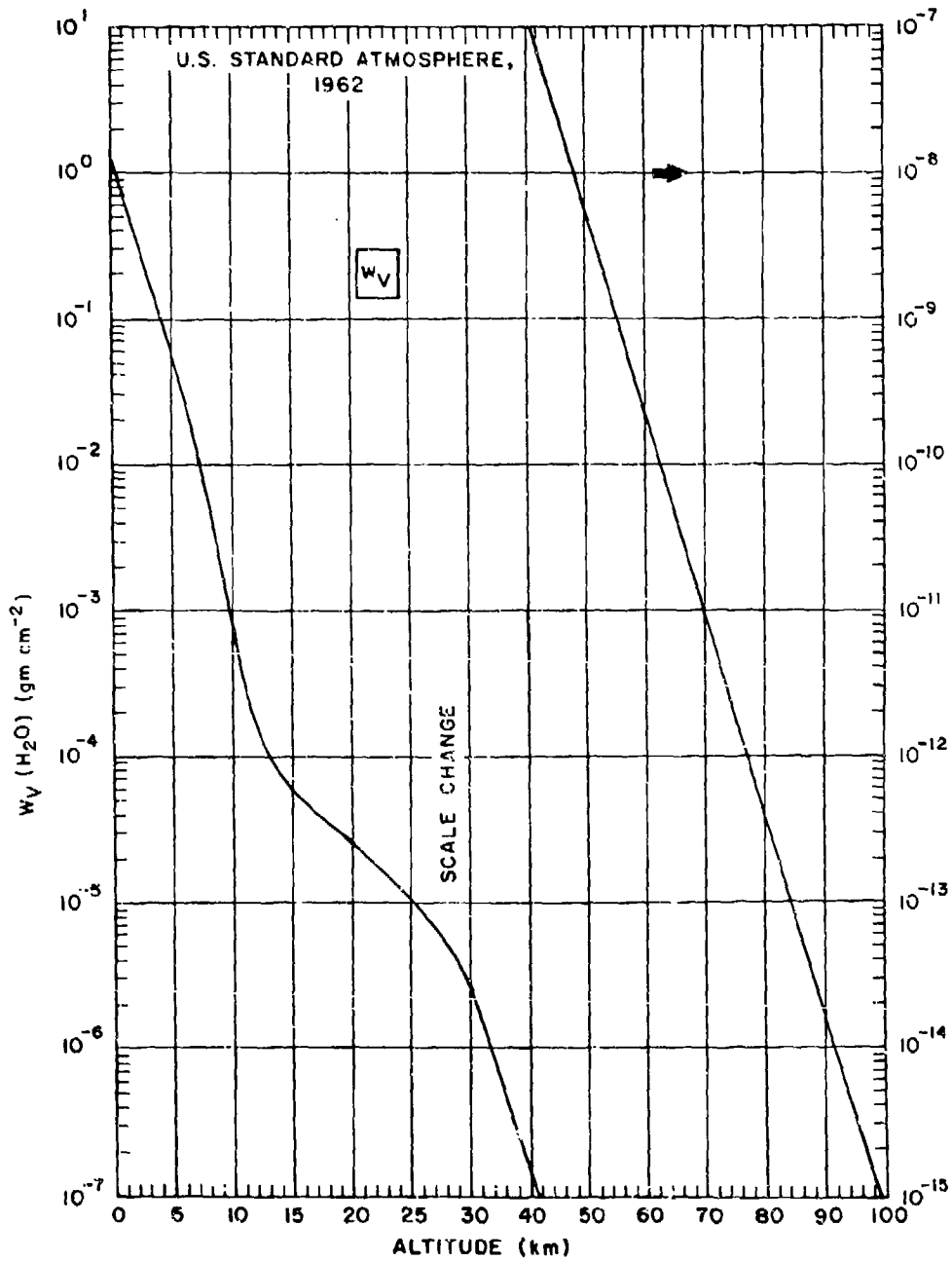


Figure B2. Equivalent Sea Level Path Length of Water Vapor as a Function of Altitude for Vertical Atmospheric Paths

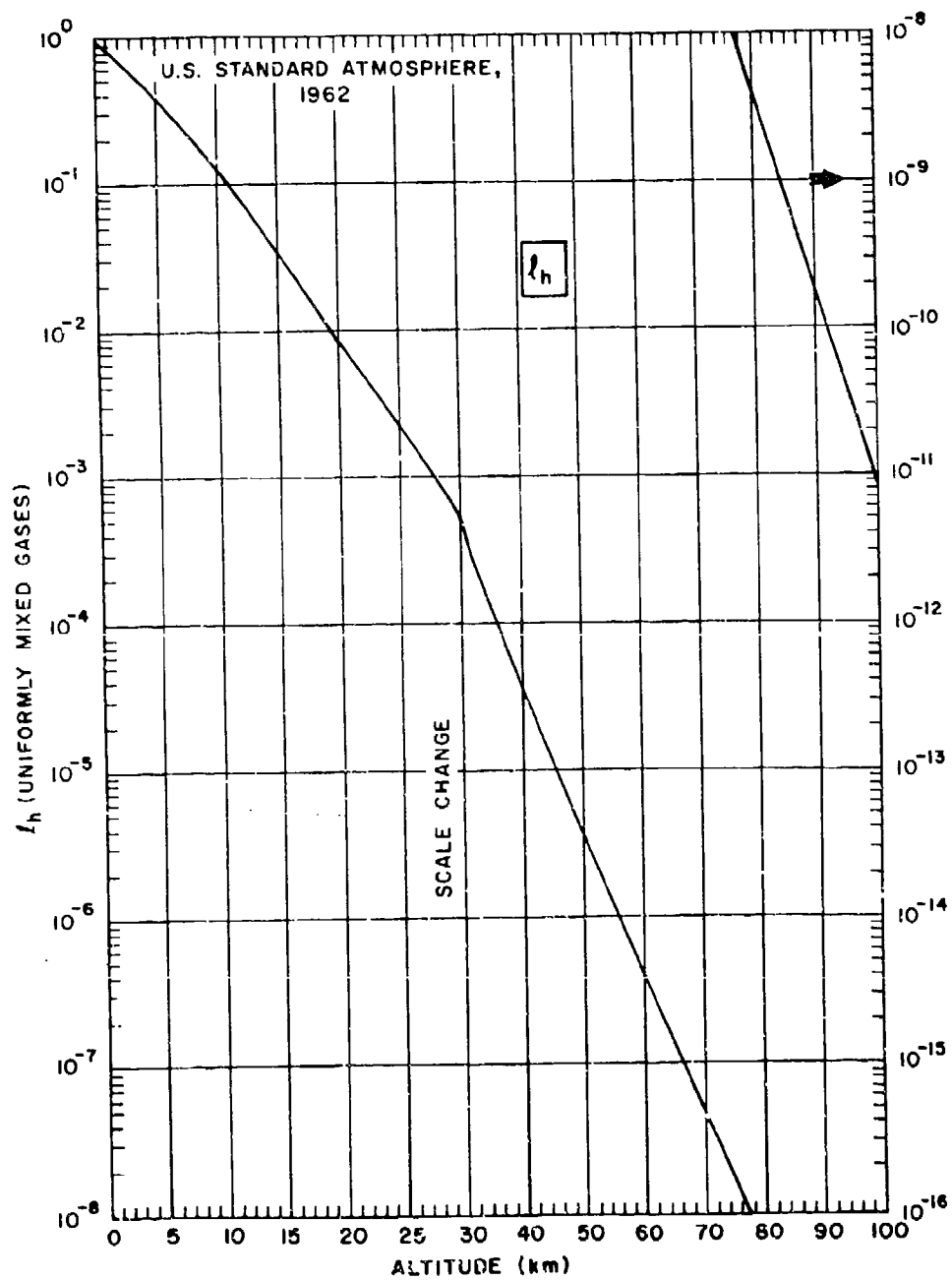


Figure B3. Equivalent Sea Level Path Length of Uniformly Mixed Gases as a Function of Altitude for Horizontal Atmospheric Paths

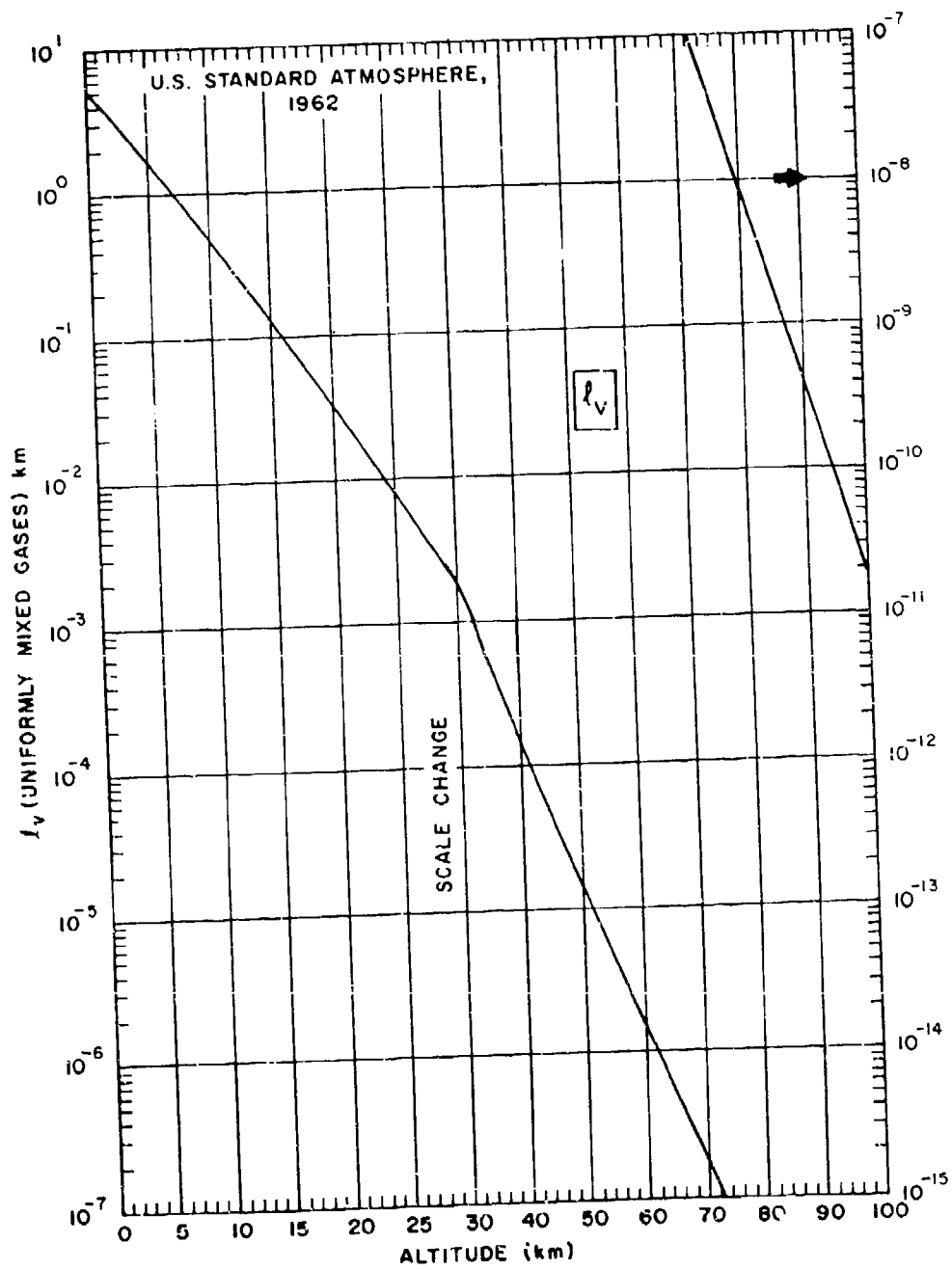


Figure B4. Equivalent Sea Level Path Length of Uniformly Mixed Gases as a Function of Altitude for Vertical Atmospheric Paths

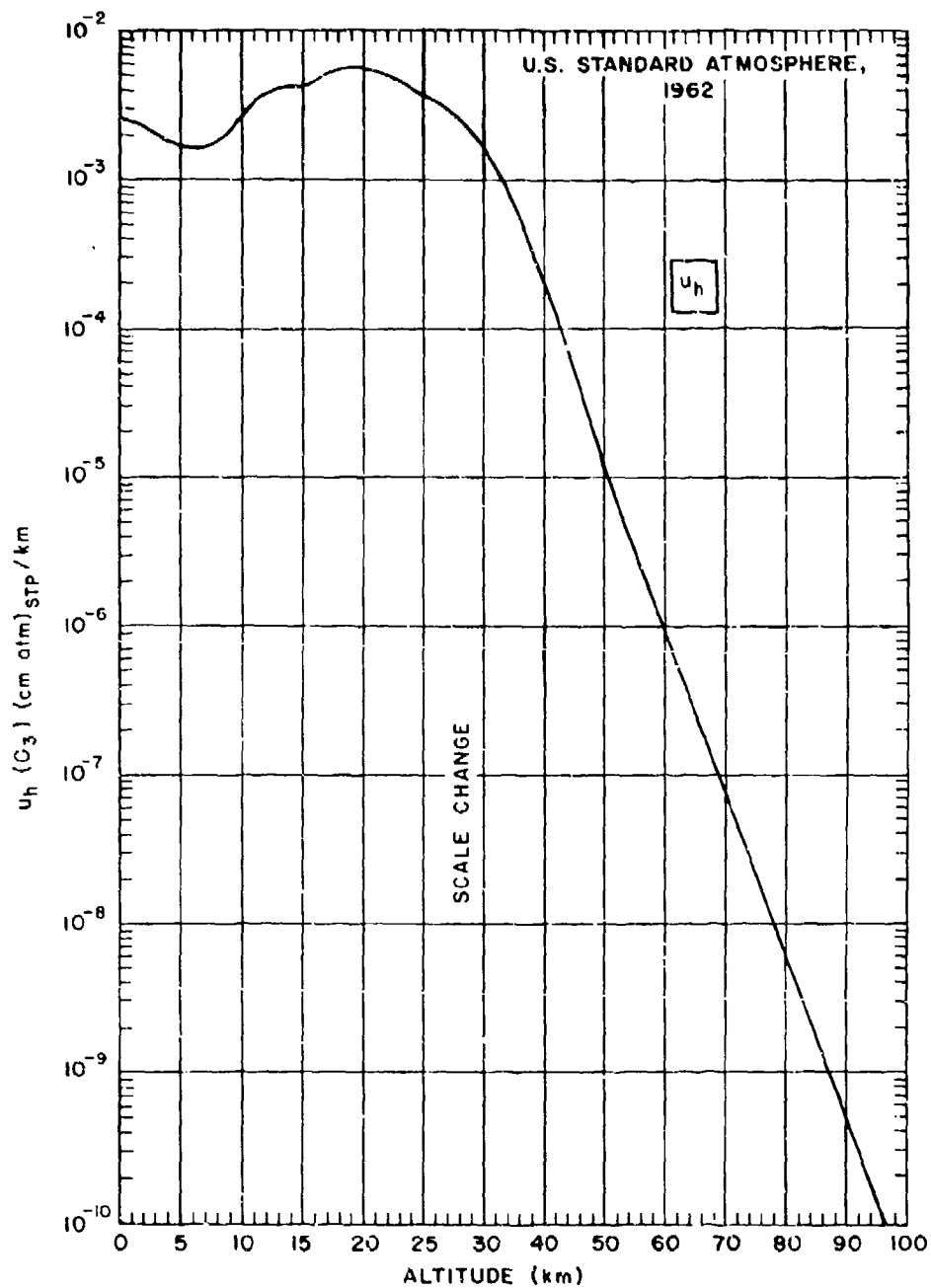


Figure B5. Equivalent Sea Level Path Length of Ozone as a Function of Altitude for Horizontal Atmospheric Paths

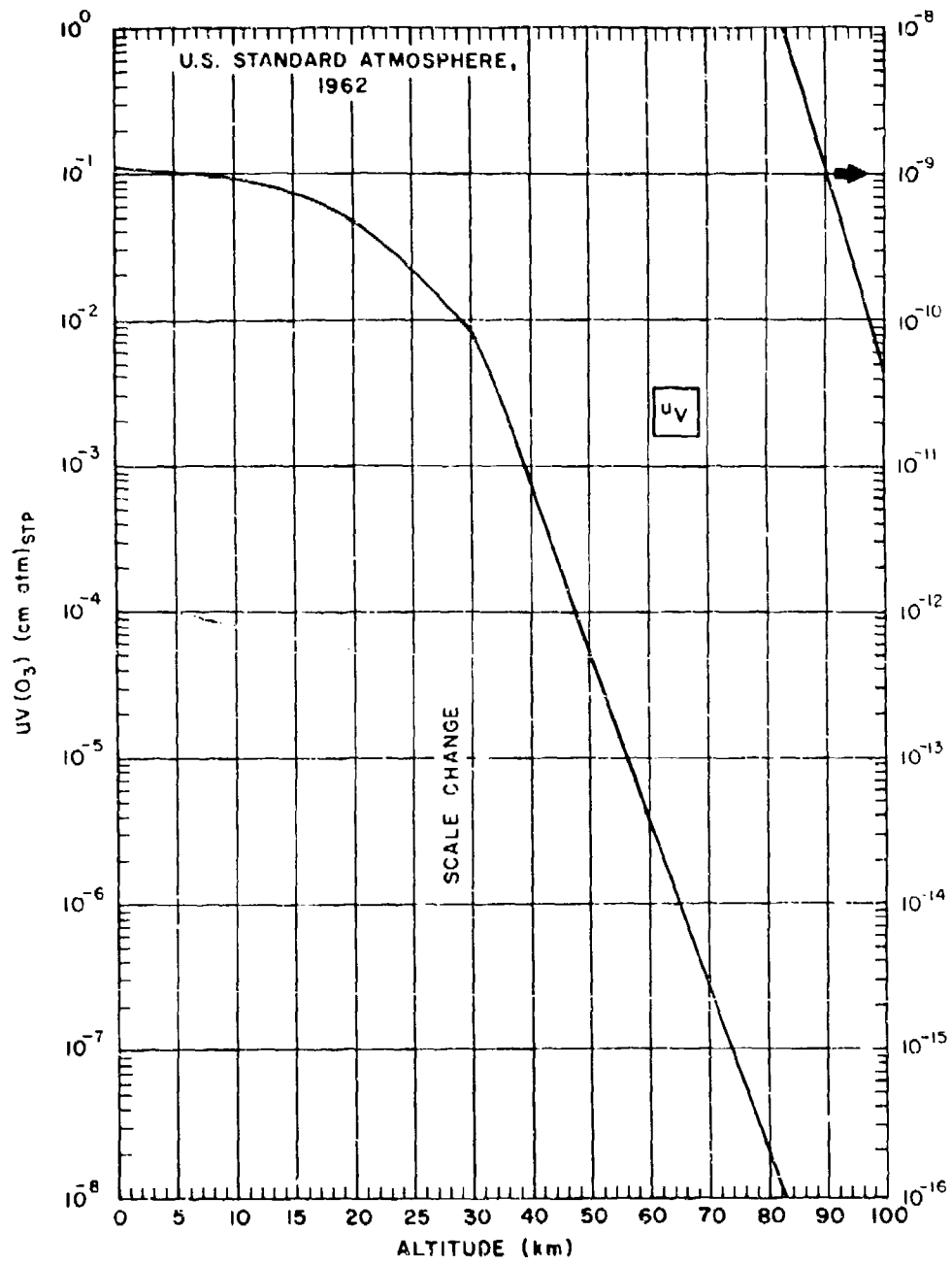


Figure B6. Equivalent Sea Level Path Length of Ozone as a Function of Altitude for Vertical Atmospheric Paths

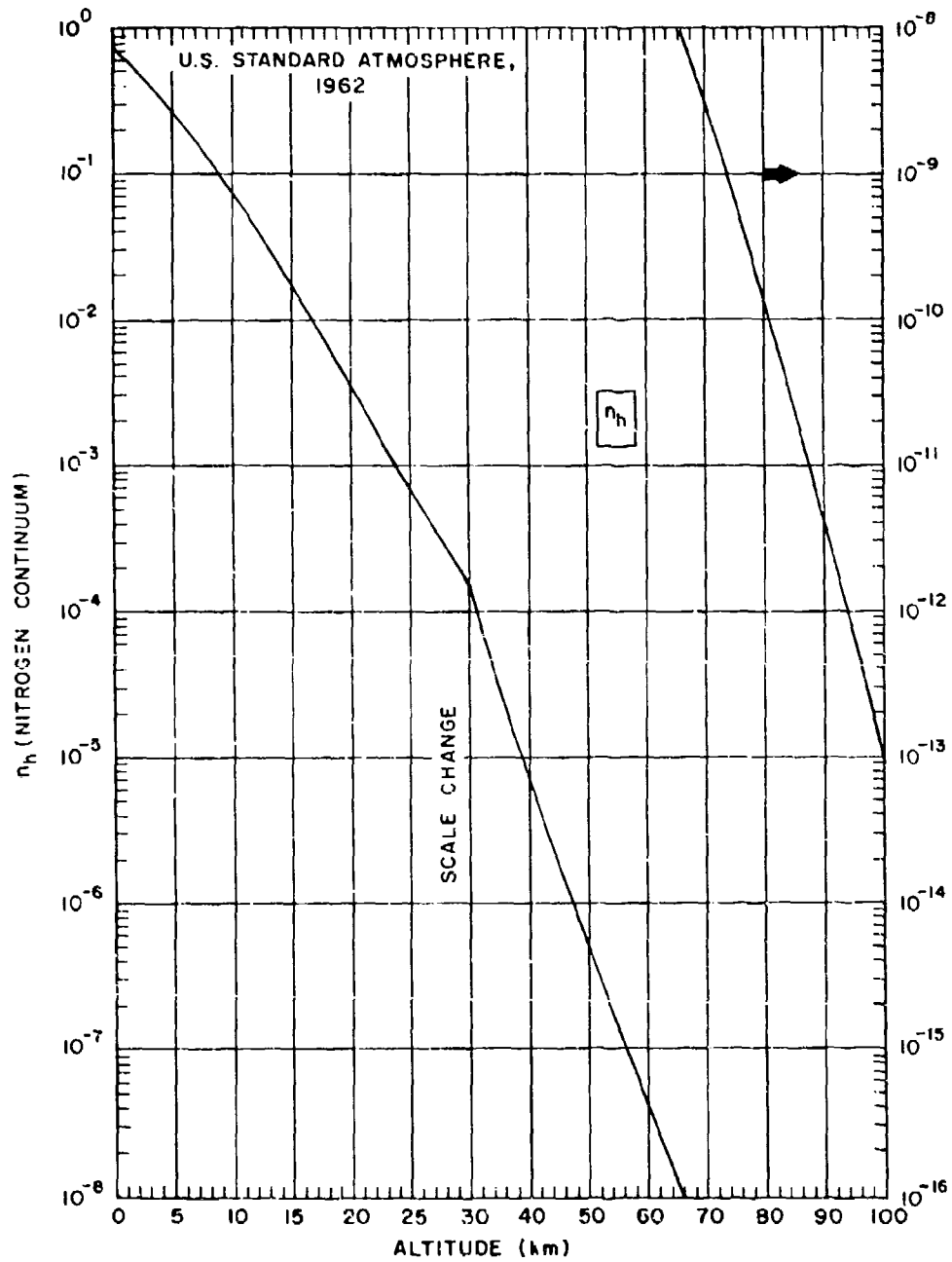


Figure B7. Equivalent Sea Level Path Length of Nitrogen as a Function of Altitude for Horizontal Atmospheric Paths

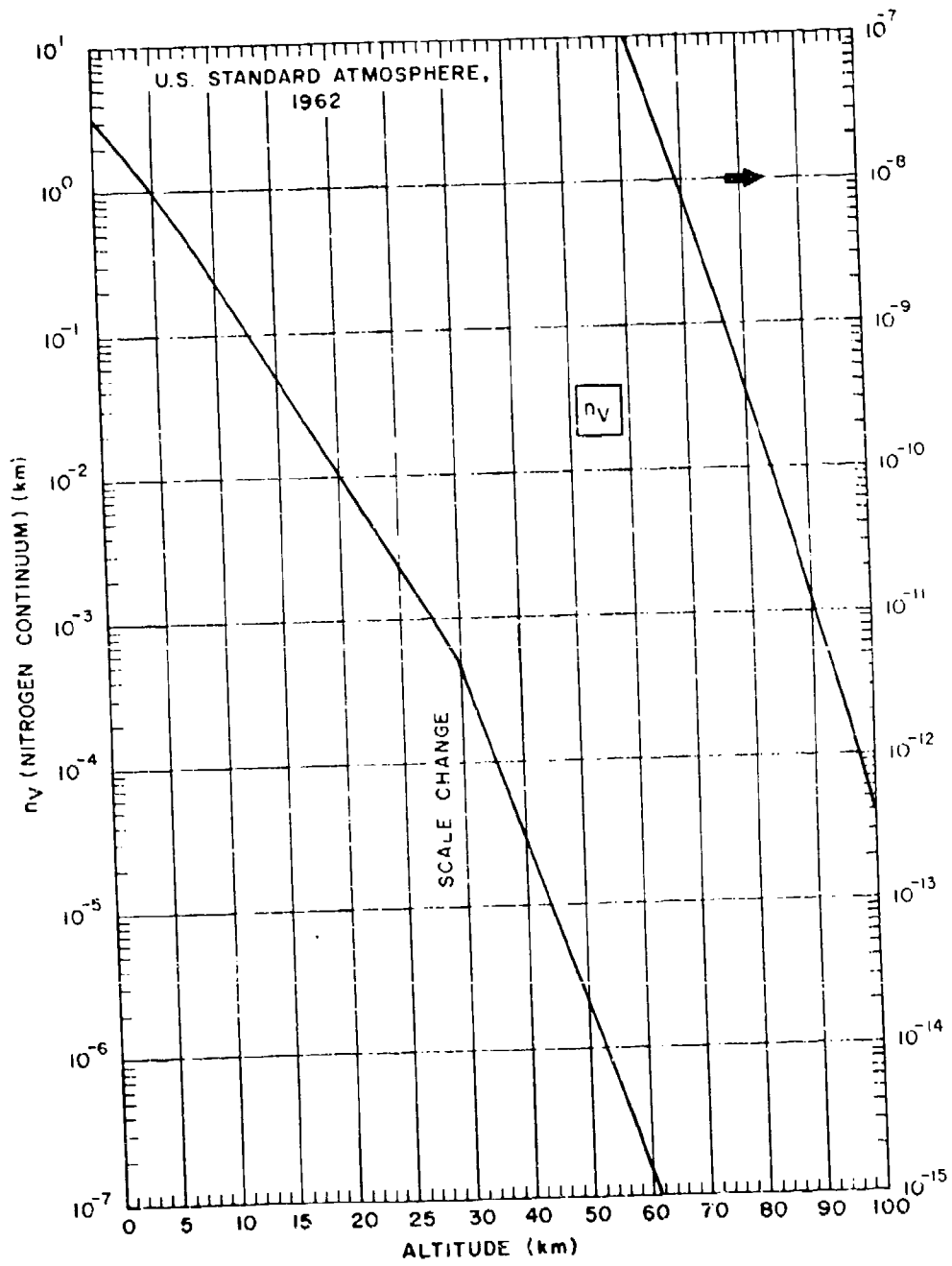


Figure B8. Equivalent Sea Level Path Length of Nitrogen as a Function of Altitude for Vertical Atmospheric Paths

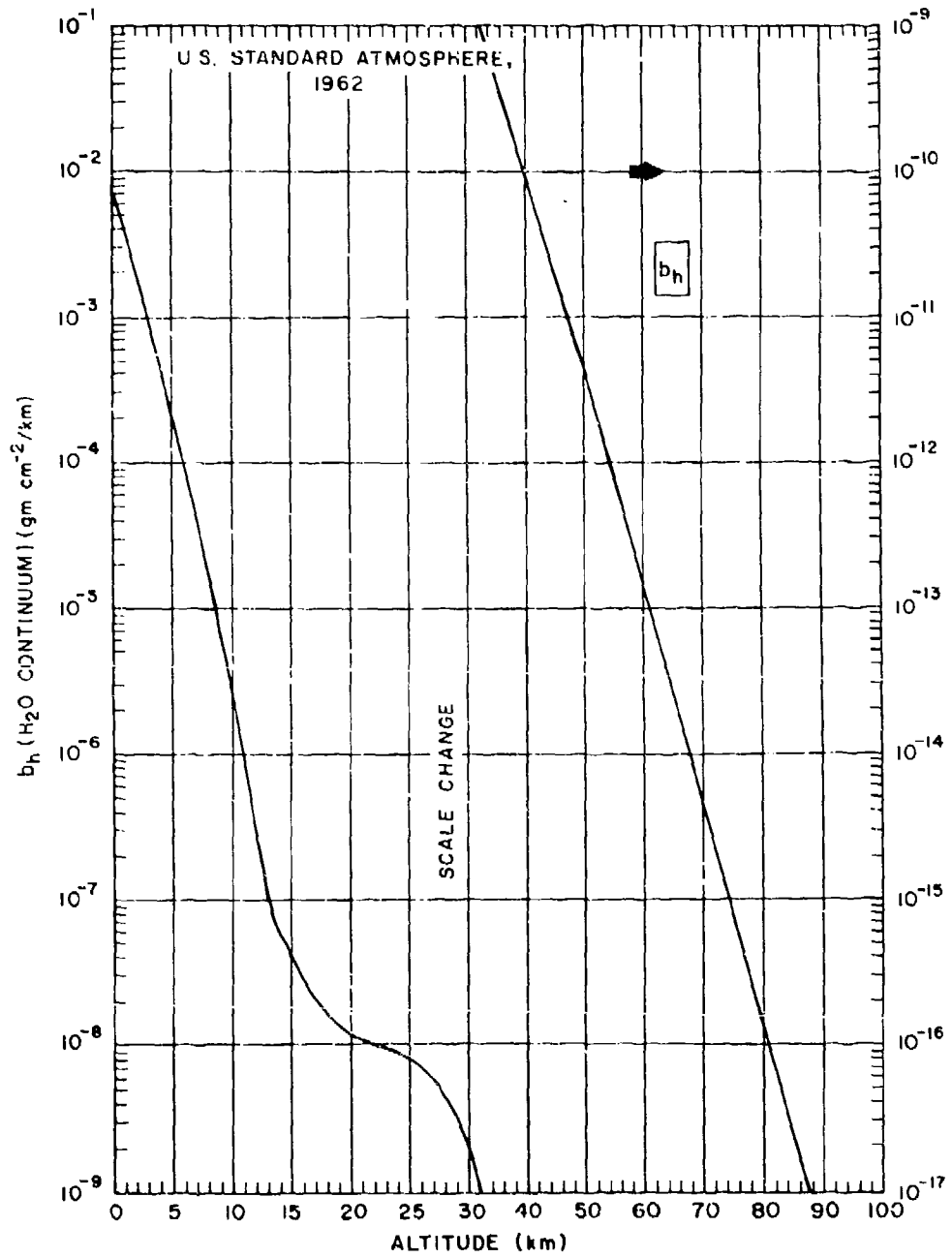


Figure B9. Equivalent Sea Level Path Length for Water Vapor Continuum as a Function of Altitude for Horizontal Atmospheric Paths.

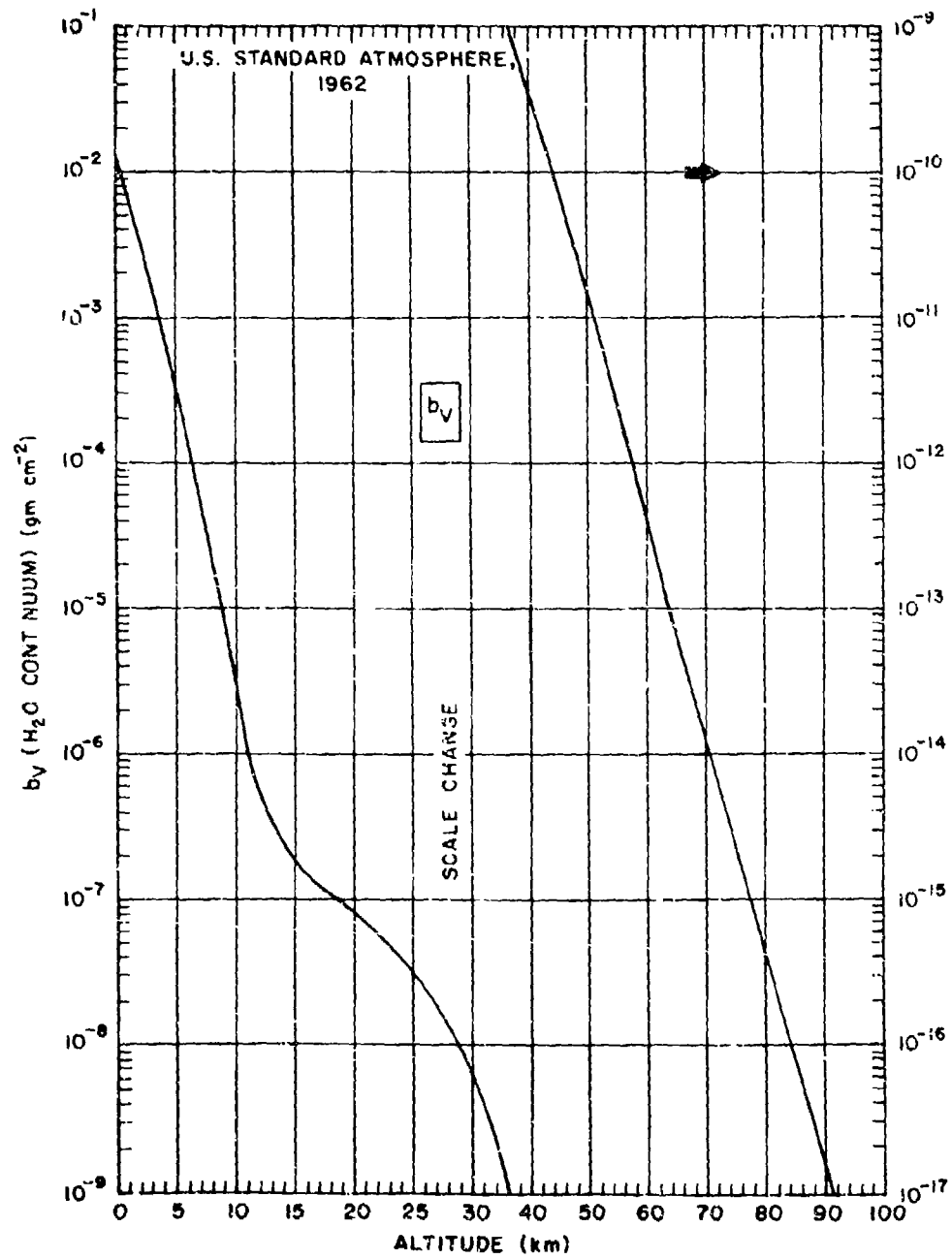


Figure B10. Equivalent Sea Level Path Length for Water Vapor Continuum as a Function of Altitude for Vertical Atmospheric Paths

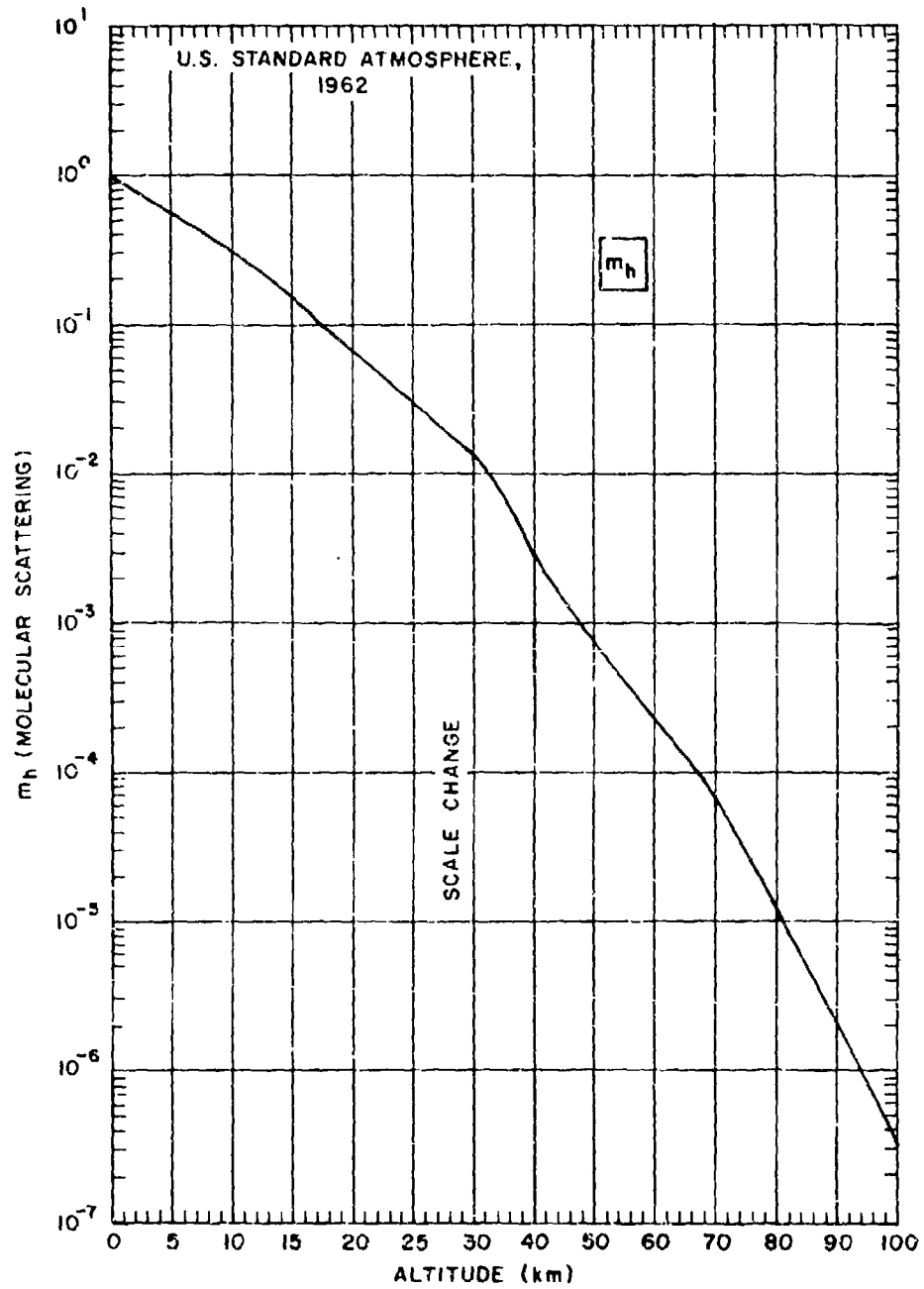


Figure B11. Equivalent Sea Level Path Length for Molecular Scattering as a Function of Altitude for Horizontal Atmospheric Paths

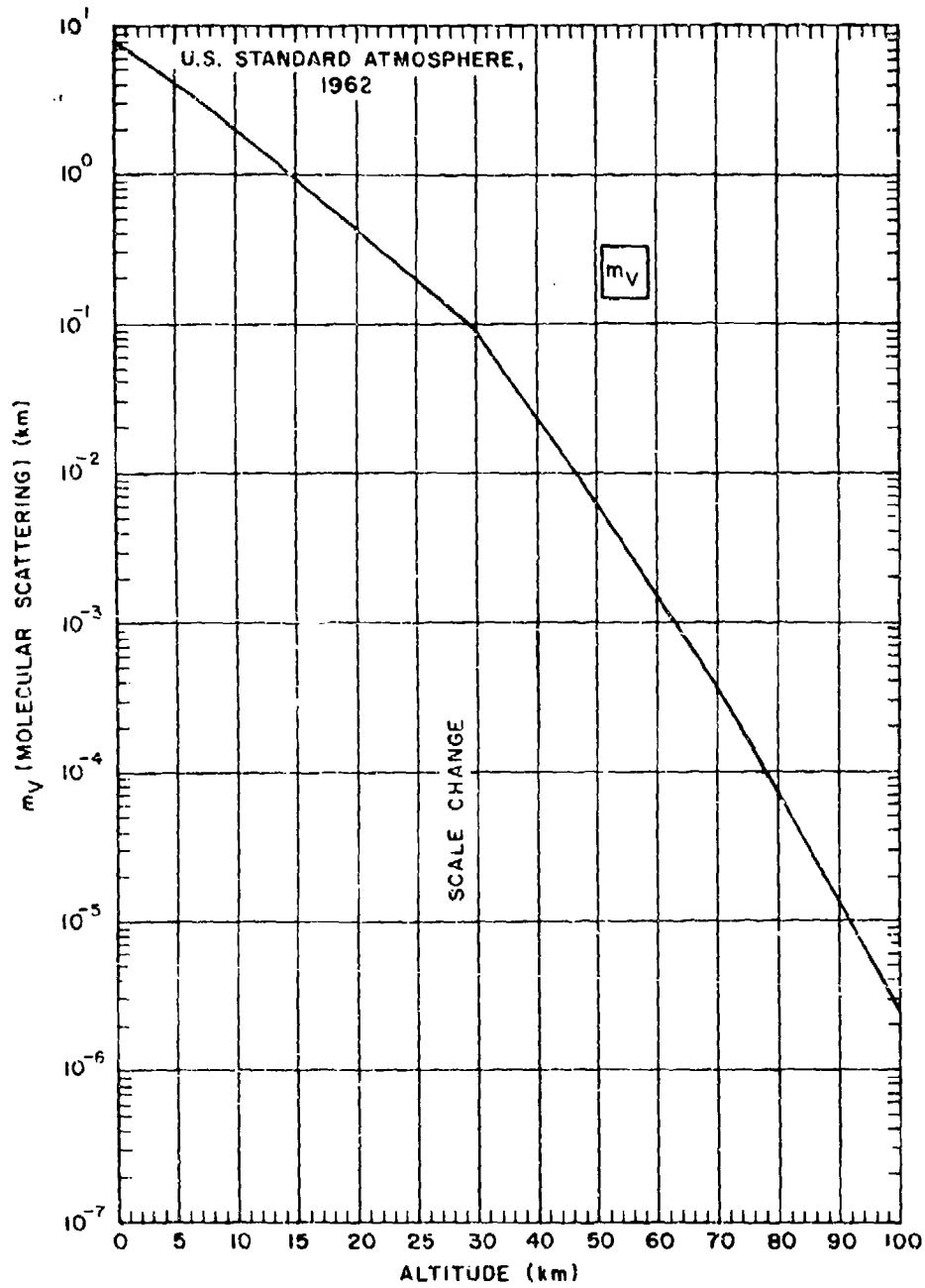


Figure B12. Equivalent Sea Level Path Length for Molecular Scattering as a Function of Altitude for Vertical Atmospheric Paths

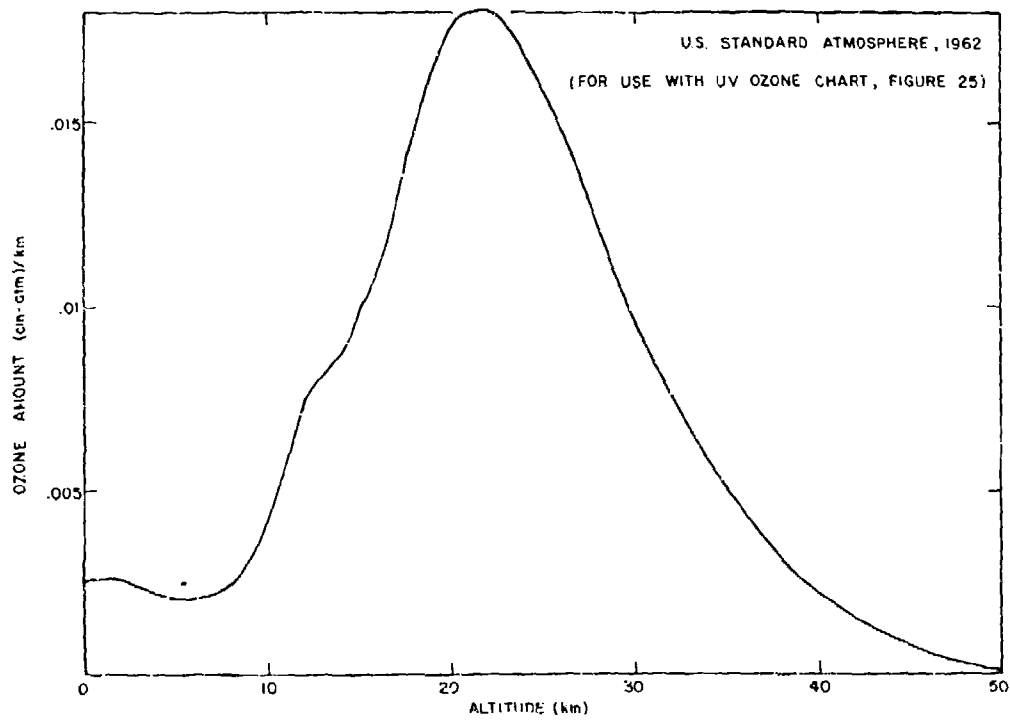


Figure B13. Equivalent Sea Level Path Length for Ozone (0.25-0.75 μm) as a Function of Altitude for Horizontal Atmospheric Paths

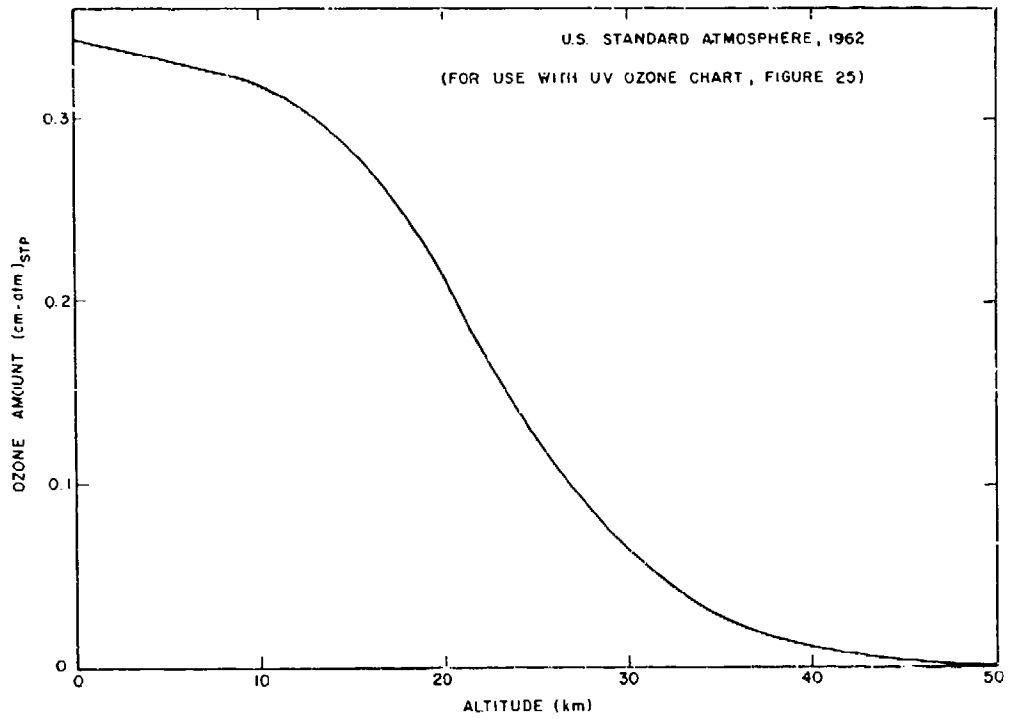


Figure B14. Equivalent Sea Level Path Length for Ozone (0.25-0.75 μm) as a Function of Altitude for Vertical Atmospheric Paths